LI
LABORATORY INVESTIGATION
THE BASIC AND TRANSLATIONAL PATHOLOGY RESEARCH JOURNAL
VOLUME 99 | SUPPLEMENT 1 | MARCH 2019

USCAP 2019

ABSTRACTS

LIVER PATHOLOGY (1509-1580)

USCAP 108TH ANNUAL MEETING

UNLOCKING YOUR INGENUITY

MARCH 16-21, 2019

National Harbor, Maryland
Gaylord National Resort & Convention Center

Published by
SPRINGER NATURE
www.ModernPathology.org

USCAP Creating a Better Pathologist
AN OFFICIAL JOURNAL OF THE UNITED STATES AND CANADIAN ACADEMY OF PATHOLOGY

EDUCATION COMMITTEE

Jason L. Hornick, Chair
Rhonda K. Yantiss, Chair, Abstract Review Board and Assignment Committee
Laura W. Lamps, Chair, CME Subcommittee
Steven D. Billings, Interactive Microscopy Subcommittee
Shree G. Sharma, Informatics Subcommittee
Raja R. Seethala, Short Course Coordinator
Ilan Weinreb, Subcommittee for Unique Live Course Offerings
David B. Kaminsky (Ex-Officio)
Aleodor (Doru) Andea
Zubair Baloch
Olca Basturk
Gregory R. Bean, Pathologist-in-Training
Daniel J. Brat
Ashley M. Cimino-Mathews
James R. Cook
Sarah M. Dry
William C. Faquin
Carol F. Farver
Yuri Fedoriw
Meera R. Hameed
Michelle S. Hirsch
Lakshmi Priya Kunju
Anna Marie Mulligan
Rish Pai
Vinita Parkash
Anil Parwani
Deepa Patil
Kwun Wah Wen, Pathologist-in-Training

ABSTRACT REVIEW BOARD

Benjamin Adam
Michelle Afkhami
Narasimhan (Narsi) Agaram
Rouba Ali-Fehmi
Ghassan Allo
Isabel Alvarado-Cabrero
Christina Arnold
Rohit Bhargava
Justin Bishop
Jennifer Boland
Elena Brachtel
Marilyn Bui
Shelley Caltharp
Joanna Chan
Jennifer Chapman
Hui Chen
Yingbei Chen
Benjamin Chen
Rebecca Chernock
Beth Clark
James Conner
Alejandro Contreras
Claudiu Cotta
Timothy D'Alfonso
Farbod Darvishian
Jessica Davis
Heather Dawson
Elizabeth Demicco
Suzanne Dintzis
Michelle Downes
Daniel Dye
Andrew Evans
Michael Feely
Dennis Firchau
Larissa Furtado
Anthony Gill
Ryan Gill
Paula Ginter
Tamara Giorgadze
Raul Gonzalez
Purva Gopal
Anuradha Gopalan
Jennifer Gordetsky
Rondell Graham
Alejandro Gru
Nilesh Gupta
Mamta Gupta
Krisztina Hanley
Douglas Hartman
Yael Heher
Walter Henricks
John Higgins
Mai Hoang
Mojgan Hosseini
Aaron Huber
Peter Illei
Doina Ivan
Wei Jiang
Vickie Jo
Kirk Jones
Neerja Kambham
Chiah Sui (Sunny) Kao
Dipti Karamchandani
Darcy Kerr
Ashraf Khan
Rebecca King
Michael Kluk
Kristine Konopka
Gregor Krings
Asangi Kumarapeli
Alvaro Laga
Cheng-Han Lee
Zaibo Li
Haiyan Liu
Xiuli Liu
Yan-Chun Liu
Tamara Lotan
Anthony Magliocco
Kruti Maniar
Jonathan Marotti
Emily Mason
Jerri McLemore
Bruce McManus
David Meredith
Anne Mills
Neda Moatamed
Sara Monaco
Atis Muehlenbachs
Bita Naini
Dianna Ng
Tony Ng
Ericka Olgaard
Jacqueline Parai
Yan Peng
David Pisapia
Alexandros Polydorides
Sonam Prakash
Manju Prasad
Peter Pytel
Joseph Rabban
Stanley Radio
Emad Rakha
Preetha Ramalingam
Priya Rao
Robyn Reed
Michelle Reid
Natasha Rekhtman
Michael Rivera
Michael Roh
Andres Roma
Avi Rosenberg
Esther (Diana) Rossi
Peter Sadow
Safia Salaria
Steven Salvatore
Souzan Sanati
Sandro Santagata
Anjali Saqi
Frank Schneider
Jeanne Shen
Jiaqi Shi
Wun-Ju Shieh
Gabriel Sica
Deepika Sirohi
Kalliopi Siziopikou
Lauren Smith
Sara Szabo
Julie Teruya-Feldstein
Gaetano Thiene
Khin Thway
Rashmi Tondon
Jose Torrealba
Evi Vakiani
Christopher VandenBussche
Sonal Varma
Endi Wang
Christopher Weber
Olga Weinberg
Sara Wobker
Mina Xu
Shaofeng Yan
Anjana Yeldandi
Akihiko Yoshida
Gloria Young
Minghao Zhong
Yaolin Zhou
Hongfa Zhu
Debra Zynger

1509 Significance of Tumor Budding in Cholangiocarcinoma

Diana Agostini-Vulaj[1], Justin Cates[2], Laura Bratton[3], Raul Gonzalez[4]
[1]University of Rochester Medical Center, Rochester, NY, [2]Vanderbilt University Medical Center, Nashville, TN, [3]Ochsner Medical Center, New Orleans, LA, [4]Beth Israel Deaconess Medical Center, Boston, MA

Disclosures: Diana Agostini-Vulaj: None; Justin Cates: None; Laura Bratton: None; Raul Gonzalez: None

Background: Tumor budding (TB) describes small clusters of tumor cells (< 5 cells) at the interface of an invasive carcinoma. It has been shown to be an adverse factor in colorectal carcinoma (CRC), increasing risk of nodal disease in pT1 cases and predicting worse survival in pT2 cases. TB has also been studied in gastric adenocarcinoma, esophageal squamous cell carcinoma, and pancreatic adenocarcinoma, and has been shown to be associated with an adverse prognosis for those malignancies. However, TB has been scarcely evaluated in cholangiocarcinoma (CC), a disease with a generally poor prognosis wherein the role for adjuvant chemotherapy following surgical resection remains somewhat unclear. We undertook this study to evaluate whether TB in CC was linked to other clinicopathologic factors or to outcome.

Design: We identified 42 cases of CC with available glass H&E slides and clinical follow-up data. Clinicopathologic features analyzed included age, sex, margin status, location, size, grade, lymphovascular invasion, perineural invasion (PNI), CC subtype (large or small duct), T stage, N status, M stage, recurrence, disease-specific survival, and TB. Budding was scored using International Tumor Budding Consensus Conference recommendations for CRC: The highest tumor bud count at the invasive tumor front in a 0.785 mm^2 area was recorded and stratified into Bd1 (0-4 buds), Bd2 (5-9 buds), and Bd3 (≥10 buds) (Figure 1A-C). Statistical analyses were performed using Fisher's exact test, Spearman's rank correlation coefficient, and Cox regression analysis, with *P*-values of <0.05 considered significant.

Results: Our cohort included 17 (40%) extrahepatic CCs and 25 (60%) intrahepatic CCs. TB was more common in higher grade lesions (*P*=0.0005) but did not relate to other factors, including lymph node metastases (*P*=0.64), CC subtype, or tumor location. High TB (Bd3) was also associated with worse disease-specific survival (*P*=0.002, hazard ratio [HR] 8.51); other factors associated with worse disease-specific survival included PNI (*P*=0.040, HR=2.49), nodal disease (*P*=0.016, HR=2.78), and distant metastases (*P*=0.004, HR=5.33).

Figure 1 - 1509

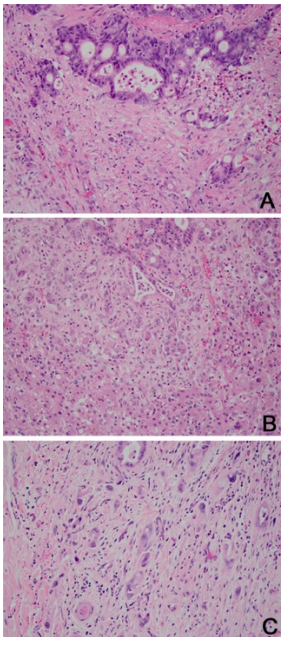

Conclusions: TB is associated with higher-grade disease in CC, and high-grade TB is associated with poor disease-specific survival, with a higher HR than distant metastases. This is analogous to its significance in other gastrointestinal malignancies. Therefore, TB may serve as useful information for clinicians with respect to patient prognosis and therapeutic considerations in CC, as in CRC.

1510 A comparison study of steatohepatitis in Belgian and Japanese cohorts regarding clinicopathological features and utility of macrophage infiltration

Tomoki Akamine[1], Nicolas Lanthier[2], Shingo Arakaki[3], Tatsuji Maeshiro[3], Kennosuke Karube[4], Mina Komuta[5]
[1]University of the Ryukyus Graduate School of Medicine, Naha City, Japan, [2]Clinique Universitaires Saint-Luc, Brussels, Belgium, [3]University of the Ryukyus, Nishihara, Japan, [4]University of the Ryukyus Graduate School of Medicine, Nakagami-gun, Japan, [5]Cliniques universitaires Saint-Luc, Brussels, Belgium

Disclosures: Tomoki Akamine: None; Nicolas Lanthier: None; Shingo Arakaki: None; Tatsuji Maeshiro: None; Kennosuke Karube: None; Mina Komuta: None

Background: Inflammation and insulin resistance play important roles in non-alcoholic steatohepatitis (NASH) progression. However, risk factors for NASH could be different between ethnic groups. For example, type 2 diabetes appears at lower levels of adiposity in Asian populations than in European populations and “lean NAFLD” was initially described in Asian populations. We hypothesized that the different backgrounds may influence the histological features of NASH. We also investigated whether macrophage infiltration correlated with the severity of inflammation and fibrosis in these two cohorts.

Design: Clinicopathological features of NASH were investigated in two independent cohorts of 75 Belgian and 45 Japanese patients, with liver biopsies graded for NASH severity, steatosis, and fibrosis. Macrophage infiltration was assessed with CD68 staining. All liver biopsies were scored based on NAS and SAF score. Fibrosis was evaluated by location; periportal, pericellular and perivenular.

Results: Clinically, the Belgian cohort was significantly more metabolic than the Japanese one, regarding body weight (mean body mass index 33.4 versus 29.9, p=0.006), waist circumference, presence of hypertension and, dyslipidaemia. Alcohol intake was also higher in the Belgian population (5.5 g/day versus 1 g/day, p<0.001). However, laboratory data showed that AST and ALT were significantly higher in Japanese group compared to Belgian group. Pathologically, the Japanese group had a significantly lower fibrotic score than the Belgian cohort (p=0.002), while the Belgian group showed more severe portal inflammation compared to the Japanese group (p=0.001). Both cohorts indicated that severe lobular inflammation was significantly associated with high fibrotic score (P=0.0028) and steatosis proportion (p=0.006). In addition, severe portal inflammation was significantly associated with high fibrotic stage, such as periportal (p=0.00012) and pericellular fibrosis (p=0.0038). Macrophage number was significantly higher with severe lobular inflammation (p=0.0011), severe portal fibrosis (p=0.0006) and severe steatosis (p=0.0269) in both cohorts.

Conclusions: There was a clear clinicopathological difference between the Belgian and Japanese cohorts, such as the incidence of metabolic syndrome, and this correlated with NASH severity, namely fibrosis and portal inflammation. Macrophage infiltration clearly correlated with NASH severity in both cohorts, indicating the possibility of a potential prognostic parameter of NASH development.

1511 Association of Histologic Features of Methotrexate Induced Hepatotoxicity with Clinical Risk Factors for Steatosis and Steatohepatitis

Ram Al-Sabti[1], Marcela Salomao[2], Rish Pai[2], Jerome Cheng[3], Maria Westerhoff[3], David Papke[4], Lei Zhao[5], Shaomin Hu[6], Nicole Panarelli[7], Katherine Boylan[8], John Hart[9]
[1]University of Chicago Medical Center, Chicago, IL, [2]Mayo Clinic Arizona, Scottsdale, AZ, [3]University of Michigan, Ann Arbor, MI, [4]Brigham and Women's Hospital, Boston, MA, [5]Brigham and Women's Hospital, Harvard Medical School, Boston, MA, [6]Montefiore Medical Center, Bronx, NY, [7]Montefiore Medical Center, Scarsdale, NY, [8]University of Utah Hospital, Millcreek, UT, [9]University of Chicago, Chicago, IL

Disclosures: Ram Al-Sabti: None; Marcela Salomao: None; Rish Pai: None; Jerome Cheng: None; Maria Westerhoff: None; David Papke: None; Lei Zhao: None; Shaomin Hu: None; Nicole Panarelli: None; Katherine Boylan: None; John Hart: None

Background: The Roenigk classification of Methotrexate (MTX) induced hepatotoxicity was created in 1977, before the concept of nonalcoholic steatohepatitis was conceived. The histologic features said to be characteristic of MTX hepatotoxicity overlap nearly completely with those of nonalcoholic fatty liver disease (NAFLD) in patients not taking MTX. Moreover, the conditions most commonly treated with (psoriasis & rheumatoid arthritis) predispose to a sedentary lifestyle that increases the risk of NAFLD. Our hypothesis is that steatosis and steatohepatitis occur only in those with clinical and laboratory risk factors for NAFLD, independent of MTX exposure. In the absence of risk factors for NAFLD, liver biopsies from patients on MTX are expected to be nearly or completely normal.

Design: From the archives of 6 institutions, 97 liver biopsies from patients receiving long term MTX were identified. The biopsies were reviewed for the reported features of MTX toxicity, including: macrovesicular steatosis (S), steatohepatitis (SH) (NIDDK system & FLIP algorithm) and fibrosis (NIDDK system) and were correlated with demographic, laboratory and clinical risk factors for NAFLD and alcohol use. Review of histologic and clinical data was conducted independently at each center; the data were pooled for central review and analysis.

Results: Demographics, indications for MTX, and the incidence of risk factors for NAFLD are shown in Table 1. A total of 88 patients (91%) had at least one known risk factor for NAFLD, including BMI>25, diabetes (DM), hyperlipidemia (HLD), chronic TPN or steroid use, or

documented alcohol abuse; of these, 66 (75%) had S or SH on biopsy. In contrast, there were only 9 patients (9%) without any of the NAFLD risk factors or ethanol abuse; of those, 3 (33%) had S and none had SH (0%). The association between known NAFLD risk factors and histologic evidence of S or SH is shown in Figure 1, and is statistically significant (p=0.016, Fisher's exact test from a 2x2 contingency table). Anisonucleosis, which is a described histologic feature of MTX exposure, was seen in only 11 cases (11%), of which 7 had no S or SH.

			No Steatosis/ Steatohepatitis N=28 (%)	**Steatosis/ Steatohepatitis N=69 (%)**
Average age (years)	54.8			
Gender	Male	34	9 (32%)	25 (36%)
	Female	63	19 (68%)	44 (64%)
Indication of MTX	Crohn's disease	11	3 (11%)	8 (12%)
	Psoriasis/ Psoriatic arthritis	28	9 (32%)	19 (28%)
	Rheumatoid arthritis	30	8 (29%)	22 (32%)
	SLE	6	1 (4%)	5 (7%)
	Other	22	7 (25%)	15 (22%)
Patients with Risk Factors (RF) for Steatosis/Steatohepatitis	No		6 (21%)	3 (4%)
	Yes		22 (79%)	66 (96%)
BMI	<25	No DM/HLD	6 (21%)	3 (4%)
		With DM/HLD	1 (4%)	2 (3%)
	25 - 29.9	No DM/HLD	4 (14%)	5 (7%)
		With DM/HLD	7 (25%)	8 (12%)
	>30	No DM/HLD	8 (29%)	23 (33%)
		With DM/HLD	1 (4%)	26 (38%)
ETOH abuse	1		0 (0%)	1 (1%)
Total Parenteral Nutrition (TPN)	2		1 (4%)	1 (1%)
Anisonucleosis		11	7 (25%)	4 (6%)

Figure 1 - 1511

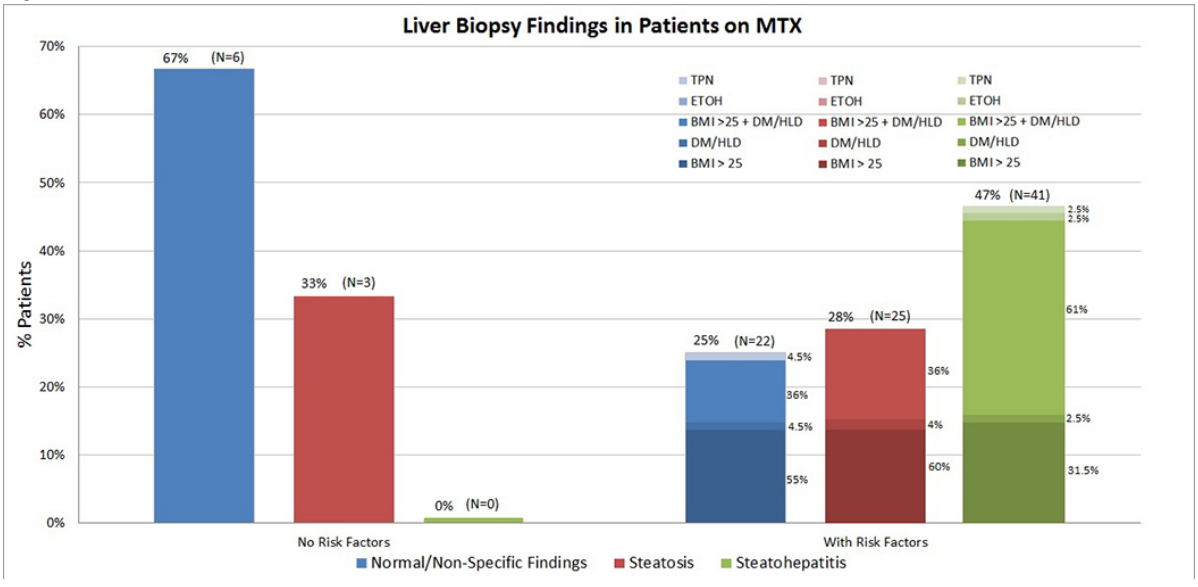

Conclusions: In patients taking MTX clinical and laboratory risk factors for NAFLD are highly prevalent (91%), and S and SH are seen almost exclusively in that group of patients. Patients on MTX without NAFLD risk factors are rare (9%) and these patients infrequently have NAFLD (33% with S and 0% with SH). The concept that MTX causes NAFLD-like changes should be re-evaluated.

1512 Pediatric Advanced Fibrosis in the Era of Genetics: A 33 Year Single Center Review

Zainab Alruwaii[1], Yang Zhang[2], James Miller[3], Tatianna Larman[3], Robert Anders[4], Kiyoko Oshima[2]
[1]Johns Hopkins Medical Institutions, Baltimore, MD, [2]Johns Hopkins Hospital, Baltimore, MD, [3]Johns Hopkins University School of Medicine, Baltimore, MD, [4]Johns Hopkins, Baltimore, MD

Disclosures: Zainab Alruwaii: None; Yang Zhang: None; James Miller: None; Tatianna Larman: None; Robert Anders: None; Kiyoko Oshima: None

Background: Advanced liver disease is a significant cause of morbidity and mortality in the pediatric population. We reviewed the evolution of etiologies of advanced liver disease and hepatic cirrhosis (HC) in children over the past 33 years, assessing the difference in frequencies of various conditions after the introduction of genetic testing in our institution.

Design: All liver specimens with severe fibrosis or cirrhosis from 1985 – 2018 in patients aged 0 -18 were identified. Cases with insufficient clinical or diagnostic information were excluded. The etiologic factors from 1985-2000 were compared with those from 2000-2018.

Results: From 399 liver samples with at least advanced fibrosis, 279 cases (136 boys, 143 girls) with an average age of 6.7 years were included. Among the causative conditions, extrahepatic biliary atresia (EHBA) comprised the most (38%), followed by Immune-related hepatitis (19%), genetic diseases (16%), cryptogenic cirrhosis (9%), infectious hepatitis (7%), congenital hepatic fibrosis (5%), and total parenteral nutrition (4%). Mixed etiologies accounted for the remaining cases. EHBA and genetic causes were more frequent in the youngest age group (<10 years), while immune-related causes predominated in older children. Viral hepatitis was more frequent in boys than in girls. Infectious causes and cryptogenic cirrhosis showed a falling trend over the study period; their proportion decreased from 10% to 4% (CI= -0.0783 to 12.5898, p-value=.048) and from 12% to 5 % (CI=0.3982 to 14.0303, p-value= 0.035) respectively(1986- 2000 vs. 2000-2018). The frequency of other causes increased less significantly over the years (Table). The distribution of EHBA remained relatively stable.

Etiology	1985 -1999			2000-2018	
EHBA	**52**	**39%**		**54**	**38%**
Immune:	**20**	**15%**		**32**	**22%**
AIH	16	12%		22	15%
SC	2	1%		8	6%
Overlap Syndrome, other	2	1%		2	1%
Genetic:	**18**	**13%**		**26**	**18%**
A1A	4	3%		5	3%
Wilson	3	2%		3	2%
CF	3	2%		5	3%
PFIC	0	0		6	4%
Alagille	4	3%		0	0
Metabolic	1	1%		5	3%
Cryptogenic	**16**	**12%**		**7**	**5%**
Infectious	**14**	**10%**		**6**	**4%**
TPN	**7**	**5%**		**5**	**3%**
Other	**8**	**6%**		**14**	**10%**
TOTAL	**135**	**100 %**		**144**	**100 %**

AIH, autoimmune hepatitis; A1A, alpha one antitrypsin deficiency; CF, cystic fibrosis; EHBA, extra-hepatic biliary atresia PFIC, progressive familial intrahepatic cholestasis; SC, sclerosing cholangitis; TPN, total parenteral nutrition.

Conclusions: Among the different etiologies of liver cirrhosis in the pediatric population, the proportion of infectious and cryptogenic cirrhosis decreased dramatically. Although genetic causes increased slightly over time, the advancement of genetic testing could be a contribution in rolling- out cryptogenic cirrhosis. Also, the spectrum of genetic diseases is changing over time; Biopsies from alagille patients disappeared since the presence of cholestasis with positive phenotype is sufficient to diagnose paucity of bile ducts. Progressive familial intrahepatic cholestasis emerged in this category, and the frequency of metabolic diseases increased between 2000 and 2018.

1513 Expression of FTO Gene is Significantly Upregulated in Hepatocellular Cancer at The RNA Level Without Increased Protein Expression

Mohammed Alsomali[1], Juan Barajas[1], Kalpana Ghoshal[1], Debbie Knight[1], Wei Chen[1], Wendy Frankel[1]
[1]*The Ohio State University Wexner Medical Center, Columbus, OH*

Disclosures: Mohammed Alsomali: None; Juan Barajas: None; Kalpana Ghoshal: None; Debbie Knight: None; Wei Chen: None; Wendy Frankel: None

Background: Hepatocellular carcinoma (HCC) is the fifth leading cause of cancer-related deaths worldwide. Thus, a better understanding of molecular aberrations involved in HCC pathogenesis is necessary for developing effective therapy. Reversible RNA modifications are emerging as a new mechanism of epitranscriptomic gene regulation. N^6-methyladenosine (m^6A) is the most prevalent internal modification in eukaryotic mRNA added predominantly at the GGACU motif of polyadenylated RNAs. m^6A is added post-transcriptionally by the m^6A methyltransferase complex and is removed by demethylases of the AlkB family including fat mass and obesity associated protein (FTO). However, the regulatory mechanism of these processes in liver is poorly understood. We studied expression of FTO in HCC and non-neoplastic liver to determine if *FTO* is dysregulated in HCC.

Design: To assess expression of *FTO* at RNA level in HCCs and benign livers, we evaluated data from The Cancer Genome Atlas (TCGA-LIHC) on HCC (n=377) and benign liver (n=50). We identified 132 cases of HCC from our archives from 1997 to 2016. Western blot analysis (n=3) and RT-PCR (n=9) were performed, and tissue microarrays were constructed using 1 mm cores in duplicate from HCC (n=132) and benign background liver (n=105). Sections were immunostained with FTO antibody (cat# ab124892, Abcam) and intensity was graded as 0 (absent), 1 (weak), or 2 (strong). Statistical analysis was performed using Graphpad Prism (chi-square and t-tests).

Results: Analysis of TCGA-LIHC data, Western blot analysis (Fig 1) and RT-PCR (Fig 2) showed significant upregulation of *FTO* RNA expression in HCCs compared to benign livers. IHC demonstrated strong nuclear expression in 36% (47/132) and weak staining in 37% (49/132) of HCCs compared to strong staining in 42% (44/105) and weak expression in 50% (52/105) of benign background livers. There was no significant difference in percentage of strong staining between HCC and benign liver (p=0.32), but overall expression was significantly reduced in HCCs compared to benign livers (p=0.0003)

Figure 1 - 1513

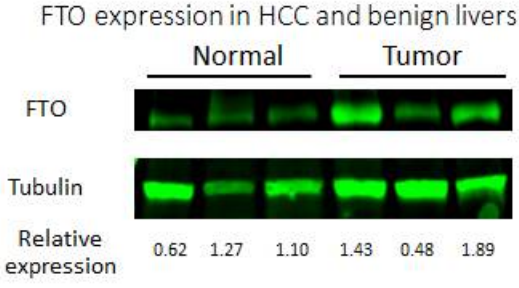

Figure 2 - 1513

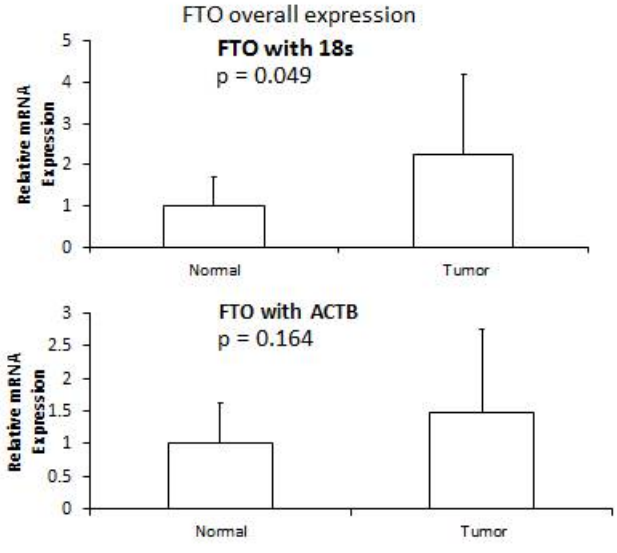

Conclusions: *FTO* gene expression is significantly greater in HCC than benign liver, but IHC showed increased nuclear staining in non-neoplastic liver compared to HCC limiting its usefulness as a predictive marker for potential targeted therapy. Further analysis may be helpful to determine whether there is any correlation of FTO protein expression with HCC etiology and prognosis.

1514 Histological Changes of Early Primary Sclerosing Cholangitis in Patients Undergoing Colon Resection for Inflammatory Bowel Disease

Manju Ambelil[1], Madhavi Rayapudi[2], Thomas Schiano[2], Maria Isabel Fiel[1]
[1]Icahn School of Medicine at Mount Sinai, New York, NY, [2]Mount Sinai Medical Center, New York, NY

Disclosures: Manju Ambelil: None; Madhavi Rayapudi: None; Thomas Schiano: None; Maria Isabel Fiel: None

Background: Primary sclerosing cholangitis (PSC) is present in a subgroup of patients with inflammatory bowel diseases (IBD) in both Crohn's disease (CD) and ulcerative colitis (UC). Definitive diagnosis of PSC is difficult on liver biopsy. We aimed to determine if changes suggestive of PSC may be incidentally found in these patients at the IBD surgery.

Design: After Institutional Review Board approval, liver biopsies (needle or wedge) were performed on IBD patients at the time of colorectal surgery (2011-2015) for either severe disease or presence of dysplasia. Demographic, clinical, type of IBD and baseline liver enzymes data was recorded. Liver biopsy slides were reviewed and detailed histologic features were scored for fibrosis (Ishak), grade of inflammation, bile duct damage and arterial wall thickening. Dilatation, luminal scalloping, atrophy, and cholangiocyte dropout were changes that defined bile duct damage.

Results: A total of 27 cases were analyzed, which include 22 (81%) UC and 5 (19%) CD, with 19 (70%) males and 8 (30%) females. Age at diagnosis of IBD ranged from 20-77 years. Baseline liver enzymes results of 25 patients were available, with mean ALT: 28.72 IU/L (r= 9 to 127), AST: 26.28 IU/L (r= 9 to 80), ALP: 126.6 IU/L (r= 53 to 419) and bilirubin: 0.53 mg/dL (r= 0.2 to 1.2). Bile duct damage was identified in 16 (59%) cases, portal inflammation in 10 (37%), portal and lobular inflammation in 1 (4%), and arterial wall thickening in 20 (74%) cases. A definitive diagnosis of PSC was made in 8 (30%) cases, with fibrosis ranging from stage 1 to 3; of these 6 were UC and 2 were CD. Among these 8 patients, 4 (50%) did not have a previous diagnosis of PSC and were considered as incidental. All 8 PSC cases showed bile duct damage (p=0.009) and 7 (88%) cases had arterial wall thickening. Analysis of severity of IBD and histologic findings revealed 13 of the 16 (81%) cases with bile duct damage had moderate to severe IBD (p=0.037); 17 of the 20 (85%) cases with arterial wall thickening also showed moderate to severe IBD at resection (p=0.049).

Conclusions: Our findings show that sub-clinical PSC may be present even in patients who were not suspected as having the disease. In addition, longer duration and severity of IBD are associated with significant histological changes in the liver such as arterial wall thickening and bile duct damage, even in the absence of significant clinical evidence and normal liver enzymes profile.

1515 High-Grade Intraductal Papillary Neoplasm as a Prognostic Marker in Intrahepatic Cholangiocarcinoma

Ahmed Bakhshwin[1], Sindhu Shetty[2], Haiyan Lu[3], Michael Cruise[2], Keith Lai[2]
[1]Robert J. Tomsich Pathology & Laboratory Medicine Institute, Cleveland Clinic, Pepper Pike, OH, [2]Cleveland Clinic, Cleveland, OH, [3]Cleveland Clinic, Beachwood, OH

Disclosures: Ahmed Bakhshwin: None; Sindhu Shetty: None; Haiyan Lu: None; Michael Cruise: None; Keith Lai: None

Background: Intrahepatic cholangiocarcinomas (ICCs) are associated with extremely poor survival and its incidence is increasing. Even in patients deemed candidates for curative resection, median survival was only 27 months in one large study. Previously, a periductal-type pattern of growth was thought to confer a poorer prognosis, and was an indication for T4 pathologic tumor staging. But recent studies do not support this, further highlighting the need for prognostic biomarkers in ICC. In this study, we examine the differences in clinical outcomes in ICC with and without an identifiable high-grade intraductal papillary neoplasm component. Intraductal papillary neoplasms of the intrahepatic bile duct (IPN) are lesions analogous to their pancreatic intraductal papillary mucinous neoplasm (IPMN) counterparts. However, less is known about IPN, rates of progression to carcinoma, and prognostic significance.

Design: Hepatic resection specimens with a diagnosis of ICC (2006-2018) were identified from the pathology archive. Slides were reviewed for the presence of an associated IPN with high-grade dysplasia. Clinical data including underlying hepatobiliary disease (such as viral hepatitis, PSC, and PBC), follow-up time and survival data were extracted from the electronic medical record. Categorical variables were analyzed using Person correlation and survival analysis with Kaplan Meier analysis.

Results: 43 hepatic resections for ICC were identified. There was a range of patient ages (mean: 60.5 years, range: 30-80 years) and a slight (53.5%) male predominance. Most patients (86%) did not have a clinical history of underlying liver disease. Three patients (7%) had viral hepatitis and 1 patient each had primary sclerosing cholangitis, autoimmune hepatitis and hemochromatosis, respectively. Clinical follow-up was available for 42 patients (mean: 47 months). IPN with high-grade dysplasia was identified in (28%) of ICC cases. Although the results do not achieve statistical significance, the presence of a high-grade IPN in ICC is associated with decreased survival at 1 year after initial diagnosis, at 3 years, and overall (Table 1, Figures 1 and 2).

		With high-grade IPN (N=12)	Without high-grade IPN (N=31)	*p*-value
Age (mean ± SD)		58.5 ± 11	61.6 ± 11.8	0.436*
Gender (% male)		58.3 %	51.6%	0.692#
Tumor differentiation (N, %)	Well	2 (17%)	5 (16%)	0.261@
	Moderate	9 (75%)	15 (48%)	
	Poor	1 (8%)	11(36%)	
Survival rate (N, %)	At 1 year	8 (66.7%)	26 (86%)	0.165®
	At 3 year	7 (58.3%)	25 (83%)	0.11®
	Overall	58.3%	74%	0.343®

*Student's T-test; # Chi-Square; @Fisher's exact test; ®Log-rank by Kaplan-Meier analysis

Figure 1 - 1515

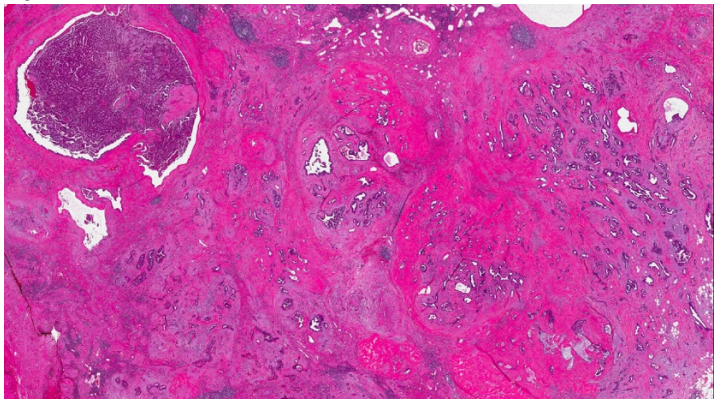

Figure 2 - 1515

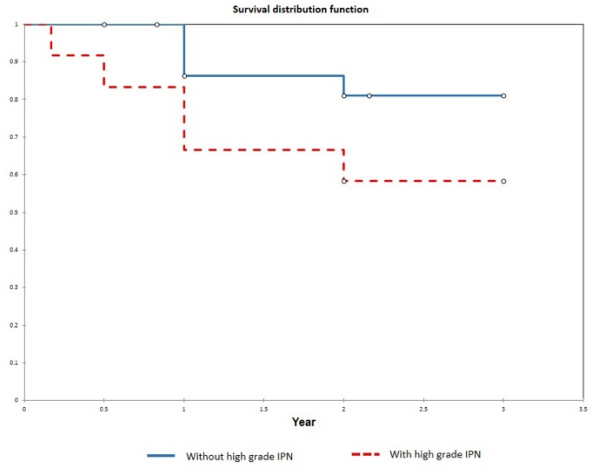

Conclusions: ICCs with an identifiable high-grade IPN component are associated with decreased survival. Although the results did not achieve statistical significance, further research into whether a high-grade intraductal component may represent an independent prognostic factor in ICC is warranted.

1516 Evaluation of HCC in Setting of Direct-Acting Antiviral Therapy

Dana Balitzer[1], Sarah Umetsu[1]
[1]*University of California, San Francisco, San Francisco, CA*

Disclosures: Dana Balitzer: None; Sarah Umetsu: None

Background: Hepatitis C virus (HCV) infection is a major cause of cirrhosis and hepatocellular carcinoma (HCC) in the United States. Direct-acting antiviral (DAA) therapies have achieved a higher rate of sustained virological response (SVR), as compared to previous treatment. The effect of treatment on HCC development is unclear, with some studies suggesting that HCC develops more frequently after DAA therapy. One proposed explanation is that interferon therapy has an immunomodulatory effect which is protective against HCC. No studies have specifically reviewed the pathology of HCC after DAA therapy.

Design: We reviewed resected cases of HCC at our institution (1995-2018) and identified patients with underlying HCV cirrhosis. Clinical data was reviewed including type of antiviral therapy, pre-resection therapy and patient demographics. Cases of entirely necrotic HCC were

excluded. We stratified these cases into patients who received therapy with DAA (n=20), traditional anti-viral therapies (n=10) and cases with untreated HCV (n=9). Pathology and staging of each case was reviewed. Immunohistochemistry for CD8 was performed on a subset of cases, and the average number of tumor-infiltrating lymphocytes (TILS) per HPF was quantified (average of 5 HPF at the center of each HCC).

Results: There was no difference in the age or gender of the patients. There was no difference in tumor size (5.1 cm vs. 3.5 cm, p= 0.15), stage greater than pT1 (70% vs 45%, p = 0.26), or multifocality (60% vs 45%, p = 0.7) in patients treated with traditional therapies versus DAA. HCC after traditional therapies had significantly more well-differentiated tumors compared to DAA therapy (80% vs. 20%, p = 0.004). There was no difference in CD8+ TIL between the therapeutic groups. Poorly differentiated HCC had significantly higher CD8+ TIL compared to well-differentiated HCC regardless of prior HCV therapy (average 54.2 versus 10.4 TIL per HPF, p =0.01)

Conclusions: A higher percentage of HCC cases after DAA showed moderately or poorly differentiated morphology compared to traditional therapies. The etiology for this finding is unclear, and may represent underlying biologic differences or selection of higher-grade tumors after complete tumor response in other patients, as necrotic HCC (which may represent complete tumor response) were excluded in this study. There was no difference in CD8+ TIL in the two groups. Further studies are needed to determine the impact of DAA-induced SVR on HCC development and recurrence.

1517 BRAF V600E and BAP1 immunohistochemistry aids in distinction between bile duct adenoma and intrahepatic cholangiocarcinoma

Dana Balitzer[1], Tara Saunders[1], Brent Molden[2], Sanjay Kakar[1], Ryan Gill[1]
[1]University of California, San Francisco, San Francisco, CA, [2]San Francisco, CA

Disclosures: Dana Balitzer: None; Tara Saunders: None; Brent Molden: None; Sanjay Kakar: None; Ryan Gill: None

Background: Bile duct adenomas may morphologically mimic adenocarcinoma and a variety of ancillary tests have been proposed to aid in distinction between bile duct adenoma and adenocarcinoma (either intrahepatic or metastatic). We aimed to assess sensitivity and specificity of BRAF V600E and BAP1 immunohistochemistry(IHC), as well as albumin in situ hybridization (ISH), in distinguishing bile duct adenoma from intrahepatic cholangiocarcinoma (ICC) in our center.

Design: 17 bile duct adenomas (5 resections, 12 biopsies) and 7 ICC resections were selected from our institution. IHC for BRAF V600E and BAP1 were performed on all samples, and we included additional BAP1 data from a prior study for comparison (19 ICC). Albumin ISH (RNAScope technology from ACD Bio) was performed on 9 cholangiocarcinomas and 12 bile duct adenomas. Staining in the lesion was graded as negative, focal (<25%), moderate (25-50%) or diffuse (>50%).

Results: BAP1 was retained by IHC in all cases of bile duct adenomas, but was lost in 27% of ICC (7 with absent BAP1 of 26 total ICC). BRAF V600E IHC was negative in all cases of ICC and was positive in 23.5% (4/17) of bile duct adenomas. Albumin ISH was diffusely positive in 17% of bile duct adenomas (2 of 12) and showed focal staining in 8% of cases (1 of 12), all of which were also positive for BRAF V600E. Albumin ISH showed focal staining in 100% (7/7 cases) of ICC. The size of BRAF V600E or Albumin ISH positive bile duct adenomas was not significantly different from the negative samples.

Conclusions: A subset of bile duct adenomas were positive for BRAF V600E (though less than previously reported, PMID: 26841202) while none of the ICC were positive, indicating low sensitivity and high specificity for a positive result in bile duct adenoma over ICC. BAP1 is lost in a minority of ICC, but none of the bile duct adenomas, indicating low sensitivity and high specificity for loss of staining in ICC over bile duct adenoma. Adding BAP1 and BRAF V600E IHC to the work up of atypical biliary lesions can aid in distinction between bile duct adenoma and intrahepatic cholangiocarcinoma. Albumin ISH stained only a minor subset of bile duct adenomas (we had notably fewer positive cases than a previous report, PMID: 26841202), but labeled all ICC; when positive, albumin ISH may be useful in excluding metastatic adenocarcinoma, but cannot be used to exclude ICC

1518 Bile Ductular and Portal Pathology in Fatty Liver Disease

Cynthia Behling[1], Cynthia Guy[2], Daniela Allende[3], Matthew Yeh[4], Oscar Cummings[5], Ryan Gill[6], Danielle Carpenter[7], Patricia Belt[8], Mark Van Natta, Melissa Contos[9], David Kleiner[10]
[1]Pacific Rim Pathology Group, San Diego, CA, [2]Chapel Hill, NC, [3]Cleveland Clinic, Avon Lake, OH, [4]University of Washington, Seattle, WA, [5]Indiana University School of Medicine, Indianapolis, IN, [6]University of California, San Francisco, San Francisco, CA, [7]St. Louis University School of Medicine, St. Louis, MO, [8]Johns Hopkins Bloomberg School of Public Health, Baltimore, MD, [9]VCU Health, Richmond, VA, [10]Rockville, MD

Disclosures: Cynthia Behling: *Consultant*, ICON; *Consultant*, Covance; Cynthia Guy: None; Daniela Allende: None; Oscar Cummings: *Consultant*, ICON / NovoNordisk; Ryan Gill: None; Patricia Belt: None; Melissa Contos: None; David Kleiner: None

Background: Steatosis, lobular inflammation and ballooning injury are typically identified in NAFLD. However, other histologic features may relate to disease progression and patient outcome. Studies of portal inflammation and ductular reaction have demonstrated associations with disease severity and natural history. We sought to develop more detailed histologic assessment of these features to correlate with clinical and other histologic features of NAFLD.

Design: From the NASHCRN database, 117 adult and 59 pediatric biopsies with complete clinical and laboratory data were selected to encompass a range of fibrosis from none to cirrhosis. Biopsies were scored 0 to 4 using pre-defined criteria for portal inflammation (PI), periportal inflammation (PI) and ductular reaction (DR). Demographic, clinical, laboratory and histologic features by PP,PI,DR categories were compared using chi-square tests for categorical measures and linear regression for continuous measures. A subset of 31 biopsies were rescored to estimate reproducibility using weighted Kappa statistic.

Results: The scores for PI,PP and DR were strongly associated ($p<0.0001$ for all pairs). In adults, the degree of PP and DR associated with age ($p=0.05$) but not gender, race or ethnicity. In children, PI and DR associated with age and PP. AST ($p=0.02$) and ALT ($p=0.05$) were only associated with PP in children. Alkaline phosphatase was associated with PP ($p=0.04$) and DR ($p=0.05$) in adults. Total bilirubin was only associated with DR in adults ($p=0.0005$). Adults with marked ductular reaction had higher fasting glucose ($p=0.02$) but no other associations with metabolic parameters. Pathology associations are reported in Table 1. Weighted kappa was 0.74 (PI, SE 0.15), 0.66 (PP, SE 0.16) and 0.70 (DR, SE 0.1).

Table 1. Association of portal inflammation and ductular reaction with other histologic components by adults and children

	Adults				Children			
		Mean (SE)				Mean (SE)		
	N	Fibrosis Stage (0-4)	Steatosis Score (0-3)	Ballooning Score (0-2)	N	Fibrosis Stage (0-4)	Steatosis Score (0-3)	Ballooning Score (0-2)
Portal Inflammation								
None	10	1.2 (1.1)	1.6 (0.7)	0.8 (0.9)	6	0.8 (0.8)	1.7 (1.0)	0.8 (0.4)
Minimal	38	1.8 (1.1)	2.0 (0.8)	1.3 (0.7)	19	1.7 (0.9)	2.1 (1.0)	1.0 (0.9)
Mild	39	2.6 (1.3)	1.6 (1.0)	1.1 (0.8)	24	2.0 (1.2)	2.2 (0.8)	1.1 (0.9)
Moderate to severe	30	2.5 (1.3)	1.6 (0.9)	1.3 (0.8)	10	2.0 (1.2)	1.7 (0.8)	1.1 (0.7)
P-value		0.001	0.29	0.21		0.09	0.40	0.86
Periportal Inflammation								
None	30	1.3 (1.1)	1.9 (0.8)	1.2 (0.8)	19	1.2 (0.9)	1.9 (1.0)	0.9 (0.7)
1-2 foci	40	2.3 (1.1)	1.8 (0.9)	1.3 (0.7)	20	1.8 (1.0)	2.0 (0.9)	1.3 (0.9)
3-5 foci	24	2.5 (1.4)	1.5 (1.0)	1.0 (0.9)	10	2.0 (1.2)	2.1 (0.9)	0.8 (0.6)
>1/3 interface	23	2.9 (1.2)	1.7 (0.9)	1.2 (0.8)	10	2.4 (1.2)	2.2 (0.8)	0.1 (0.9)
P-value		<0.0001	0.47	0.77		0.03	0.87	0.30
Ductular Reaction								
None	15	1.2 (1.0)	2.1 (0.8)	1.1 (0.9)	3	1.3 (0.6)	0.3 (0.6)	0.3 (0.6)
1-2 duct structures	53	1.7 (1.0)	2.0 (0.8)	1.2 (0.8)	34	1.4 (0.9)	2.1 (0.8)	1.2 (0.8)
3-5 duct structures	37	2.7 (1.3)	1.6 (0.9)	1.2 (0.7)	19	2.0 (1.1)	2.1 (0.9)	0.9 (0.8)
6+ duct structures	12	3.8 (0.4)	0.8 (0.7)	1.0 (0.9)	3	4.0 (0.0)	2.0 (1.0)	1.0 (1.0)
P-value		<0.0001	<0.0001	0.82		0.0003	0.008	0.31

Conclusions: Portal and periportal inflammation and ductular reaction correlated with fibrosis stage in both adults and children. The relative lack of consistent correlation of any of these features with other histological and clinical parameters typical of NAFLD leaves open the possibility that one or more of these proposed scales would have independent predictive value. The proposed scoring system for these features shows reproducibility. Systematic evaluation of portal disease in NASH may add benefit to existing scoring systems and provide additional insight into therapeutic response and clinical progression of disease.

1519 Chromatin Remodeling and DNA Repair in Intrahepatic Cholangiocarcinoma: A Possible Driver of Tumorigenesis

Margaret Black[1], George Jour[2], Matija Snuderl[3]
[1]NYU, Long Island City, NY, [2]NYU Langone Health, New York, NY, [3]New York University, New York, NY

Disclosures: Margaret Black: None; George Jour: None; Matija Snuderl: None

Background: Intrahepatic cholangiocarcinoma (IHCC), the second most common primary liver cancer, has poor survival and a poor response to standard chemotherapy. Molecular mechanisms underlying tumorigenesis are poorly understood, with some reports of IDH1/2, *KRAS* mutations, and *FGFR2* translocations. Herein, we investigate the molecular landscape of IHCC in a single tertiary care center.

Design: Twelve cases were selected. DNA was extracted from FFPE after selection of areas with highest tumor content. Matched tumor and normal tissue were analyzed using our customized panel targeting 580 exomes in cancer related genes for single nucleotide variation (SNV), insertions/deletions (InDels), copy number variation (CNV), and tumor mutational burden (TMB) using our clinically validated pipeline.

Results: All of the tested samples showed a strikingly low TMB (range, 0.05 – 1.75 mutations per megabase). *FLT4*, *ATM*, *NUP98*, *LCG1*, and *SYNE1* were among the most commonly mutated genes and were altered by SNV or indels in up to 33% of the tested cases. Mutually exclusive *IHD1* R132C mutation and *BRAF* V600E mutation were identified in two separate cases. *Her2/ERBB2* amplification (copy number = 32) was identified in one case with low tumor mutational burden.

Figure 1 - 1519

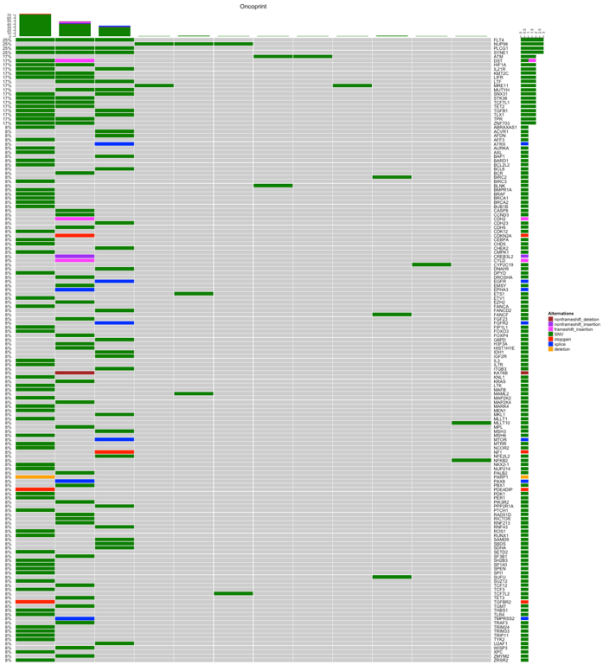

Conclusions: Our data suggests that IHCC is a cold tumor with low TMB. Chromatin remodeling and DNA repair genes are the most commonly implicated pathways as drivers in IHCC tumorigenesis. Targetable events in MAPK and Kinase (BRAF/HER2) pathways with currently available FDA approved drugs have a low frequency in IHCC. The low TMB suggest that epigenetic events may be implicated and may contribute to tumor development. Further epigenetic studies are warranted.

1520 LFABP-Negative Hepatocellular Adenoma: Spectrum of Morphologic and Molecular Characteristics with Emphasis on Atypical Features

Annika Blank[1], Nancy Joseph[1], Ryan Gill[1], Sanjay Kakar[1]
[1]*University of California, San Francisco, San Francisco, CA*

Disclosures: Annika Blank: None; Nancy Joseph: None; Ryan Gill: None; Sanjay Kakar: None

Background: Loss of liver fatty acid binding protein (LFABP) by immunohistochemistry is used for diagnosis of hepatocyte nuclear factor (HNF)1?-mutated hepatocellular adenoma (H-HCA). H-HCA typically show steatosis and no cytoarchitectural atypia. Tumors with LFABP loss can show variant and atypical features, and LFABP loss can occur in HCC (PMID:26997447).

Design: Morphology, reticulin and glutamine synthetase (GS) staining were assessed in 24 LFABP-negative tumors and categorized as H-HCA (n=13, no atypical features) and atypical hepatocellular neoplasms (AHN, n=9). Cases were considered atypical (AHN) when the following were present: cytoarchitectural atypia (involving 20x field or more), reticulin loss/fragmentation in non-fatty areas and/or diffuse GS. Additionally, there were 2 cases of HCC arising in H-HCA. Overt hepatocellular carcinoma (HCC) cases without HCA component were excluded. Reticulin loss/fragmentation and 'packeting' (nests of tumor cells completely wrapped by reticulin) was recorded as present when involving at least a 20x field. Capture-based next generation sequencing (NGS) targeting 510 cancer genes and copy number alterations (CNA) were evaluated in 6 AHNs.

Results: Majority of H-HCA occurred in women >50 years (Table). Variant features in H-HCA included peliosis and no fat (16%), reticulin 'packeting' (46%) and reticulin loss in fatty area (62%). In 9 AHNs, atypia was due to prominent pseudoacini (n=3), reticulin loss in non-fatty area (n=3) and diffuse GS (n=3). H-HCA portion of 2 cases with associated HCC (50/F, 55/F) did not show atypical features (both H-HCA and HCC were LFABP-negative). NGS was done in 6 AHN (3 with prominent pseudoacini, 3 with diffuse GS). *HNF1A* mutations were present in all 3 AHN with prominent pseudoacini and 2 with diffuse GS (both lacked *CTTNB1* mutation). *CTTNB1* mutation without *HNF1A* mutations was seen in 1 case with diffuse GS (Table).

	Typical H-HCA (n=13)	**LFABP-negative AHNs** (n=9)
Age >50 years	8 (62%)	0
Women	13 (100%)	5 (56%)
Fat	9 (69%)	2 (22%)
>50%	2 (15%)	1 (11%)
5-50%	2 (16%)	5 (67%)
0-5%		
Peliosis	2 (16%)	0
Reticulin stain	6 (46%)	5 (56%)
'Packeting'	8 (62%)	3 (33%)
Loss in fatty area	0	3 (33%)
Loss in non-fatty area		
Prominent pseudoacini	0	3 (33%)
Diffuse GS staining	0	3 (33%)
NGS (6 LFABP-negative AHNs)		
	Prominent pseudoacini (n=3)	Diffuse GS staining (n=3)
HNF1A Mutations	3	2
CTNNB1 Mutation	0	1
Copy number alterations	0	1 (8q gain)
Gains	1 (8p,12p)	0
Losses		

Conclusions: H-HCA most often occurs in older women and can show variant features such as lack of fat and peliosis. Reticulin 'packeting' and loss in fatty areas is common and should not be mistaken for HCC. LFABP-negative AHN occurs in both genders, and may show prominent pseudoacini, reticulin loss in non-fatty areas and/or diffuse GS. Rare cases of HCC can arise in H-HCA. Most AHN with LFABP loss including those with diffuse GS show *HNF1A* mutation. *HNF1A* mutation and *CTNNB1* mutation did not occur together in any case. The reason for diffuse GS in 2 cases without *CTNNB1* mutation is not clear.

1521 Development of a Tumor Regression Grading Score for Hepatocellular Carcinoma Recurrence Following Transarterial Chemoembolization

Adam Booth[1], Judy Trieu[1], Omar A. Saldarriaga[1], Heather Stevenson-Lerner[1]
[1]*University of Texas Medical Branch, Galveston, TX*

Disclosures: Adam Booth: None; Judy Trieu: None; Omar A. Saldarriaga: None; Heather Stevenson-Lerner: None

Background: Hepatocellular carcinoma is the 3rd most common cancer-related death in the world and 7th in the US. Transcatheter arterial chemoembolization (TACE) may increase survival by preventing hepatocellular carcinoma (HCC) progression or by downstaging tumors while patients await liver transplant. At this time, a histologic tumor regression grading (TRG) system that evaluates treatment responses to TACE on HCC progression/recurrence does not exist. The main goal of this study was to develop a standardized HCC TRG (HTRG) scoring system that would facilitate assessment of TACE-related treatment responses in hepatectomy and resections. The score will then be correlated with clinical outcomes.

Design: We retrospectively reviewed livers explanted from 2010-2018 and eligibility criteria included patients who received TACE at least once prior to transplantation. Demographic/clinical data were obtained. Based on scoring systems used for colorectal liver metastasis, we developed an HTRG scoring system to assess the percentage of viable tumor vs necrosis in the HCC nodules (Figure 1). Histopathologic findings included fibrous capsular breach, percent viable tumor versus tumor necrosis, and +/- microscopic lymphovascular invasion. A non-TACE control group was evaluated for comparison.

Results: Seventy-nine explanted livers were reviewed and 27 cases met criteria; 36 total nodules were evaluated. Twenty-four patients were male with an average age of 58.5. Hepatitis C infection was the etiology of HCC in 22 cases and fatty liver disease in 5. Average listing model for end-stage liver disease (MELD) for liver transplantation was 23.4. Comparison of TACE and non-TACE outcomes for recurrent HCC was not statistically significant (p=0.131), with only one and three patients with recurrence in each group, respectively. Follow-up time was statistically significant between groups (p=0.013), TACE 26.7 months vs control 58.1 months. Histologically, 19 of 36 nodules demonstrated capsular breach, 9 of 36 microscopic lymphovascular invasion, and 5 of 36 clear cell change. Mean viable tumor was 27.7% in the TACE group vs 65.0% in the control group.

Figure 1 - 1521

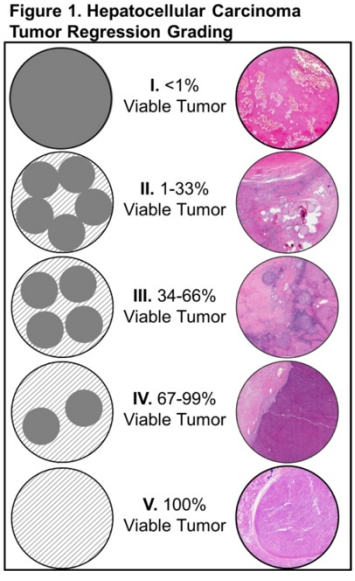

Conclusions: The HTRG score facilitated assessment of treatment responses. Preliminary outcome data suggests lower rates of recurrence in TACE groups. A larger cohort is necessary to increase the power of our study. Use of the HTRG system will increase consistency in pathology reporting and synoptic data, which then can be correlated with clinical outcomes in larger studies.

1522 Albumin RNA in situ hybridization as a marker of neoplasms of hepatic origin

Diane Brackett[1], Martin Taylor[2], Lawrence Zukerberg[3], Anthony Mattia[4], Lipika Goyal[2], Andrew Zhu[5], Vikram Deshpande[5]
[1]Massachusetts General Hospital, East Sandwich, MA, [2]Boston, MA, [3]Auburndale, MA, [4]Newton-Wellesley Hospital, Sudbury, MA, [5]Massachusetts General Hospital, Boston, MA

Disclosures: Diane Brackett: None; Martin Taylor: None; Lawrence Zukerberg: None; Anthony Mattia: None; Lipika Goyal: None; Vikram Deshpande: *Grant or Research Support*, ACD

Background: Distinguishing intrahepatic cholangiocarcinoma (ICC) from metastatic adenocarcinoma represents a major diagnostic challenge. It has recently been shown that albumin RNA in situ hybridization (ISH) is a sensitive and specific marker in resected ICCs. In this study, we assessed the accuracy of albumin RNA ISH performed on formalin-fixed paraffin-embedded tissue in a cohort of tumors of uncertain origin, comparing the results with clinical, immunohistochemical, and molecular data.

Design: A pathology database was used to identify 120 patient samples of primary and metastatic lesions in which albumin RNA ISH had been performed clinically, as part of the diagnostic workup. Cases with no clinical history or followup were excluded. 7 cases remained unclassifiable with respect to primary site and were excluded. Targeted tumor sequencing was performed in 55% of cases. Immunohistochemistry for arginase 1 and glypican 3 was performed in selected cases.

Results: Approximately 75% of all specimens were directly sampled from the liver vs. an extrahepatic site. 88% of ICCs (46 of 52) and 96% of HCCs (23 of 24) were positive for albumin RNA ISH, whereas only one case of extrahepatic cholangiocarcinoma was positive **(Table 1)**. Overall, 48% of HCCs were evaluated as high grade or poorly differentiated (11 cases). None of the cases determined to be metastatic (i.e. nonhepatic) malignancies were positive for albumin RNA ISH; the most common primary sites were pancreas (n = 11) and lung (n = 11). The specificity and sensitivity of albumin RNA ISH for neoplasms of hepatic origin is 91% and 98%, respectively. Targetable genetic alterations (*IDH* mutations and *FGFR2* fusions) were identified in 31% of ICCs (10 of 32 cases). *TERT* mutations were identified in 92% of HCCs (11 of 12 cases).

Table 1.

Classification	Total no. of cases	Tissue site		Biopsies		Resections		Albumin RNA ISH	Molecular Studies Performed		Most common molecular alterations (n)
		Liver (n)	Extrahepatic (n)	(n)	%	(n)	%		(n)	%	
Albumin-positive ICC	46	42	4	41	89%	5	11%	Pos: all	29	57%*	*TP53* (7) *TERT* (1) *IDH1* (5) *FGFR2* (5) *KRAS* (4)
Albumin-negative ICC	6	4	2	5	83%	1	17%	Neg: all	3	50%	n/a (each mutation occurred only once)
HCC	24	15	9	24	100%	0	0%	Pos: 23 Neg: 1	12	55%*	*TERT* (11)
ECC	7	4 **	2**	4	57%	3	43%	Pos: 1 Neg: 6	4	57%	*SMAD4* (3) *KRAS* (2) *TP53* (2)
Nonhepatic carcinomas	37	25	12	34	92%	3	8%	Neg: all	n/a	n/a	n/a
Total	120	90	29	110	88%	13	10%		48	55%	

*Excludes instances of multiple cases from the same patient.

**One case included tissue from both intrahepatic and extrahepatic sites.

Conclusions: Albumin RNA ISH is highly sensitive and specific for distinguishing an intrahepatic primary from a metastatic carcinoma. It is also a sensitive test for poorly differentiated HCC. Given the high prevalence of targetable mutations in ICC, albumin RNA ISH is an integral component in the workup of tumors of uncertain origin, and can be used to prompt appropriate molecular testing and targeted therapy for *IDH* and *FGFR2* alterations.

1523 Peritumroal expression of PSMA as a diagnostic marker in Hepatocellular Carcinoma

Wei Chen[1], Amad Awadallah[1], Wei Xin[2]
[1]*University Hospitals Cleveland Medical Center, Cleveland, OH,* [2]*Case Western Reserve University, Cleveland, OH*

Disclosures: Wei Chen: None; Amad Awadallah: None; Wei Xin: None

Background: Recently radiologists have found that radio-labeled prostate-specific membrane antigen (PSMA), previously used as an imaging tracer for prostate cancer evaluation, could help distinguish hepatocellular carcinoma (HCC) from benign adenoma and cirrhotic nodules on PET-CT. In this report, we would like to study whether immunohistochemical stain of PSMA could differentiate HCC from benign lesions.

Design: Formalin-fixed paraffin-embedded blocks of liver tumors were retrieved. In total, 22 cases of HCC and 5 hepatic adenomas were selected. Immunostains of PSMA were performed by our hospital diagnostic immunohistochemical lab. Clinical information and histological features, including viral infection, background cirrhosis and steatosis, were analyzed as well.

Results: Mean age was 60.5 years (ranging from 35-89 years) with a male-to-female ratio of 1.5:1. PSMA was not expressed in any normal liver tissue nor in non-neoplastic cirrhosis. PSMA expression were identified in peritumoral neo-vessels in 68.1% (15/22) of HCC cases, and none of the adenomas show similar expression patterns. Among the HCCs, 10 had cirrhotic background and 12 HCCs arose from non-cirrhotic liver. PMSA peritumoral vascular expression was significantly more common in HCC with cirrhosis (9/10, 90.0%) than in non-cirrhotic HCC (6/12, 50%)($p<0.05$), see Table 1. Further analysis showed that in 15 PSMA positive cases 11 (11/15, 73.3%) had Hepatitis C or Hepatitis B infection, significantly higher than the non-viral infected cohort (4/15, 26.7%) ($p=0.03$), suggesting a possible relationship between virus-induced cirrhosis and PSMA neovascular expression in HCC. PSMA was absent in all the adenoma cases (0/5, 0.0%), which was expected for benign lesions. No tumor cell positivity is identified in our study.

Table 1. PSMA neovascular expression in primary liver tumors.

	HCC		Adenoma
	Cirrhotic	Non-Cirrhotic	
PSMA			
Positive	9(90.0%)*	6(50.0%)	0(0.0%)
Negative	1(10.0%)	6(50.0%)	5(100.0%)

*$p<0.05$, compared to non-cirrhotic HCCs.

Conclusions: Similar to findings by radiologists, some HCCs can induce PSMA expression on the peritumoral vessels, especially in HCCs developed from viral hepatitis with cirrhosis. PMSA can thus be used as an important ancillary marker to help differentiate HCCs from cirrhotic nodules in morphologically challenging cases. Whether PSMA plays any role in HCC carcinogenesis may need further investigation.

1524 An Assessment of the Heterogeneous Expression of Glypican-3 (GPC3) in Hepatocellular Carcinoma (HCC) in the Era of GPC3 as a Biomarker

Brian Cox[1], Kevin Waters[1], Deepti Dhall[1], Brent Larson[1], Maha Guindi[2]
[1]*Cedars-Sinai Medical Center, Los Angeles, CA,* [2]*Cedars-Sinai Medical Center, Beverly Hills, CA*

Disclosures: Brian Cox: None; Kevin Waters: None; Deepti Dhall: None; Brent Larson: None; Maha Guindi: None

Background: GPC3 plays an important role in cell growth, differentiation, and migration. To date, its main use is for HCC diagnosis. Recently, utilization of GPC3 as a biomarker for targeted therapy is being studied using a monoclonal antibody that targets GPC3, and bi-specific monoclonal antibodies (BiTES) that direct T-cells against cancer cells. Heterogeneous GPC3 staining in HCC has been observed, but not systematically studied. Given that new GPC3 targeted agents bind to the tumor cell surface, we systematically evaluated the heterogeneity of GPC3 expression, which may potentially impact response to therapy.

Design: From 2012-2017, a total of 47 untreated moderate and poorly differentiated HCC in resections/explants (r/e) (N=28) and biopsies (N=19) were retrospectively identified for analysis. HCC patterns and Edmondson-Steiner nuclear grade were determined for each case. Immunostaining for GPC3 (GC33, Ventana, Roche Diagnostics) was performed. GPC3 membranous and cytoplasmic staining was

each scored in terms of its staining pattern, percentage, and overall intensity (Table 1). GPC3 staining was considered heterogeneous if it differed by two or more overall score points within the same tumor. An independent samples T-test was utilized to determine differences in heterogeneity between r/e and biopsies.

Results: 96% (N=27/28) of r/e specimens and 79% (N=15/19) of biopsies expressed either cytoplasmic or membranous GPC3. Similarly, cytoplasmic staining was seen in 96% of r/e specimens and 79% of biopsies. Membranous staining was less prevalent: 57% of r/e and 47% of biopsies. Combined staining was seen in 43% of r/e and 47% of biopsies. Heterogeneity of GPC3 staining was seen in 46% r/e but only 16% of biopsies (p=0.03). GPC3 heterogeneity within a given HCC pattern was 46% in r/e specimens versus 0.5% in biopsies (p<0.01). Heterogeneity of staining between tumor patterns within the same specimen was 21% in r/e specimens and 0% of biopsies (p=0.03).

Membranous Staining		Cytoplasmic Staining	Overall Score
<10%; 0+	and	<10%; 1-3+	0
<10%; 1-3+	and/or	10-50%; 1-3+	1
≥10%; 1-2+ <10%; 3+	+/-	10-50%; 1-3+	2
≥10%; 3+	or	≥50%; 3+	3

Conclusions: GPC3 staining is heterogeneous in nearly 50% of r/e HCC specimens. GPC3 heterogeneity is encountered significantly less often in biopsies, which may be due to sampling effect. When compared to cytoplasmic staining, membranous staining is less prevalent and is often patchy or focal. GPC3 heterogeneity [and/or lack of membranous localization?] could explain the lack of a significant clinical response in a previous monoclonal antibody study. This could potentially impact HCC response to the investigational monoclonal antibody or BiTE.

1525 Hepatic Disease in CVID is Characterized by a Combination of Sinusoidal Fibrosis and Nodular Regenerative Hyperplasia

Rory Crotty[1], Lawrence Zukerberg[2], Anthony Mattia[3], Martin Taylor[4], Jocelyn Farmer[1], Vikram Deshpande[1]
[1]Massachusetts General Hospital, Boston, MA, [2]Auburndale, MA, [3]Newton-Wellesley Hospital, Sudbury, MA, [4]Boston, MA

Disclosures: Rory Crotty: None; Lawrence Zukerberg: None; Anthony Mattia: None; Martin Taylor: None; Vikram Deshpande: None

Background: Common variable immunodeficiency (CVID) is an immunodeficiency syndrome of heterogeneous etiology, characterized by failure of B-cell maturation and deficient immunoglobulin production. CVID can be associated with distinct histologic patterns of organ involvement. CVID involving the liver is a known phenomenon, but the histologic characteristics are not well described in the literature.

Design: We identified six liver biopsies taken between 2013 and 2018 at our institution. These biopsies came from five patients with known CVID. Histologic slides were reviewed, and pathologic and clinical features were evaluated for each case.

Results: ALT, AST, and alkaline phosphatase levels were elevated in one, five, and five of six cases, respectively, with median values of 37 U/L (normal 10-55 U/L), 54 U/L (10-40 U/L), and 193 U/L (45-115 U/L). Three of the five patients had biopsies demonstrating CVID involvement of other organs, of which two were granulomatous-lymphocytic interstitial lung disease and one was CVID enteritis.

All liver biopsies of CVID demonstrated a distinct pattern of predominantly centrizonal sinusoidal fibrosis, with panlobular involvement in four of six cases (67%). A nodular regenerative hyperplasia (NRH)-like pattern of nodularity was present in all cases. Bridging fibrosis and cirrhosis were not identified in any case.

Portal hepatitis was present in all six cases (5 with mild inflammation, and 1 with moderate inflammation). Lobular hepatitis was also identified in all cases (5 mild, 1 moderate). Lymphocyte trafficking was identified in five of six cases (83%). Plasma cells were not identified in any biopsy. Additional findings included granulomatous or giant cell inflammation, identified in four biopsies (67%). Two of six cases also demonstrated focal copper deposition.

Conclusions: Hepatic disease in CVID is commonly associated with mild elevations in AST and alkaline phosphatase and histologically demonstrates a distinctive pattern of involvement on liver biopsies, characterized by a combination of sinusoidal fibrosis, NRH-like changes, lymphocyte trafficking, absence of plasma cells, and mild lobular lymphocytic infiltrates.

1526 Progressive Familial Intrahepatic Cholestasis- An Inexpensive DNA mass Spectrometry Based Study To Predict The Disease In The Offsprings

Ashim Das[1], Suvradeep Mitra[2], Aditi Sharma[1], Arnab Pal[2], Sadhna Lal[2]
[1]PGIMER, Chandigarh, India, [2]Postgraduate Institute of Medical Education & Research, Chandigarh, India

Disclosures: Ashim Das: None; Suvradeep Mitra: None; Aditi Sharma: None; Arnab Pal: None; Sadhna Lal: None

Background: Progressive familial intrahepatic cholestasis, a type of infantile cholestasis syndrome, is a complex disorder on clinico-biochemically and also histologically. Several types of progressive familial cholestasis exist including PFIC I to IV. PFIC II is the most common form. A detailed molecular characterisation can be achieved only by next generation sequencing which is expensive. A new method by DNA mass spectrometry can identify already known mutations and is relatively inexpensive. Hence, we tried to evaluate the molecular diagnosis of PFIC by using DNA mass Spectrometry in predicting the disease in offsprings.

Design: A total of 41 families (102 DNA samples from 2 ml of EDTA blood) of infantile cholestasis syndrome was selected and includes progressive familial intrahepatic cholestasis, congenital hepatic fibrosis, Extrahepatic biliary atresia, paucity of intrahepatic bile ducts, bile acid synthetic defects and one autopsy case of cystic fibrosis with clinical features of infantile cholestasis. The two loci of PFIC II gene i.e c.1772A>G (p.Asn591Ser) and c.1331T>C (p.Val444Ala) and two loci of PFIC III gene c.523A>G (p.Thr175Ala) and c.1954A>G (p.Arg652Gly) were studied by DNA mass spectrometry to identify mutations and heterozygous status.

Results: Two cases showed mutations at the first locus of PFIC II gene i.e c.1772A>G (p.Asn591Ser). Out of these, one case showed mutations even in both parents in the same locus; but the second case showed double heterozygous status in the mother but the father showed mutation in the other locus c.1331T>C (p.Val444Ala). On the other hand, twent nine samples (14 cases of PFIC and 15 family members) showed mutations at the second locus c.1331T>C (p.Val444Ala). Out of these, two showed mutation in both parents.

None of the cases showed mutation in the gene of PFIC III locus c.523A>G (p.Thr175Ala) but one case showed mutations at the PFIC III gene locus c.1954A>G (p.Arg652Gly) with the heterozygous parents. One child showed hetergyzous mutation at the PFIC III gene locus c.1954A>G (p.Arg652Gly) but one family member showed mutation in the same locus of PFIC III gene.

2	CASE	5_Sample no	C	A	MT/WT
	MOTHER	6_G2MPEIC05	T	G	WT/MT
	FATHER	7_G2MPEIC06	CT	GA	HET/HET
3	CASE	44_G2MPEIC43	T	G	WT/MT
	FATHER	45_G2MPEIC44	T	G	WT/MT
	MOTHER	46_G2MPEIC45	T	GA	WT/HET
4	CASE	47_G2MPEIC46	T	G	WT/MT
	FATHER	48_G2MPEIC47	T	G	WT/MT
	MOTHER	49_G2MPEIC48	T	GA	WT/HET
5	CASE	50_G2MPEIC49	T	G	WT/MT
	FATHER	51_G2MPEIC50	T	G	WT/MT
	MOTHER	52_G2MPEIC51	T	GA	WT/HET
6	CASE	53_G2MPEIC52	T	G	WT/MT
	FATHER	54_G2MPEIC53	T	G	WT/MT
	MOTHER	55_G2MPEIC54	T	G	WT/MT
7	MOTHER	66_G2MPEIC65	T	G	WT/MT
	FATHER	67_G2MPEIC66	T	GA	WT/HET
	CASE	68_G2MPEIC67	T	G	WT/MT
8	CASE	70_G2MPEIC69	T	G	WT/MT
	FATHER	71_G2MPEIC70	T	G	WT/MT
	MOTHER	72_G2MPEIC71	T	GA	WT/HET
9	CASE	91_G2MPECI_90	T	G	WT/MT
	FATHER	92_G2MPECI_91	T	G	WT/MT
	MOTHER	93_G2MPECI_92	T	G	WT/MT
10	CASE	99_G2MPECI_98	T	G	WT/MT
	FATHER	100G2MPECI_99	T	GA	WT/HET
	MOTHER	101G2MPECI_100	T	G	WT/MT

Figure 1 - 1526

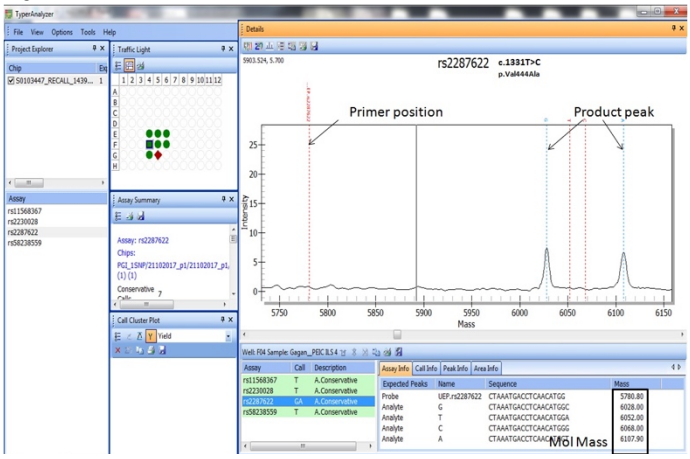

Figure 2 - 1526

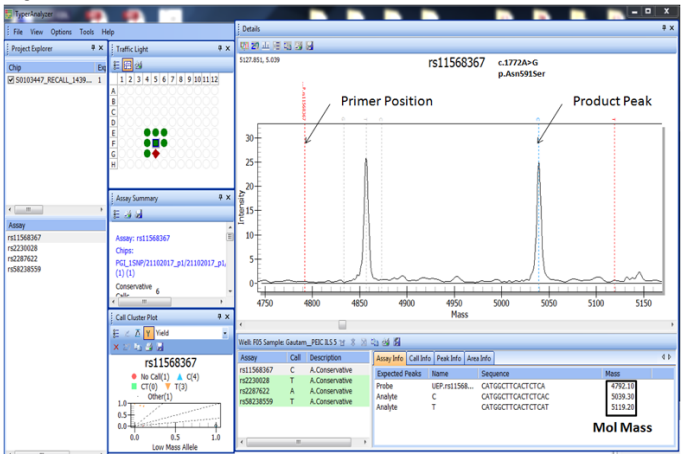

Conclusions: PFIC is extremely heterogeneous disease. A complete molecular study is required for its characterization. An inexpensive method like DNA mass spectrometry may help as NGS is extremely expensive. A prenatal check up for the parents can help us in predicting this disease in the offspring

1527 A comparative study of PD-L1 immunohistochemistry assays for primary liver cancer

Min Du[1], Wujian Zhang[2], Yumeng Cai[3], Bo Wei[2], Zhuyue Si[2], Xi Zhang[2], Lixing Li[2], Lingtong Hao[2], Yuan Ji[3], Shaoping Ling[2]
[1]Hua Dong Hospital, Fudan University, Shanghai, China, [2]Genowis.Inc, Beijing, China, [3]Zhongshan Hospital of Fudan University, Shanghai, China

Disclosures: Min Du: None; Wujian Zhang: None; Yumeng Cai: None; Bo Wei: None; Zhuyue Si: None; Xi Zhang: None; Lixing Li: None; Lingtong Hao: None; Yuan Ji: None; Shaoping Ling: None

Background: Due to the importance of PD-L1 expression quantification in terms of using checkpoint inhibitor drugs, several PD-L1 IHC assays have been approved by FDA accompanied with corresponding drugs. However, PD-L1 expression quantification in primary liver cancer hasn't been standardized, and the consistency of these assays in primary liver cancer is also not well studied. This study particularly focused on primary liver cancer (mainly hepatocellular carcinoma (HCC), and intrahepatic cholangiocarcinoma (ICC) patients), aiming to reveal the performance of each assay in primary liver cancer.

Design: 142 surgically resected tumor tissue samples, including HCC, ICC, were collected from Zhongshan hospital, Fudan University, ShangHai, China. All clinical data were approved by ethical commitment, and the informed consent was obtained from patients. Three types of anti-PD-L1 antibodies (SP142, 28-8, E1L3N) were considered in this study. The agreement of three antibodies in both tumor and immune cells were compared. A 1% and a 5% cutoffs of PD-L1 expression were selected to show the concordance of three reagents in tumor cells. The association of PD-L1 expression with recurrence was investigated.

Results: The results show that [SP142] stains higher percent of both tumor and immune cells, while [28-8] and [E1L3N] behave concordance. The results from pairwise comparisons show that [SP142] stains higher percent of tumor cells than [28-8] and [E1L3N], and stains higher percent of immune cells than [28-8] (Fig 1b). The concordance analysis of three reagents based on two cutoffs (1% and 5%) reveals that total 105 (73.9%) samples show concordance across 3 reagents (Fig 1c). Furthermore, higher expression of [SP142] in tumor cells and higher expression of [E1L3N] in immune cells are associated with longer survival ($p<0.05$) (Fig. 2).

Table 1. Number of Cases used in each figure 4 group

Tumor cells (N = 68)						
Reagent	SP142		28-8		E1L3N	
PD-L1	<= 5%	>5%	<= 5%	>5%	<= 5%	>5%
Number of Cases	56	12	62	6	59	9
Immune cells (N = 68)						
Reagent	SP142		28-8		E1L3N	
PD-L1	<= 5%	>5%	<= 5%	>5%	<= 5%	>5%
Number of Cases	35	33	51	17	37	31

Figure 1 - 1527

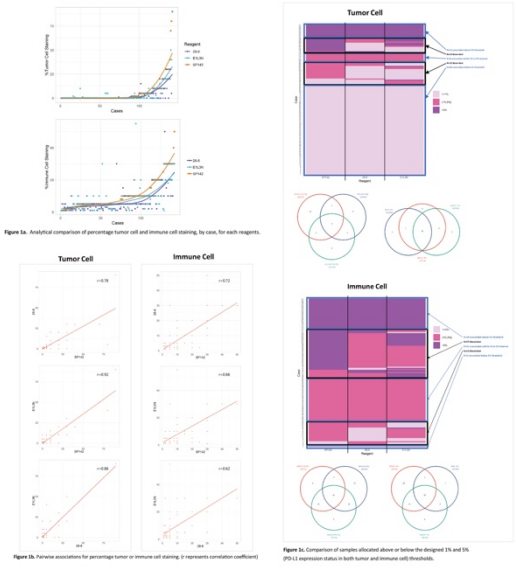

Figure 2 - 1527

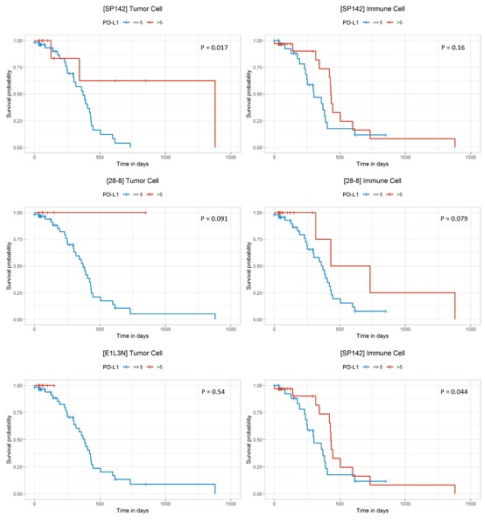

Figure 2. Recurrence free survival (RFS) analysis by comparing high (>5%) and low(<=5%) PD-L1 expression levels.

Conclusions: We conclude that [SP142] is a stronger PD-L1 staining reagent than [28-8] and [E1L3N] in both tumor and immune cells, while [28-8] and [E1L3N] behave almost the same in tumor cells. Since both concordance and discordance exist across all three types of reagents, a unique, specialized cutoff is needed for each reagent. Moreover, higher expression of [SP142] in tumor cells and [E1L3N] in immune cells might be indicators of better survival. Although the RFS curves are not significantly differentiated in both [28-8] and [E1L3N] stained tumor cell region, all the cases with high PD-L1 expression have no recurrence during the observation period.

1528 Evaluation of Clinicopathologic Presentation and Outcomes in Parenchymal Rejection Versus Acute Cellular Rejection in Liver Transplant Biopsies

Daffolyn Rachael Fels Elliott[1], Mehdi Tavakol[1], Bilal Hameed[1], Linda Ferrell[1], Sanjay Kakar[1], Ryan Gill[1]
[1]University of California, San Francisco, San Francisco, CA

Disclosures: Daffolyn Rachael Fels Elliott: None; Mehdi Tavakol: None; Bilal Hameed: None; Linda Ferrell: None; Sanjay Kakar: None; Ryan Gill: None

Background: Parenchymal rejection (PR) may occur in isolation or in combination with acute cellular rejection (ACR). The aim of this study was to evaluate clinicopathologic features and outcomes in PR cases and compare to cases of ACR.

Design: PR and ACR cases were identified by a database search (1990-2017). PR was defined as centrizonal lymphocyte predominant inflammation and hepatocellular necrosis, with or without portal features of mild to moderate ACR. Immunohistochemistry for C4d was performed on a subset of PR and ACR cases.

Results: 173 biopsies were evaluated, including 49 isolated PR (iPR), 35 combined PR and mild to moderate ACR (PR/ACR), 34 mild ACR, 52 moderate ACR and 3 atypical rejection (plasma cell hepatitis pattern) cases. The median time from transplant was longer for iPR (1175 days, p<.01) compared to PR/ACR (270 days), mild ACR (21 days), and moderate ACR cases (69 days). iPR patients were younger at time of biopsy (p<.01) and transplant (p<.01). Compared to mild ACR, PR/ACR showed increased AST (p<.01) and ALT (p=.03), similar to moderate ACR (AST p=.04, ALT p=.03). There was no significant difference with respect to mild ACR and iPR. Within 7 days after biopsy AST and ALT decreased in all groups, indicating a response to therapy; the response was most pronounced for PR/ACR (AST and ALT p<.01) and iPR (AST p<.01) in comparison to mild ACR. One iPR case and one moderate ACR case showed strong C4d staining of venules (DSA testing not performed). Future ACR episodes developed in 2/49 (4%) iPR cases compared to 8/35 (23%) PR/ACR, 7/34 (21%) mild ACR, and 13/52 (25%) moderate ACR cases (p=.03). There were no significant differences for future episodes of PR, chronic rejection, centrizonal fibrosis, re-transplant, or death.

Conclusions: PR represents a form of lobular injury that is associated with delayed onset after transplant and may affect younger patients. iPR cases show elevations in liver enzymes similar to mild ACR, and are less likely to have future episodes of ACR. PR/ACR cases show overlap in clinicopathologic features with iPR and moderate ACR. C4d immunostaining does not aid in diagnosis of PR. We recommend separate reporting of portal-based and parenchymal rejection. Standardization of terminology for parenchymal forms of rejection can facilitate appropriate management decisions.

1529 Determination of Donor Versus Native Origin of Hepatocellular Carcinoma Occurring in Liver Transplants Originally Transplanted with Hepatocellular Carcinoma using Short Tandem Repeat (STR) Analysis

Kurt Fisher[1], James Wisecarver[2], Fedja Rochling[1], Marco Olivera[1], Jennifer Sanmann[1], Pamela Althof[1]
[1]University of Nebraska Medical Center, Omaha, NE, [2]Omaha, NE

Disclosures: Kurt Fisher: None; James Wisecarver: None; Fedja Rochling: None; Marco Olivera: None; Jennifer Sanmann: None; Pamela Althof: None

Background: Orthotopic liver transplantation (OLT) is an effective therapeutic option for patients with cirrhosis and hepatocellular carcinoma (HCC). However, recurrent HCC occurs in 3.5%-21% of OLT and can recur within a few months or as late as 10+ years after the transplant. Case reports have shown that HCC can arise *de novo* in a transplanted liver as early as 2 years post-transplant. The wide range of recurrence time raises the question about whether the tumor in the transplanted liver arose from the native or donor liver.

Design: DNA was extracted from one H&E stained slide from formalin fixed paraffin embedded tissue from 1) the native liver, 2) the donor liver, and 3) the hepatocellular carcinoma arising in the transplanted liver. Using the AmpFISTR Identifiler PCR amplification kit, 16 STR loci were amplified with 30 cycles of PCR and the PCR products were separated by capillary electrophoresis. STR loci with signals greater than 100 Relative Fluorescent Units (RFU) were considered adequate for evaluation. The 3 STR profiles were compared to assess the origin of the hepatocellular carcinoma. IRB approval #: 661-16-EP.

Results: A review of 2823 orthotopic liver transplants performed at the University of Nebraska Medical Center from 1986 to 2016 identified 6 patients who were transplanted with HCC that developed HCC in the transplanted liver 2 years post-transplant and tissue was available for analysis in the FFPE tissue archives. Tumors arose between 2.5-17 years after transplantation. Based on STR analysis, all 6 samples are consistent with an origin from the HCC present at time of transplant. FISH for X and Y chromosomes was attempted in all 6 cases, and the results supported the above findings in 2 cases. The other 4 cases were gender matched transplants or failed to hybridize. These findings suggest that the recurrent tumors are remote metastases from the original tumor.

Conclusions: STR analysis is a viable technique to determine the origin of HCC occurring in transplanted livers, and the findings suggest that these tumors represent metastatic/recurrent disease and may help direct therapeutic options.

1530 Reassessing the Histological Features Associated with Antibody-Mediated Rejection in Liver Transplants

Catherine Forse[1], Morteza Tarokh[1], Chao Tu[1], Bijan Eghtesad[1], Scott Robertson[1], Daniel Roberts[1], Lisa Yerian[1], Daniela Allende[2]
[1]Cleveland Clinic, Cleveland, OH, [2]Cleveland Clinic, Avon Lake, OH

Disclosures: Catherine Forse: None; Morteza Tarokh: None; Chao Tu: None; Scott Robertson: None; Daniel Roberts: None; Lisa Yerian: None; Daniela Allende: None

Background: The diagnosis of antibody-mediated rejection (AMR) in liver allografts is complex and requires consideration of histological features, C4d immunohistochemistry (IHC) and donor specific antibodies (DSA). According to recent Banff guidelines, AMR shows characteristic histologic features (endothelial cell hypertrophy, sinusoidal dilation, leukocyte sludging/ margination and edema); however, we infrequently see these features in our clinical practice. We therefore aimed to identify histological features associated with AMR and compare them to the Banff criteria.

Design: Liver allograft biopsies with corresponding C4d IHC and DSA tests were collected from 2012 to 2018. All cases included were ABO-compatible allografts. Histologic assessment and diagnosis was based on Banff criteria (Am J Transplant, 2016). Using the Banff criteria (histology, positive DSA and positive C4d), cases were classified as certain AMR (3/3 features), possibly AMR (2/3, positive DSA required) or unlikely AMR (0-1/3, no positive DSA).

Results: A total of 73 liver biopsies were reviewed. Summarized findings are shown in Table 1. The “signature” histology as proposed by the Banff working group was not seen in any cases. Histologic findings frequently associated with “certain AMR” were endothelial cell hypertrophy/ swelling ($p=0.007$), lobular inflammation (mainly in a sinusoidal distribution) ($p<0.001$), and bile duct injury ($p=0.04$). When assessing the same histologic features independently of C4d expression, only the absence of cholestasis was significantly associated with positive DSA ($p=0.03$).

Table 1. Summarized results of the cohort with values representing the absolute number of cases with the histological feature. The signature histological features for AMR as proposed by the Banff Working Group are in bolded font.

Histological Features	Unlikely AMR (n=41)	Possible AMR (n=20)	Certain AMR (n=12)	p-value
Portal inflammation present	35	18	12	NS
Lobular inflammation present	27	16	10	See below
Sinusoidal inflammation present	1	2	3	<0.001
Perivenulitis present	5	5	4	NS
Hepatocellular injury present	21	10	6	NS
Regenerative hepatocellular changes present	29	15	10	NS
Endothelitis present	6	5	3	NS
Lymphocytic necrotizing arteritis present	0	0	0	NS
Endothelial cell hypertrophy/ swelling present	8	8	8	0.007
Sinusoidal dilatation present	0	0	0	NS
Microvascular disruption/interstitial hemorrhage present	12	7	5	NS
Fibrin thrombi present	2	0	0	NS
Portal edema present	0	0	0	NS
Leukocyte sludging/margination present	0	0	0	NS
Intimal arterial hyperplasia present	0	0	1	NS
Foamy cell arterial change present	0	0	0	NS
Bile duct injury	11	11	7	0.04
Senescent bile changes/loss present	0	0	0	NS
Bile duct proliferation present	26	13	11	NS
Cholestasis present	16	6	2	NS
Fibrosis present	7	8	4	NS

Conclusions: The proposed AMR "signature histologic criteria" are uncommonly seen in clinical practice. In our cohort, endothelial cell hypertrophy/ swelling, lobular inflammation (sinusoidal pattern in particular) and bile duct injury were significantly associated with the presence of AMR. The presence of cholestasis is not necessarily associated or a common feature of AMR. Pathologists should be aware that these histologic features may warrant further work-up for AMR in liver transplants to potentially increase the detection rate.

1531 Challenges in C4d Immunostain Interpretation in the Diagnosis of Antibody-Mediated Rejection in Liver Transplants

Catherine Forse[1], Morteza Tarokh[1], Chao Tu[1], Bijan Eghtesad[1], Scott Robertson[1], Daniel Roberts[1], Lisa Yerian[1], Daniela Allende[2]
[1]Cleveland Clinic, Cleveland, OH, [2]Cleveland Clinic, Avon Lake, OH

Disclosures: Catherine Forse: None; Morteza Tarokh: None; Chao Tu: None; Scott Robertson: None; Daniel Roberts: None; Lisa Yerian: None; Daniela Allende: None

Background: The Banff criteria for diagnosis of antibody-mediated rejection (AMR) in liver allografts (Am J Transplant, 2016) include C4d immunohistochemistry (IHC). C4d interpretation presents challenges, and data on interobserver agreement is lacking. This study aims to (1) determine if C4d staining correlates with the presence of donor specific antibodies (DSA) and (2) assess interobserver agreement of C4d scoring.

Design: Liver allograft biopsies stained for C4d were retrospectively identified in a pathology database search (2012-2018). Clinical data was obtained from medical records. C4d IHC (American Research Products, rabbit polyclonal, 1:50) was performed on formalin-fixed paraffin embedded tissue and assessed independently by 3 liver pathologists. Intensity and distribution of staining (portal vessels, central veins, sinusoids and portal stroma) were recorded. Raters assigned each biopsy a positive, indeterminate or negative for C4d score based on the Banff criteria. A consensus C4d score was generated and compared to the original C4d interpretation and to DSA serology.

Results: The 73 biopsies were originally interpreted as positive (n =19), indeterminate (n=29) and negative (n=25) for C4d. Upon slide review, strong staining was noted in 14/73 cases. 53/73 cases had C4d expression in portal vessels. Sinusoidal C4d staining was seen in 16/73 cases; 13 of which also had C4d expression in portal vessels. Central vein staining was noted in a minority of cases (2/73). Portal stroma C4d staining was identified in 34/73 cases (29 of which also had portal vessel staining). The consensus C4d score resulted in reclassification of 44% (32/73) of cases (Table 1). Five of the 19 cases originally interpreted as positive were reclassified as negative upon consensus C4d read. Eight of 25 C4d (32%) negative cases were reclassified as indeterminate or positive based on consensus C4d read. Interobserver agreement for C4d interpretation was moderate (κ=0.442, p<0.001). Approximately 47% of the consensus C4d scores correlated with the expected (positive or negative) DSA serology.

Table 1. C4d immunostain interpretation reclassification based on initial and consensus reads.

	Initial read			
		Negative	Indeterminate	Positive
Consensus Read	Negative	17	11	5
	Indeterminate	7	16	6
	Positive	1	2	8

Conclusions: Portal vessel C4d staining was the most frequent pattern. C4d in portal stroma is frequently seen and can hinder assessment of portal vessels. We found only moderate interobserver agreement on C4d interpretation and relatively low correlation between C4d IHC and DSA serology. Our findings illustrate that C4d interpretation is problematic and better markers are needed to improve the reproducibility of AMR diagnosis.

1532 Diagnosis of Liver Allograft Antibody Mediated Rejection: Reappraisal of the 2016 Banff Criteria and Implications on Patient Management

Yuna Gong[1], Brian Lee[1], Michael Koss[2], Jeffrey Kahn[1], Shefali Chopra[3]
[1]University of Southern California, Los Angeles, CA, [2]Keck Medical Center of USC, Los Angeles, CA, [3]University of Southern California, San Marino, CA

Disclosures: Yuna Gong: None; Brian Lee: None; Michael Koss: None; Jeffrey Kahn: None; Shefali Chopra: None

Background: Antibody mediated rejection (AMR) and donor specific antibodies (DSA) have been implicated in graft dysfunction and failure in many organ transplants such as the kidney and the heart. In liver, however, the diagnosis of AMR remains a source of controversy. In 2016, the Banff Working Group on Liver Allograft Pathology published an introduction on the diagnostic criteria for AMR. The purpose of this study is to evaluate the application of the diagnostic criteria in clinical practice.

Design: Allograft liver biopsies with concurrent C4d immunohistochemistry over a period of 3 years (2015-2018) were retrospectively identified. The diagnostic criteria for AMR as described in the Banff schema were applied based on the four criteria (h-score, C4d-score, DSA positivity, exclusion of other insults) and the cases were classified as definite, suspicious, indeterminate or negative for acute AMR. Clinicopathologic data including DSA level, index disease, biopsy results and treatment rendered, were collected on these cases.

Results: A total of 50 allograft cases were retrieved, of which 34 showed elevated DSA levels and 16 did not. None of the cases could be classified as definite for acute AMR due to inability to exclude other causes that might cause similar patterns of injury. Of the DSA-positive cases, 12 of 34 (35.3 %) cases were classified as suspicious for acute AMR. Of these 12 suspicious cases, 3 were treated with IVIG/plasmapheresis with significant response. The remaining 9 suspicious cases received treatment based on clinical and biopsy findings, such as steroids for T-cell mediated cellular rejection and ERCP for bile duct obstruction. Six cases showed clinical improvement while 3 were refractory to treatment. In addition, the DSA-positive cases showed moderate positive correlation between the C4d- and h-scores.

Pathologic features		DSA positive (n=34)	DSA negative (n=16)
Acute AMR			
	Definite	0 (0%)	0 (0%)
	Suspicious	12 (35.3 %)	0 (0%)
	Indeterminate	7 (20.6%)	5 (31.3%)
	Negative	15 (44.1%)	11 (68.7%)
Chronic active AMR			
	Probable or possible	0 (0%)	0 (0%)
	Negative	34 (100%)	16 (100%)
Biopsy diagnosis			
	ACR	9 (25.5%)	5 (31.25%)
	CDR	1 (2.9%)	1 (6.25%)
	Ischemia/preservation injury	3 (8.8%)	3 (18.75%)
	Bile obstruction	5 (14.7%)	1 (6.25%)
	Recurrent index disease	3 (8.8%)	0 (0%)
	Others*	13 (38.2%)	6 (37.5%)
H score			
	0	20 (58.8%)	11 (68.75%)
	1	8 (23.5%)	4 (25%)
	2	5 (14.7%)	1 (6.25%)
	3	1 (29.4%)	0 (0%)
C4d score			
	0	12 (35.3%)	5 (31.25%)
	1	6 (17.6%)	7 (43.75%)
	2	10 (29.4%)	4 (25%)
	3	6 (17.6%)	0 (0%)

*Others include cases with nonspecific minimal to mild portal/lobular inflammation, cholestasis, venous outflow obstruction and de novo AIH. AMR = antibody mediated rejection; ACR = acute cellular rejection; CDR = chronic ductopenic rejection.

Conclusions: The histopathologic pattern of injury of acute AMR as described in the Banff criteria is relatively nonspecific and overlaps with other patterns of injury, rendering exclusion of other causes difficult and precluding definitive diagnosis of acute AMR. The above cases classified as suspicious consist of variety of cases that include probable acute AMR, concurrent AMR with other pathologies, and histologic mimics of AMR. Considering these results, the Banff diagnostic criteria may need to be revisited or the treatment protocol of the suspicious category of cases may need adjustment to accomodate for the various pathologies that constitute this group.

1533 Histopathologic Findings in Allograft Liver Biopsies in the Era of Direct Acting Antiviral Agents

Yuna Gong[1], Elise Nguyen[2]
[1]University of Southern California, Los Angeles, CA, [2]USC/LAC+USC Medical Center, Los Angeles, CA

Disclosures: Yuna Gong: None; Elise Nguyen: None

Background: Recurrence of HCV was considered almost universal in patients who have undergone transplants prior to widespread use of direct acting antiviral agents (DAA). Liver biopsies, along with serologic testing for HCV RNA, have long been an integral part of diagnosis and management for patients with HCV before and after liver transplants; however, it's role may be changing with the advent of DAA agents. The purpose of this study is to examine the changing landscape of allograft liver biopsies in patients who have undergone treatment with DAA and attained sustained virologic response (SVR) prior to the transplant.

Design: A single center, retrospective analysis will be conducted on all allograft liver biopsies performed at our institution between 2015 and 2018 after treatment with DAA and attainment of SVR. Data will be obtained by review of pathology department's specimen database and review of associated medical charts. Clinicopathologic data including post-transplant follow-up interval, liver biopsy results and laboratory data (HCV RNA, liver function tests) are recorded. The rate of HCV recurrence as documented by serum HCV RNA and any concurrent histologic evidence is recorded.

Results: Total of 20 patients are identified with mean follow up of 662 (184-1270) days post-transplant. None of the patients showed definite evidence of recurrent HCV as documented by serum HCV RNA measurements. Of the 20 patients, 7 were biopsied due to abnormal liver enzymes with a total of 19 biopsies. The most common histologic finding was acute cellular rejection 7/19 (36.8%), followed by minimal to mild nonspecific portal and lobular inflammation 5/19 (26.3%). Bile obstruction 2/19 (10.5%), ischemia 2/19 (10.5%), steatosis/steatohepatitis 2/19 (10.5%) and other pathologies 1/19 (5.3%) comprise the remaining cases. All cases of ACR occurred within 6 months from the time of transplant.

Conclusions: The most common pathology seen in patients who have received pre-transplant DAA is no longer recurrent HCV, but ACR occurring within 6 months of transplant date. No definite histologic or serum HCV RNA evidence of recurrent HCV were seen in the biopsies; however, the possibility of low-level, recurrent, HCV infection cannot be entirely excluded as the etiology of the nonspecific portal/lobular inflammation is unknown in a subset of cases and other studies have shown presence of occult HCV RNA in hepatocytes despite treatment with DAA. The clinical relevance of this subset of cases needs further study.

1534 Viral Integration in Genome of Hepatocellular Carcinoma

Katie Hsia[1], Metabolic and Epigenetic Control of RNA expression Cancer[2], Shaolei Lu[3]
[1]Alpert Medical School of Brown University, Providence, RI, [2]Rhode Island Hospital/Brown University, Providence, RI, [3]Providence, RI

Disclosures: Katie Hsia: None; Metabolic and Epigenetic Control of RNA expression Cancer: None; Shaolei Lu: None

Background: Viral interference has been shown to play a role in the progression of hepatocellular carcinoma (HCC). HCC is the 5th most common cancer and the 3rd deadliest cancer. The incidence of HCC has tripled since the 1980s and is expected to increase with the associated peak of the Hepatitis C virus, as well as the rise of non-alcoholic fatty liver disease and non-alcoholic steatohepatitis. The integration of Hepatitis B viral material has been found in HCC. This study explored the prevalence of viral genetic material in HCC. Better understanding of the prevalence of viral material in hepatocellular carcinoma can inform future studies exploring the mechanisms involved in and risk factors for HCC.

Design: All 1,212 cases of archived HCC genome in The Cancer Genome Atlas (TCGA) were downloaded to a local computer cluster. Genomic sequences of 7,500 viruses were obtained from viruSITE. Using VirusFinder2.0, VERSE algorithm was applied to determine if the hepatocellular carcinoma genome contained portions of viral genomes. The algorithm was designed to identify viral integration sites, ie. viral insertions flanked by human sequences.

Results: Viral insertions were found in 1,095 of the 1,212 samples (90%). There was a total of 1,289 viral insertions, for an average of 1.064 viral insertions per sample. A total of 4 different human viruses were found, and the remainders were predomantly Enterobacteria phages. Of 80 unique samples containing human viruses (6.6%), there are 3 samples with Human herpesvirus 6B (each with 2 insertions) and Human betaherpesvirus 6A (each with 2 insertions), 3 samples with Human adenovirus C (each with 1 insertion), and 74

samples with Hepatitis B (each with 1 insertion). Genomic information could be correlated to clinical data for 671 patients. Unfortunately, no clinical information was available for the 80 samples with human virus insertions. Supprisingly, all the 351 cases with known Hepaitis B infection did not have Hepatitis B viral insertion.

Conclusions: It is the largest reported study that searched all the 7,500 known virus sequences in all the 1,212 HCC genomes archived in TCGA. The prevalence of viral genomic material was found in over 90% of HCC genomes. Human-related viruses were found integrated in 6.6% of the HCCs, with HBV found in 92% of these. The pervalance of hepatitis virus integration may not be as high as indicated by smaller localized studies. Hepatitis B viral integration may not be the universal mechanism of HCC tumorigenesis.

1535 CTNNB1 and TP53 mutations are Mutually Exclusive Molecular Drivers in a Subset of Hepatocellular Carcinomas and are Independent of Etiology of Liver Disease

Upasana Joneja[1], Jonathan Lake[2], David Lieberman[3], Danielle Fortuna[4], Emma Furth[5], Rashmi Tondon[4]
[1]Hamilton, NJ, [2]University of Pennsylvania Health System, Philadelphia, PA, [3]The Hospital of the University of Pennsylvania, Philadelphia, PA, [4]Hospital of the University of Pennsylvania, Philadelphia, PA, [5]University of Pennsylvania, Philadelphia, PA

Disclosures: Upasana Joneja: None; Jonathan Lake: None; David Lieberman: None; Danielle Fortuna: None; Emma Furth: None; Rashmi Tondon: None

Background: Mutations in *TP53*, *CTNNB1* and *TERT* promoter are key drivers in hepatocellular carcinoma (HCC). However, clinical associations with mutational signatures in HCCs are in their infancy. Greater understanding in this realm may be helpful in the development of early detection methods. We therefore examined the mutational profile and its clinicopathologic associations in our institution.

Design: Clinicopathologic data of all HCCs with available molecular results between 2014-2018 was reviewed. Molecular characterization was performed using a 47 gene solid tumor sequencing panel in 27 patients.

Results: The patient characteristics were as follows: 17 (63%) males, 10 (37%) females, and mean age- 62.3 yrs. Six patients had no known underlying liver disease/fibrosis while 20 patients had known underlying liver disease with different stages of fibrosis. No clinical history was available on one patient. Underlying liver diseases included Hepatitis C (44%), Hepatitis B (7%), Steatohepatitis (15%), and Hemochromatosis (4%). Interestingly, 32% of cases showed no pathogenic mutations. When present, the most frequent pathogenic mutations were *TP53* (7 (30%)) and *CTNNB1* (6 (26%)). Other mutations included *BAP1* (9%), *ARID1* (9%), *PTEN* (9%), *BRAF* (4%), *IG1R* (4%), *TRAF7* (4%), and *ERCC2* (4%). In addition to conventional morphology with different degrees of differentiation (WHO classification and Edmondson-Steiner scheme), HCC variants included steatohepatitic (4%) and clear cell variant (11%). Poorly differentiated HCCs (67%) showed a correlation with *TP53* mutations while well-moderately differentiated tumors (100%) showed a correlation with *CTNNB1* mutations (p –value: 0.04, Fischer's exact test). Attesting to differing molecular pathways, *TP53* and *CTNNB1* mutations were mutually exclusive. However, presence or absence of underlying liver disease, etiology of liver disease, underlying cirrhosis, gender, and AFP levels greater or less than 100 did not show any statistically significant correlation with the mutational signatures.

Conclusions: Most frequently mutated genes, *TP53* and *CTNNB1,* were mutually exclusive implicating divergent molecular pathways for hepatocarcinogenesis. As the underlying etiologies and presence or absence of liver disease were independent of the molecular signature, developing molecular markers for early detection may be feasible. However, only 68% of HCCs had detectable mutations implying other mutations and/or epigenetic factors are important for hepatocarcinogenesis.

1536 Liver Biopsy Interpretation Using Smartphone Video

Richard Judelson[1], Xiaofei Wang[2]
[1]University of Massachusetts Medical School, Worcester, MA, [2]UMass Memorial Health Care, Worcester, MA

Disclosures: Richard Judelson: None; Xiaofei Wang: None

Background: Most liver biopsies are for diagnosis of acute liver failure and evaluation of post-transplant liver rejection; many of them are from outside hospitals. They require a fast and accurate assessment to guide the management. Our objective is to evaluate if a microscopic video of liver biopsy taken by a Smartphone can provide an accurate interpretation, which can be used as an effective tool for liver pathologists.

Design: 20 liver biopsy cases were selected from our institution's archives. The cases included medical liver biopsies (8 Cases) and post-transplant liver biopsies (12 Cases). One H&E stained slide and one trichrome stained slide from each case were used. An iPhone 8 was attached to the eyepiece of the microscope using a Smartphone mount. A video was taken of the entire biopsied tissue by scanning tissue under 200 magnifications. The video was then stored in a shared folder in iCloud or was texted to the liver pathologist for interpretation. Only basic clinical information, such as elevated LFTs, acute liver failure or post-transplant liver, was available to pathologist. A checklist of histopathologic features was assessed, including portal inflammation, interface activity, lobular inflammation, steatosis, liver cell injury,

necrosis, bile duct injury and vascular injury as well as fibrosis. A final diagnosis or limited differential diagnosis was also rendered based on the video image and then compared to the original report.

Results: Of the 20 cases, there was concordance of final or differential diagnosis in all cases. These included acute cellular rejection (ACR), autoimmune hepatitis, steatohepatitis, cirrhosis, drug induced injury, reperfusion injury and obstructive biliary disease. All transplant cases assessing for ACR had a concordant diagnosis with minor discrepancy on severity in 3 cases. The concordance rates for assessing presence of portal inflammation, bile duct injury and steatosis were 100%, 90% and 95% respectively. Concordance among the remaining features ranged from 80% to 100%.

Conclusions: Our data shows that Smartphone video of liver biopsies can make concordant interpretations over a wide range of pathological diagnoses. It is feasible for a liver pathologist to render fast and accurate diagnoses of liver biopsies remotely when necessary.

1537 Hepatocellular carcinoma in patients with MDR3 deficiency

Saime Kirimlioglu[1], Laura Bull[2], Nancy Joseph[2], Sanjay Kakar[2], Kevin Bove[3], Linda Ferrell[2], Umit Ince[4], Grace Kim[2]
[1]University of Acibadem, Istanbul, Spring Hill, TN, [2]University of California, San Francisco, San Francisco, CA, [3]Cincinnati, OH, [4]University of Acibadem, Istanbul, Istanbul, Turkey

Disclosures: Saime Kirimlioglu: None; Nancy Joseph: None; Sanjay Kakar: None; Linda Ferrell: None; Grace Kim: None

Background: Progressive familial intrahepatic cholestasis3 (PFIC3) is caused by mutation in the *ABCB4* gene that encodes multidrug resistance–associated protein 3 (MDR3). Negative or faint MDR3 immunostaining is diagnostic of MDR3 deficiency, but normal canalicular staining has also been observed. Increased risk of developing hepatocellular carcinoma (HCC) is known for BSEP deficiency (PFIC2); however, HCC has only rarely been reported in MDR3 deficiency.

Design: Explant livers from PFIC3 cases received at one institution between 2010-2017 were reviewed. Genetic analysis was performed in two patients. MDR3 immunohistochemical stain was performed on formalin-fixed, paraffin-embedded tissue block for all 6 cases and reticulin stain on 3 cases.

Results: Liver transplantation was done on all 6 cases due to liver failure (Table). All patients had been previously treated with ursodeoxycholic acid, without prior surgical intervention. All patients were offspring of consanguineous marriages (fourth cousins).

Homozygous p.A953D mutation, a known pathogenic variant, was detected in patient 2 (*sibling of patient 1). Homozygous p.A523G mutation (unknown variant) was detected in patient 5. The explant livers in all patients demonstrated cirrhosis and three patients also had <2 cm well-differentiated hepatocellular carcinoma; two occurred in siblings (*patients 1 and 2). Diffuse strong canalicular staining for MDR3 was seen in 4 cases, while 2 revealed areas with loss of staining. At 3-76 months follow-up, all patients were alive after liver transplantation.

Table 1. Clinicopathologic information.

Patient	Gender	Age at diagnosis (yrs)	Age at explant (yrs)	Genetics	MDR3 stain	HCC (cm)
1*	Male	2	8	Not performed	+	1.5
2*	Female	3	5	*ABCB4* gene (p.A953D) homozygous	+	1.1
3	Male	2	6	Not performed	+	1.4
4	Male	10	17	Not performed	Focal loss	-
5	Male	13	14	*ABCB4* gene (p.A523G) homozygous	Focal loss	-
6	Male	6 mts	7 mts	Not performed	+	-

Conclusions: Small HCCs may be discovered on careful examination of the explant liver in PFIC3 cases. Presence of a homozygous *ABCB4* missense mutation p.A523G in one of the six patients suggests this is likely a pathogenic variant causative of disease.

1538 Autoimmune hepatitis with prominent IgG4-positive plasma cell infiltrates

Hee Eun Lee[1], Michael Torbenson[2], Lizhi Zhang[1]
[1]Rochester, MN, [2]Mayo Clinic, Rochester, MN

Disclosures: Hee Eun Lee: None; Michael Torbenson: None; Lizhi Zhang: None

Background: IgG4-associated autoimmune hepatitis (AIH) is a recently identified and possibly new disease entity that affects older aged men. We aimed to describe clinicopathologic features of such cases, which remain unclear at present.

Design: In order to identify possible cases, IgG4 immunostain was performed on liver sections from patients with atypical AIH (male and over 45 years old, n=17), primary biliary cirrhosis (PBC) (19), AMA negative PBC (19), primary sclerosing cholangitis (PSC) (20), typical AIH (19) and AIH-PBC overlap syndrome (16). 8 cases with ≥10 IgG4+ plasma cells/HPF were finally selected for study group. Various clinical, laboratory, and histologic findings were recorded.

Results: All 8 patients with AIH with prominent IgG4+ plasma cells were male with a median age of 52 years (range, 36-79). All had clinical and/or histological findings of AIH including 2 with AIH and PSC overlap syndrome without clinical suspicion of IgG4-related disease. Histologic findings were summarized in Table 1. Median number of IgG4+ plasma cells/HPF was 24 (range, 13-88). One patient had an increased serum IgG4 level (269 mg/dL) and the remaining patients were not tested for it. All liver sections in other groups, except for a single case of PSC showed <10 IgG4+ plasma cells/HPF.

Table 1. Histologic findings of AIH with prominent IgG4+ plasma cell infiltrates*

Case	Portal inflammation	Interface activity	Lobular activity	Confluent necrosis	Fibrosis (stage)	Storiform fibrosis	Venulitis	Plasma cell predominance	Eosinophils >5/HPF	IgG4+ cells/HPF
1	2	1	2	0	3	Absent	Focal	Mild predominance	Present	18
2	3	4	4	5	0	Absent	Absent	Present	Absent	66
3	2	3	3	2	0	Absent	Absent	Present	Absent	22
4	3	3	3	1	3-4	Absent	Absent	Present	Absent	26
5	3	4	4	4	0	Absent	Absent	Present	Present	32
6	2	2	3	4	0	Absent	Absent	Present	Present	88
7	3	4	3	3	4	Absent	Focal	Present	Absent	13
8	2	1	2	2	1	Onion skin-like periductal fibrosis	Absent	Mild predominance	Present	20

*Portal inflammation, interface activity, lobular activity, and confluent necrosis; and fibrosis were scored according to the modified HAI and Batts-Ludwig system, respectively.

Conclusions: We show that a subset of AIH cases in older aged men contains prominent IgG4+ plasma cells, and such cases show similar clinical and histological findings as AIH. It is uncertain at present whether they are part of systemic IgG4-related disease or a variant of AIH. Further study of this unique patient cohort will allow characterization of this distinctive pattern of injury: AIH with prominent IgG4-positive plasma cell infiltrates.

1539 Molecular Characteristics of Hepatocellular Carcinoma with Epigenetic Activation of the 9p21.3 Locus

Yongchao Li[1], Jatin Gandhi[1], Jinjun Cheng[2], Yaohong Wang[1], Shuyu E[1], Jacob Abel[1], Joe Kaminsky[1], Adel Abdallah[1], Ali Saad[3], Mahul Amin[4], Ian Clark[1], Meiyun Fan[5]
[1]University of Tennessee Health Science Center, Memphis, TN, [2]National Cancer Institute/NIH, Bethesda, MD, [3]Methodist/LeBonheur Health System, Memphis, TN, [4]Methodist University Hospital, Memphis, TN, [5]The University of Tennessee Health Science Center, Memphis, TN

Disclosures: Yongchao Li: None; Jatin Gandhi: None; Jinjun Cheng: None; Yaohong Wang: None; Shuyu E: None; Jacob Abel: None; Joe Kaminsky: None; Adel Abdallah: None; Ali Saad: None; Ian Clark: None; Meiyun Fan: None

Background: LIHC typically arises in the background of chronic liver disease that is most commonly caused by alcohol consumption, virus infection, autoimmunity or non-alcoholic fatty liver disease. It is unclear how this inflammatory environment shapes molecular abnormalities

of tumor cells by exerting selective pressures and how it is refined by tumor cell intrinsic factors. The objective of this study is to examine the association of epigenetic activation of 9p21.3 loci with molecular and clinicopathological features of LIHC.

Design: Integrated analyses of multiple data platforms of LIHC in the TCGA database was conducted to exploit the cause and consequence of transcriptional activation of 9p21.3 locus. FFPE tissues prepared for diagnosis purpose by the Methodist University Hospital were examined for CDKN2A and IFNB1 expression at single cell resolution by using IHC and RNAscope 2.5 LS in situ hybridization Assay (ACDbio), respectively, to confirm the association of CDKN2A and IFNB1 expression in tumor and stromal cells with clinicopathological characteristics retrieved from the surgical reports.

Results: 1) Homozygous deletion of 9p21.3 locus that hosts CDKN2A occurs in 5.4% of LIHC. Paradoxically, elevated expression of CDKN2A, along with multiple genes encoded by the 9p21.3 locus, were detected in 43.7% LIHC. (Fig 1) . 2) Four CpG islands that are strongly methylated in normal liver tissues were found to be demethylated in LIHC tumor tissues comparing with adjacent normal tissues (P<0.0001). Expression levels of multiple mRNAs encoded by the 9p21.3 locus, including CDKN2A, CDKN2B and IFNB1, are inversely correlated with the methylation intensities of these CpGi. 3) Tumors with epigenetic activation of 9p21.3 locus exhibit adverse molecular features such as high indices of aneuploidy, proliferation, stemness and unfavorable immune contexture. (Table 1). 4) Epigenetic activation of 9p21.3 locus is associated with is positively associated with high RS65 score, a which predicts short overall survival of patients after surgical resection for LIHC and predict short survival interval.

	Correlation with CDKN2A expression			Correlation with cg14069088 methylation			Comparison of deM,hiEx to M.lowEx LIHC	
	Number of XY Pairs	Pearson r	P value	Number of XY Pairs	Pearson r	P value	P value	Description
Genomic alterations								
Aneuploidy Score	355	0.0637	0.2311	243	-0.1361	0.0339	8.48E-03	Higher in deM,hiEx
Fraction Altered	361	0.1499	0.0043	248	-0.2652	< 0.0001	4.83E-07	Higher in deM,hiEx
Homologous Recombination Defect score	355	0.2684	< 0.0001	243	-0.4041	< 0.0001	1.04E-09	Higher in deM,hiEx
Immune cell infiltration								
Th17 Cells1	362	-0.1247	0.0176	244	0.1527	0.017	4.30E-03	Lower in deM,hiEx
CTA (Cancer testis antigens) Score	356	0.3052	< 0.0001	241	-0.4416	< 0.0001	2.74E-16	Higher in deM,hiEx
Natural killer T cell	369	0.2596	< 0.0001	252	-0.1910	0.0023	5.32E-04	Higher in deM,hiEx
Plasma cells	369	0.1167	0.0249	252	-0.2195	0.0004	7.23E-03	Higher in deM,hiEx
Th1 cells	369	0.2956	< 0.0001	252	-0.2482	< 0.0001	3.32E-08	Higher in deM,hiEx
Th2 Cells	362	0.3199	< 0.0001	244	-0.3796	< 0.0001	3.07E-11	Higher in deM,hiEx
Tumor stroma								
Stroma_notLeukocyte_Floor	356	-0.1975	0.0002	243	0.2122	0.0009	1.32E-05	Lower in deM,hiEx
Endothelial cells	369	-0.1866	0.0003	252	0.3384	< 0.0001	2.15E-12	Lower in deM,hiEx
Fibroblasts	369	-0.1900	0.0002	252	0.2561	< 0.0001	2.89E-09	Lower in deM,hiEx
Myocytes	369	-0.1438	0.0057	252	0.1795	0.0043	5.40E-05	Lower in deM,hiEx
Tumor cell characteristics								
mDNAsi (stemness indices)	369	0.3180	< 0.0001	253	-0.4045	< 0.0001	1.70E-15	Higher in deM,hiEx
mRNAsi (stemness indices)	369	0.3519	< 0.0001	250	-0.4117	< 0.0001	7.28E-17	Higher in deM,hiEx
Proliferation	362	0.3935	< 0.0001	244	-0.5150	< 0.0001	5.55E-24	Higher in deM,hiEx
Wound Healing	362	0.4274	< 0.0001	244	-0.4788	< 0.0001	5.11E-19	Higher in deM,hiEx

deM.hiEx: LIHC with cg14069088 demethylation (b value >0.5) and high CDKN2A expression (fold change >2, compared to average expression in normal liver tissues); M.lowEx: LIHC with cg14069088 methylation and low CDKN2A expression.

Figure 1 - 1539

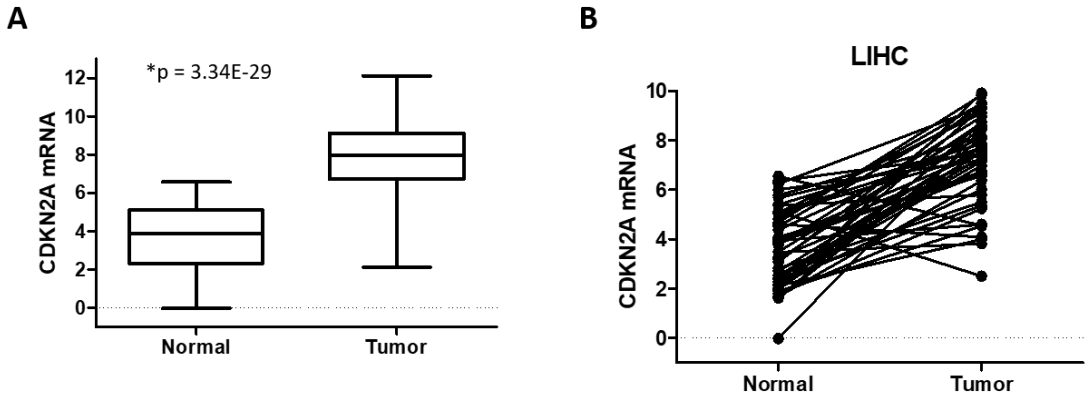

Fig. 1. Elevated expression of CDKN2A in LIHC. ***A.*** Comparison of CDKN2A mRNA levels in LIHC tumor tissues (n=371) to tumor-adjacent normal liver tissues (n=50). *Student's t-test. ***B.*** Comparison of CDKN2A mRNA levels in paired tumor and adjacent normal liver tissues (n=50). P < 0.0001, paired t-test. The mRNA expression data were retrieved form the TCGA database (PanCanAtlas).

Figure 2 - 1539

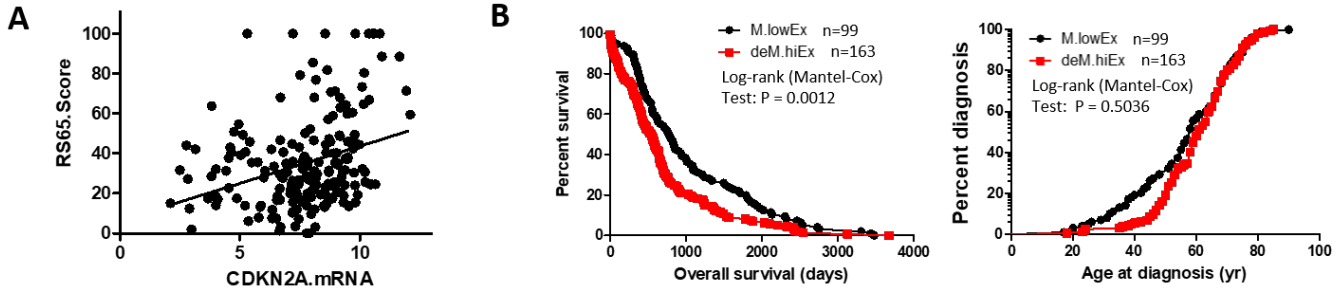

Fig. 2. cg14069088 demethylation and elevated CDKN2A expression are associated with poor prognosis of LIHC. **A.** CDKN2A expression is positively associated with RS65 score, a 65-gene–based risk classifier that predicts short overall survival (OS) of patients after surgical resection for LIHC. **B.** cg14069088 demethylation and elevated CDKN2A expression are associated with short interval of overall survival but not age at cancer diagnosis. deM.hiEx: LIHC with cg14069088 demethylation (β value >0.5) and high CDKN2A expression (fold change >2, compared to average expression in normal liver tissues); M.lowEx: LIHC with cg14069088 methylation and low CDKN2A expression.

Conclusions: Our results from the integrated analyses of multiple data platforms of LIHC in the TCGA database pointed to a role of increased expression of CDKN2A/CDKN2B and IFNB1, as a consequence of epigenetic activation of the 9p21.3 loci, in modulating cell cycle regulation and immune contexture of tumors and predicting short overall survival of patients after surgical resection and short survial interval.

1540 Low Interobserver Agreement Hinders Diagnosis of Obliterative Portal Venopathy

Jiancong Liang[1], Safia Salaria[1], Won Jae Huh[1], Hernan Correa[1], William Dupont[2], Chanjuan Shi[3], Mary Washington[1]
[1]Vanderbilt University Medical Center, Nashville, TN, [2]Vanderbilt University School of Medicine, Nashville, TN, [3]Nashville, TN

Disclosures: Jiancong Liang: None; Safia Salaria: None; Won Jae Huh: None; Hernan Correa: None; William Dupont: None; Chanjuan Shi: None; Mary Washington: None

Background: Obliterative portal venopathy (OPV), also called hepatoportal stenosis, is a form of idiopathic non-cirrhotic portal hypertension characterized by alterations in portal vein branches, including dilated veins herniated into adjacent parenchyma, abnormal periportal vessels, and obliterated or stenotic portal veins. The histopathologic diagnosis of OPV by liver biopsy is challenging. We aimed to assess the interobserver agreement in diagnosis of OPV with the goal towards a consistent and standardized approach to diagnosis.

Design: Liver biopsy specimens previously diagnosed as either positive for/suggestive of (n=42) or possible for/raising the consideration of (n=11) OPV were retrieved. High resolution virtual slides (H&E and trichrome/reticulin) of all cases were randomized and independently reviewed in a blinded fashion by six hepatopathologists and categorized as positive, negative, or indeterminate for OPV. Histopathologic

features of OPV (herniated portal veins and portal vein stenosis) were separately assessed. Interobserver agreement was calculated by kappa statistics.

Results: Interobserver agreement on positive, indeterminate and negative for OPV was fair (κ=0.21), poor (κ<0), and slight (κ=0.19), respectively, while the overall interobserver agreement was slight (κ=0.15). Agreement between individual pathologists and the group ranged from 71% (κ=0.40) to 59% (κ=0.18). While portal vein stenosis (p<0.001), portal fibrosis (p<0.001) and nodular regenerative hyperplasia (p=0.032), but not herniated portal veins (p=0.499), were found to be significant predictors of HPS by univariate logistic regression analysis, only portal vein stenosis remained independent by multivariate analysis (p=0.016). The strength of these predictors correlated with the degree of interobserver agreement for the corresponding histopathologic features, with higher agreement for portal vein stenosis (κ=0.25) and lowest for herniated portal veins (κ=0.15).

Conclusions: The interobserver agreement in the histopathologic diagnosis of OPV was low among experienced hepatopathologists. Portal vein stenosis appeared to be the most useful histopathologic feature in the diagnosis of OPV.

1541 A Phenotypic Reappraisal of the Stroma of Mucinous Cystic Neoplasm of the Liver

Mira Lotfalla[1], Taofic Mounajjed[1], Roger Moreira[1], Daniela Allende[2], Michelle Reid[3], Sarah Kerr[1], Rondell Graham[1]
[1]Mayo Clinic, Rochester, MN, [2]Cleveland Clinic, Avon Lake, OH, [3]Emory University Hospital, Atlanta, GA

Disclosures: Mira Lotfalla: None; Taofic Mounajjed: None; Roger Moreira: None; Daniela Allende: None; Michelle Reid: None; Sarah Kerr: None; Rondell Graham: None

Background: Mucinous cystic neoplasm of the liver (MCN-L) is a rare hepatic tumor that predominantly occurs in females. Histologically, it is composed of mucinous or biliary epithelial lining and ovarian-like stroma. This stroma is known to express hormonal receptors, ER and PR and is believed to be responsive to estrogen and progesterone. A detailed comparison of the stroma of MCN-L to true ovarian stroma has not been performed. Steroidogenic factor-1 (SF-1) is a master regulator of steroid hormone synthesis and is believed to be a highly specific immunohistochemical marker for the diagnosis of a sex cord stromal tumor or adrenocortical tumor.

Design: Whole tissue sections of 13 MCN-L and 19 primary ovarian mucinous tumors were reviewed. Immunohistochemical stains for SF-1, ER, PR, Calretinin, Inhibin, Melan A, were performed on all cases.

Results: Histologically the stroma of MCN-L closely resembled that seen in the stroma of primary ovarian tumors in all cases. Diffuse positive nuclear staining for SF-1, ER, PR, was identified in the stromal cells in 100% of MCN-L (13/13) and 100% of mucinous ovarian tumor (19/19). Focal expression of Calretinin, inhibin, and Melan A was identified in 84% (11/13), 84% (11/13), and 76% (10/13) of MCN-L, and in 100% (19/19), 100% (19/19), and 73% (14/19) of ovarian mucinous tumors, respectively.

Conclusions: The stroma of MCN-L and mucinous ovarian tumors shows consistent striking phenotypic similarity at both morphologic and immunohistochemical levels. The expression of SF-1, calretinin, inhibin and Melan-A indicate that the stroma of MCN-L is not only hormonally responsive but is also capable of hormone production. This raises interesting biological questions regarding the origin, development, and maintenance of MCN-L stroma. Also, these data show, for the first time, that the expression of SF-1 in a spindle cell stroma of an abdominal mass cannot be used as sole confirmation that the sampled specimen is from a eutopic or ectopic ovary.

1542 Longitudinal assessment of Nonalcoholic Fatty Liver Disease in Young Adults

Haiyan Lu[1], Lisa Yerian[2], Daniela Allende[3]
[1]Cleveland Clinic, Beachwood, OH, [2]Cleveland Clinic, Cleveland, OH, [3]Cleveland Clinic, Avon Lake, OH

Disclosures: Haiyan Lu: None; Lisa Yerian: None; Daniela Allende: None

Background: Background & Aims: Histological characteristics of nonalcoholic fatty liver disease (NAFLD) in young adults and their pathological evolution remains poorly understood. We aimed to perform a longitudinal assessment of NAFLD in this cohort.

Design: Design: We retrospectively identified 91 biopsies from patients age 18-35 with diagnosis of NAFLD from 01/2002 to 12-2008 using the terms “steatosis” and “steatohepatitis”. Only patients with paired liver biopsies (baseline and follow up) and follow up data were included. Pathology data was obtained from review of available H&E and trichrome stained slides. Clinical data was obtained from electronic medical records. Patients were divided upon baseline diagnosis into bariatric surgery or not.

Results: Results: Among our initial cohort of 91 cases, 16 cases had paired biopsies and follow up (17.5%), 7 male (43.8%). Mean follow up was 41.4 months. Nine patients (9/16) were in the bariatric surgery group, while the rest (7/16) were followed for medical reasons: At baseline biopsy, steatosis (NAFL) was diagnosed in 62.5% and steatohepatitis (NASH) in 37.5%. Most patients (12/16) remained in the same category, NAFL or NASH, in the follow up biopsy independent of bariatric status (Table1, *p*=0.110), although bariatric patients showed a significant decrease in BMI compared to non-bariatric patients (Table1, *p*=0.022). Similarly, 7/16 cases revealed no change in

fibrosis stage while 3/16 showed fibrosis progression and fibrosis regressed in the others (Table1, p=0.635). Increased total NAS score correlated more with steatosis (r=0.740, *p*<0.01) and lobular inflammation (r=0.745, *p*<0.01) than with portal inflammation (*p*=-0.152, p>0.05). Liver enzyme improvements at follow up correlated with steatosis and total NAS score (AST: with steatosis: r=0.532, p<0.05; with total NAS score: 0.581, p<0.05; ALT: with steatosis: r=0.527, p<0.05; with total NAS score: 0.576; p<0.05). Evidence of diabetes at follow up showed correlation with fibrosis (r=0.511, p<0.05).

Table 1: Follow up of clinico-pathological features in bariatric and non-bariatric patients

Clinico-pathological features		Total (n: 16)	Bariatric (n: 9)	Non-bariatric (n: 7)	P-value
Follow up time (months)	Mean ± SD	46.11±39.49	44.97±32.04	47.57±50.25	NS**
	median (range)	41.4 (3-127.5)	60.4 (4-85.5)	15.5 (3-127.5)	
Age at follow up (years)	Mean ± SD	34.69±4.85	35.11±2.98	34.12±6.82	NS**
Diagnosis evolution, baseline to follow up (N (%))	NASH to NASH	2 (12.5)	1 (11.11)	1 (14.29)	NS*
	NAFL to NAFL	10 (62.5)	6 (66.67)	4 (57.14)	
	NAFL to NASH	3 (18.75)	1 (11.11)	2 (28.57)	
	NASH to NAFL	1 (6.25)	1 (11.11)	0 (0.00)	
Fibrosis stage (N (%))	Worse	3 (18.75)	1 (11.11)	2 (28.57)	NS*
	Same	7 (43.75)	4 (44.44)	3 (42.86)	
	Better	6 (37.5)	4 (44.44)	2 (28.57)	
Diabetes mellitus (DM) (N (%))	DM to DM	5 (31.25)	3 (33.33)	2 (28.57)	0.06*
	Non-DM to Non-DM	6 (37.50)	2 (22.22)	4 (57.14)	
	Non-DM to DM	5 (31.25)	4 (44.44)	1 (14.28)	
BMI (mean ± SD)	Baseline	48.30±17.34	58.15±16.86	48.73±9.23	0.004**
	Follow up	43.51±9.98	35.64±6.36	36.81±6.49	0.011**
	Change from baseline	-4.79±9.60	-9.42±10.76	1.16±1.49	0.022**
	Percentage of change	-6.09±13.81	-13.40±14.40	3.31±4.17	0.010**
AST (mean ± SD)	Baseline	49.56±19.96	44.89±11.88	55.57±27.08	NS**
	Follow up	33.19±20.85	30.78±16.87	36.29±26.22	NS**
	Change from baseline	-16.38±18.22	-14.11±15.78	-19.29±21.91	NS**
	Percentage of change	-31.58±30.78	-29.42±32.50	-34.35±30.72	NS**
ALT (mean ± SD)	Baseline	73.56±43.14	53.89±20.91	98.86±52.38	0.033**
	Follow up	45.63±39.33	32.56±22.59	62.43±50.99	NS**
	Change from baseline	-27.93±26.70	-21.33±23.74	-36.43±29.68	NS**
	Percentage of change	-36.21±37.16	-34.59±43.75	-38.29±29.86	NS**

*Fisher's exact test; ** Student's T-test

Conclusions: Conclusion: Our study suggests that in a longitudinal assessment of fatty liver disease in young adults, most had persistent NAFL or NASH on follow up independent of bariatric surgery status. AST/ALT correlated with steatosis and total NAS score improvement. Diabetes status at follow up may represent a potential predictor of fibrosis stage.

1543 Reliability Of Visual Inspection Of Routine Stained Liver Biopsies For The Quantitation Of Steatosis In Evaluating The Suitability Of A Donor Liver For Transplant

Mark Luquette[1], Aastha Chauhan[2], Mahmoud Khalifa[1], David Berger[3], Tetyana Mettler[4], Regina Plummer[5], Kevin Ha[2], Amy Beckman[6]
[1]University of Minnesota, Minneapolis, MN, [2]University of Minnesota, Saint Paul, MN, [3]Woodbury, MN, [4]Chanhassen, MN, [5]Plymouth, MN, [6]University of Minnesota, St. Paul, MN

Disclosures: Mark Luquette: None; Aastha Chauhan: None; Mahmoud Khalifa: None; David Berger: None; Tetyana Mettler: None; Regina Plummer: None; Kevin Ha: None; Amy Beckman: None

Background: In assessing the suitability of a donor liver for transplant, it is generally agreed that significant steatosis in the donor is a marker for poor clinical outcome. The threshold most frequently cited is 30 percent steatosis, but the details of how to make that determination are less clear. Overall, assessment of hepatic fat has been reported using histologic examination of routine and Oil Red-O stained sections, image analysis, biochemical analysis, and radiologic imaging. In this study we review the reliability of assessment using visual inspection.

Design: 20 formalin fixed paraffin embedded needle biopsies of liver were selected (per IRB approved protocol) with varying degrees of steatosis in the absence of other space occupying histologic change. Three pathology staff and four residents were asked to make a rapid assessment of the percent steatosis of each case to mimic the conditions of a frozen section request. These results were compared with morphometric assessment of fat content done by hand (tracing the tissue, zones of steatosis and the individual lipid droplets). Comparison of the results within and between the groups as well as with morphometric results was done.

Results: Comparing staff to residents, the mean scores were higher from staff in 18 of 20 cases, and the standard deviations were wider in 11 of 20 cases (with 3 cases being the same and 6 wider in the resident group). However, using z-scores (95% CI), only 5 of 20 samples showed statistically different results between the groups. In comparison with morphometry, tested cases showed consistent overestimate of the fat content by visual assessment ranging from 10 to 44% overestimate.

Conclusions: Given that both groups tended to significantly overestimate the fat content in the biopsies, it would appear that the detection of subtle distinctions flanking a 30% threshold for rejecting a donor for use is an unrealistic expectation. A more practical intraoperative approach appears indicated, and better definition of the threshold is needed.

1544 Metastases can Occur in Cirrhotic Livers with Patent Portal Veins and Mild Fibrous Remodeling

Zaid Mahdi[1], Raul Gonzalez[2], Mark Ettel[3], John Hart[4], Lindsay Alpert[4], Jiayun Fang[5], Natalia Liu[6], Jerome Cheng[7], Joel Greenson[5], Paul Swanson[8], Suntrea Hammer[9], Maria Westerhoff[7]
[1]Beth Israel Deaconess Medical Center, Newton, MA, [2]Beth Israel Deaconess Medical Center, Boston, MA, [3]University of Rochester, Rochester, NY, [4]University of Chicago, Chicago, IL, [5]University of Michigan Hospitals, Ann Arbor, MI, [6]Ann Arbor, MI, [7]University of Michigan, Ann Arbor, MI, [8]University of Washington, Bainbridge Island, WA, [9]University of Texas Southwestern Medical Center, Dallas, TX

Disclosures: Zaid Mahdi: None; Raul Gonzalez: None; Mark Ettel: None; John Hart: None; Lindsay Alpert: None; Jiayun Fang: None; Natalia Liu: None; Jerome Cheng: None; Joel Greenson: None; Paul Swanson: None; Suntrea Hammer: None; Maria Westerhoff: None

Background: Metastases are common in non-cirrhotic livers but are considered unlikely in the setting of cirrhosis. In non-cirrhotic livers, carcinomas (CA) may access the liver through the dominant blood supply of the portal vein (PV). With cirrhosis, however, scarring may deter entry of metastases. But cirrhosis is not the “all or nothing,” irreversible process as previously believed. There can be degrees or a spectrum of fibrosis; hence metastases may potentially access the liver vasculature. We hypothesized that metastases can occur in cirrhotic livers if the fibrous remodeling is not severe or if abnormal veno-arterial shunting is present to override an obstructed PV system.

Design: We searched departmental archives for cirrhotic livers with masses. H&E, CD34, and trichrome stains were evaluated on metastatic cases. Cirrhosis was categorized by Laennec fibrosis staging: 4A = mild cirrhosis (delicate fibrous septa), 4B = moderate (having at least 2 broad septa), 4C = severe cirrhosis (at least 1 very broad septa or many minute nodules). Clinical history, lab & radiologic data were reviewed.

Results: Of 1080 cirrhotic livers with masses, 1057 were primary liver tumors and 23 were metastases (2%). Colon CA was the most common metastasis (8), followed by neuroendocrine tumor (5), pancreas (3), upper GI (3), breast (2), Müllerian (1), & lung (1). By Laennec staging, the majority of livers had 4A or 4B cirrhosis (n=17; 73%). Mean albumin was 3.2 g/dL, mean platelet count was 168K, and 15/23 had sequelae of cirrhosis (ascites, varices, jaundice). Of 17 pts evaluated by ultrasound Doppler, 4 with Laennec 4C had reversal of PV flow, but all 4A & 4B patients had patent PV without reversed flow. Echocardiograms (available for 11, including 4 Laennec 4C) did not show ventricular or atrial septal defects or AV shunts. CD34 did not show evidence of sinusoidal capillarization to indicate severe PV obstruction in any cases.

Conclusions: Metastases are uncommon in cirrhotic livers, accounting for 2% of masses in this setting. Most had mild or moderate cirrhosis (Laennec 4A/4B) & patent PV. None of the livers (including Laennec 4C) had diffuse CD34 expression to indicate severe PV obstruction. As there were some Laennec 4C cases with metastases, it is evident that mild cirrhosis & patent PV may not be the only factors for metastatic access; the role of arterial entry is not discounted. Overall, however, we show that metastases to cirrhotic livers occur primarily in pts with mild fibrous remodeling and patent PV.

1545 Hepatic Syphilis: A Rare Diagnosis with Varied Patterns of Histologic Injury

Grace Malvar[1], Diana Cardona[2], Joseph Misdraji[3], Oyedele Adeyi[4], Deyali Chatterjee[5], Laura Lamps[6], Raul Gonzalez[1]
[1]Beth Israel Deaconess Medical Center, Boston, MA, [2]Duke University Medical Center, Durham, NC, [3]Massachusetts General Hospital, Harvard Medical School, Boston, MA, [4]Toronto General Hospital, Toronto, ON, [5]Washington University, St. Louis, MO, [6]University of Michigan Hospital, Ann Arbor, MI

Disclosures: Grace Malvar: None; Diana Cardona: None; Joseph Misdraji: None; Oyedele Adeyi: None; Deyali Chatterjee: None; Laura Lamps: None; Raul Gonzalez: None

Background: The rate of syphilis in the United States has been increasing steadily in the past decade, but it remains an uncommon diagnosis in tissue biopsies. Most of the pathology literature on hepatic syphilis consists of older series or case reports. This study aimed to systematically characterize the histologic spectrum of hepatic syphilis.

Design: We identified 10 biopsy cases of hepatic syphilis from 2012-2018, based on convincing clinical and/or pathologic evidence. Gummas and congenital syphilis were excluded. For each case, we recorded patient age, sex, sexuality, presenting symptoms, and known HIV and syphilis status; presence and character of inflammation (including granulomas and phlebitis) and biliary-type changes (e.g., ductitis, portal edema); and *Treponema* immunohistochemistry (IHC) results (available on all cases).

Results: All 10 cases were from men (age range: 31-57 years); six had HIV, and a different subset of six were known to have sex with men. Three had prior syphilis, though hepatic syphilis was the primary clinical diagnosis in only one. Common symptoms included jaundice, rash, and abdominal pain; all had elevated AST (mean 289 IU/L, range 66-1382), ALT (mean 431 IU/L, range 58-2122), and alkaline phosphatase (mean 620 IU/L, range 186-1511). Three biopsies showed nonspecific inflammation (Fig. 1A), four showed biliary-pattern injury mimicking obstruction or drug reaction (Fig. 1B; obstruction was not evident clinically), and one each showed acute hepatitis (Fig. 1C), autoimmune hepatitis-like inflammation with prominent plasma cells, and a necroinflammatory mass lesion (Fig. 1D). All 10 showed portal and lobular lymphocytes and plasma cells; seven had duct inflammation. Occasional focal findings included hepatocyte dropout/necrosis (n=5), granulomas (n=4), phlebitis (n=3), and prominent eosinophils (n=1). *Treponema* IHC was positive in six. Eight patients had RPR testing before or after biopsy, with 1:64 or higher titer; this included three cases with negative *Treponema* IHC. All patients who received penicillin or doxycycline recovered.

Figure 1 - 1545

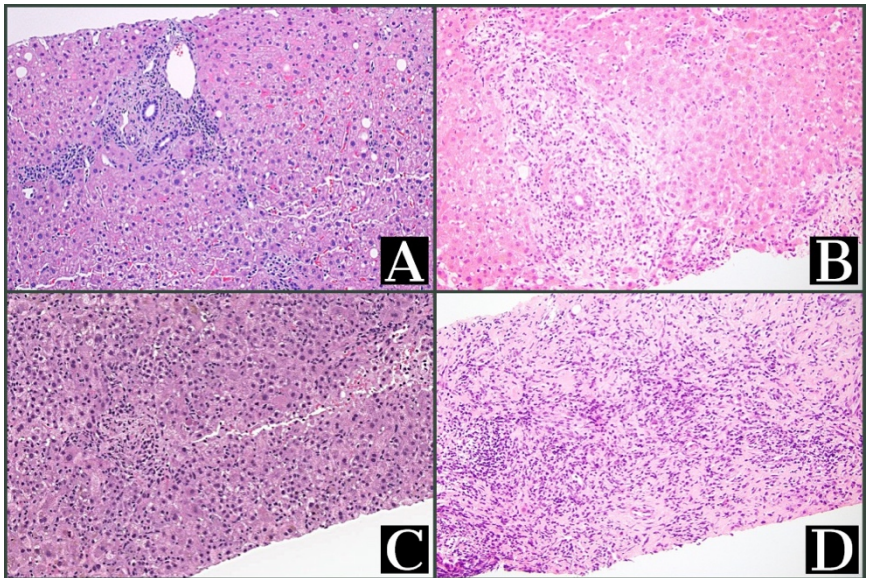

Conclusions: Hepatic syphilis is rarely diagnosed but likely under-recognized. It can have several histologic appearances, including nonspecific inflammation, biliary obstruction-like features, and inflammatory pseudotumor formation. Granulomas and phlebitis may also be seen. Negative *Treponema* IHC does not exclude the diagnosis. Syphilis should be considered in several hepatic differential diagnoses, especially in men who have sex with men.

1546 TERT Promoter Mutations in Tumors Characterized as Intrahepatic Cholangiocarcinoma

Elena Maryamchik[1], Martin Taylor[2], Vikram Deshpande[1]
[1]Massachusetts General Hospital, Boston, MA, [2]Boston, MA

Disclosures: Elena Maryamchik: None; Martin Taylor: None; Vikram Deshpande: None

Background: Intrahepatic cholangiocarcinoma (ICC), the second most common liver cancer, is associated with poor prognosis and limited response to conventional chemotherapy; targeted therapy for IDH1/2 and FGFR2 alteration has yielded promising results. Somatic mutations in the *TERT* promoter, which cause cancer-specific increase in telomerase activity, is the most prevalent mutation in hepatocellular carcinomas (HCC) 44-64%, but are not described in ICC. We have noted *TERT* promoter mutation in cases classified as ICC. Incorrect classification of intrahepatic neoplasm may deny a patient appropriate targeted therapy, and hence our aim was to evaluate the appropriate classification of these *TERT* promoter mutated ICCs.

Design: Using SNaPshot NSG and Solid Fusion Assay, we conducted a mutational analysis of 232 tumors previously classified as ICC based on histology and immunohistochemistry. Mixed tumors and those classified as HCC were excluded. Tumors harboring a *TERT* mutation were analyzed for the presence of other mutations that would support hepatic or bile duct differentiation, based on the data from publicly available databases. Immunohistochemistry/in-situ-hybridization studies for arginase-1, glypican-3, hep par 1, albumin, keratin 7 and keratin 19 were performed in selected cases.

Results: *TERT* promoter mutation was identified in 7 of 232 (3%) tumors characterized as ICC. The tumors displayed two distinct phenotypes. 5 of 7 tumors were undifferentiated, and showed nests of large cells with abundant eosinophilic cytoplasm. Immunohistochemical and mutational profile of these tumors is presented in Table 1. The second subgroup included two tumors with a well-differentiated ICC-like tubular architecture and desmoplastic stroma; both tumors had concurrent *FGFR2* fusion (*FGFR2-SORBS1* and *FGFR2-WAC*).

Table 1. Immunohistochemical and Molecular Profile of Poorly Differentiated Tumors.

Case	Immunohistochemistry	Mutations
1	Arginase-1 -, Glypican-3 -, Albumin -	TERT, APC, PTCH1, MAP2K1, TP53
2	Arginase-1 -, Glypican-3 -, CK7 +, CK19 +, Albumin focal +	TERT, MYC, POLE, TP53, AURKA
3	Albumin rare +	TERT, TFG-MET gene fusion
4	Arginase 1 -, Glypican-3 -, Hep Par 1 +, CK7 +, CK19 +, Albumin +	TERT, ERBB2, MYC, TP53
5	Arginase 1 -, CK19 +, CK 7 -, Albumin focal +	TERT, PDGFRA, CDKN2A, KIT, KDR, TSC1

Conclusions: *TERT* promoter mutation is an uncommon but significant finding in tumors previously characterized as ICC, and are grouped into two categories: 1) well-differentiated ICC-like phenotype with concurrent *FGFR2* fusion, 2) undifferentiated carcinomas without definitive morphologic, genetic or immunohistochemical evidence of hepatocellular or cholangiocarcinoma differentiation. The precise lineage of these TERT promotor mutation positive undifferentiated carcinomas is uncertain.

1547 Liver electron microscopy in the molecular era: A ten-year retrospective study shows it is still a valuable diagnostic tool

Cherise Meyerson[1], Bita Naini[2]
[1]UCLA Medical Center, Reseda, CA, [2]UCLA Medical Center, Santa Monica, CA

Disclosures: Cherise Meyerson: None; Bita Naini: None

Background: In the second half of the 20th century, diagnosis in liver pathology was enhanced by electron microscopy (EM), particularly for metabolic or cholestatic disorders in pediatric patients. However, with the advancement of biochemical and molecular testing, EM has been supplanted by other ancillary tests that can provide more definitive diagnoses. Nonetheless, we hypothesized that there may be cases in which EM provides valuable diagnostic findings that can have an impact on the clinical management.

Design: We searched for liver specimens at UCLA from 2008-2018 in which tissue was collected for EM. Patient age, sex, and type of specimen were recorded. We determined whether the tissue was collected in glutaraldehyde by the clinician, by the pathologist, or post-fixed from formalin-fixed paraffin-embedded (FFPE) tissue. We compared the final histopathologic diagnosis with the EM results and classified the results as follows: EM confirmed light microscopic (LM) findings; EM showed new findings; EM was non-diagnostic.

Results: EM was performed on 99 of 117 cases in which tissue was collected in glutaraldehyde. Median patient age was 1.4 y (range: 10 d-60 y) with 72 males and 45 females. Of those in which EM was performed, 90 were biopsies and 9 were total hepatectomies. Two were allograft livers, and the rest were native livers. Of the 99 cases, 83 had tissue collected in glutaraldehyde by clinicians at time of biopsy; 5 were collected by pathologists at time of grossing; 11 were post-fixed after formalin fixation. In 87 cases, the EM findings confirmed the LM

findings and did not show additional abnormalities. In 8 cases, EM showed diagnostic findings that were not seen by LM or suspected clinically (Table 1), including abnormal lysosomes consistent with Niemann-Pick disease, viral inclusions, mitochondrial abnormalities consistent with Reye syndrome, abnormal bile suggestive of progressive familial intrahepatic cholestasis type 1 (PFIC1), and inclusions consistent with fibrinogen storage disease. All of the non-diagnostic EM cases were those post-fixed from FFPE tissue.

Table 1. Cases with new electron microscopy findings

Age	Sex	Clinical Presentation	Light Microscopic Findings	Electron Microscopic Findings
4 y	M	Liver enzyme abnormalities, abdominal pain	No histopathologic abnormality	Microvesicular steatosis with normal mitochondria, suggestive of a metabolic disorder
5 y	F	Fever, cough, hepatosplenomegaly, pancytopenia	Enlarged hepatocytes and scattered Kupffer cells with swollen, foamy cytoplasm	Lysosomal figures, some with a lamellar internal configuration, consistent with Niemann-Pick disease
7 y	M	Fulminant hepatic failure of unknown etiology but suspected HHV-6 with positive PCR on serum	Severe acute hepatitis with massive hepatic necrosis	Viral inclusions consistent with HHV-6
10 y	F	Cough, fever, fatigue, altered mental status, with abnormal liver enzymes, hyperammonemia	Macrovesicular steatosis, occasional microvesicular steatosis	Microvesicular steatosis and swollen mitochondria with disrupted cristae, consistent with Reye syndrome
1 y	F	Cholestasis, pruritus, jaundice, diarrhea	Mild cholestasis and small duct injury	Canaliculi with brush border attenuation and coarse granular bile, suggestive of PFIC1
9 y	M	Incidentally found liver enzyme abnormalities	No histopathologic abnormality	Intracytoplasmic vacuoles with fingerprint-like inclusions, consistent with fibrinogen storage disease
60 y	M	Status post OLT for HCV cirrhosis with pruritus and jaundice	Allograft with recurrent chronic hepatitis C; mild steatosis and Mallory-Denk bodies	Secondary lysosomes with lamellar/whorled substructure, consistent with amiodarone toxicity
2 m	M	Jaundice, hyperbilirubinemia, failure to thrive	Paucity of intrahepatic bile ducts; no viral inclusions seen	Cytomegalovirus inclusion

Abbreviations: HHV-6, human herpes virus 6; PFIC1, progressive familial intrahepatic cholestasis type 1; OLT, orthotopic liver transplant; HCV, hepatitis C virus

Conclusions: Although EM confirmed the LM findings in the majority of cases, a few cases showed new diagnostic findings. All of the non-diagnostic EM cases were those procured from FFPE tissue. Therefore, collecting fresh tissue in glutaraldehyde and performing EM based on clinician and/or pathologist judgment, especially when there is suspicion for a metabolic disorder, is still recommended so as not to miss the rare cases.

1548 FGFR2 Alterations in Primary Intrahepatic Cholangiocarcinoma: Driving New Routes for Therapy

Kanish Mirchia[1], Laurie Gay[2], Julia Elvin[3], Jo-Anne Vergilio[3], J. Keith Killian[3], Nhu Ngo[3], Shakti Ramkissoon[4], Eric Severson[4], Amanda Hemmerich[4], Jon Chung[3], Siraj Ali[2], Alexa Schrock[3], Venkataprasanth Reddy[3], Vincent Miller[3], Robert Corona[5], Jeffrey Ross[6]

[1]SUNY Upstate Medical University, Syracuse, NY, [2]Cambridge, MA, [3]Foundation Medicine, Cambridge, MA, [4]Foundation Medicine, Morrisville, NC, [5]Syracuse, NY, [6]Upstate Medical University, Syracuse, NY

Disclosures: Kanish Mirchia: None; Laurie Gay: *Employee*, Foundation Medicine, Inc.; Julia Elvin: *Employee*, Foundation Medicine, Inc; Nhu Ngo: None; Eric Severson: *Employee*, Foundation Medicine, Inc.; Amanda Hemmerich: *Employee*, Foundation Medicine, Inc.; Alexa Schrock: *Employee*, Foundation Medicine, Inc.; Vincent Miller: *Employee*, Foundation Medicine Inc.; *Advisory Board Member*, Revolution Medicines; Jeffrey Ross: *Employee*, Foundation Medicine, Inc.

Background: Primary intrahepatic cholangiocarcinoma of the liver (CCA) is increasing which has encouraged the development of new therapy strategies targeting *FGFR2*. We performed a comprehensive genomic profiling (CGP) study designed to evaluate the clinical and genomic alteration (GA) features of *FGFR2* driven CCA.

Design: FFPE tissues from 2,975 clinically advanced CCA underwent hybrid-capture based comprehensive genomic profiling (CGP) to evaluate all classes of genomic alterations. Tumor mutational burden (TMB) was determined on ~1.1 Mbp of sequenced DNA and microsatellite instability (MSI) was determined by principal components analysis of optimized loci. PD-L1 expression was determined by immunohistochemistry on a subset of cases.

Results: CCA with *FGFR2* GA (FGFR2+) occur in slightly younger patients who are more often female (P-0.0001) (Table), when compared to CCA without *FGFR2* GA (FGFR2-). The number of GA per tumor was slightly higher in FGFR2- than FGFR2+ cases. The FGFR2+ cases included 83% with FGFR2 gene rearrangements/fusions, 11% with *FGFR2* short variant mutations, 2.5% with *FGFR2* amplifications,

and 3% with multiple *FGFR2* GA. Among clinically relevant (CR) GA, *IDH1*, a potential target in CCA, was significantly more frequently altered in the FGFR2- tumors as were *BRAF* and *ERBB2*. In the FGFR2+ group, additional genomic targets beyond FGFR2 were uncommon, but included MTOR pathway genes (*PIK3CA*, *PTEN*, *NF1*). *TP53* and *KRAS* GA were more common in FGFR2- cases and the *CDKN2A/B* GA frequency was similar in both. TMB, MSI high status and PD-L1 expression levels were slightly higher in FGFR2- than FGFR2+ tumors. Responses of FGFR2+ patients to FGFR inhibitors will be presented.

	CCA with *FGFR2* GA (FGFR2+)	CCA without *FGFR2* GA (FGFR-)
Number of Cases	354 (12%)	2,621 (88%)
Males/Females	M 35% F 65%	M 50% F 50%
Median age, years (range)	56 (21-87)	62 (16-88)
GA/tumor	3.6	4.0
Top Non-CR GA	*BAP1* 31% *CDKN2A* 29% *CDKN2B* 22% *TP53* 10% *ARID1A* 9%	*TP53* 34% *CDKN2A* 29% *KRAS* 24% *CDKN2B* 20% *ARID1A* 18%
Top CR GA	*FGFR2* 100% *PBRM1* 7% *PIK3CA* 7% *PTEN* 5% *IDH1* 3% *NF1* 1%	*IDH1* 18% *PBRM1* 12% *PIK3CA* 7% *BRAF* 6% *ERBB2* 5% *IDH2* 4%
MSI-High	0.3% (198 cases tested)	1% (2174 cases tested)
Mean TMB	2.3	3.1
Median TMB	1.7	2.4
TMB>10 mut/Mb	1.1%	3.4%
TMB>20 mut/Mb	0.6%	1.2%
PD-L1 IHC Positive	4.6% (43 cases tested)	7.6% (366 cases tested)

Conclusions: In CCA, FGFR2- tumors differ significantly in genomic profiles from FGFR2+ tumors with more opportunities for non-FGFR targeted therapies and more frequent presence of biomarkers predictive of positive responses to immunotherapies. For patients with refractory CCA, additional clinical studies for appropriate personalized therapy appears warranted.

1549 Distinct Histologic Differences in Response to TACE and Y90 Treatments in Hepatocellular Carcinoma and a Potential Diagnostic Pitfall

Recep Nigdelioglu[1], Xianzhong Ding[2], Stefan Pambuccian[3], Xiuzhen Duan[3], Yihong Ma[4]
[1]Loyola University, Maywood, IL, [2]Northbrook, IL, [3]Loyola University Medical Center, Maywood, IL, [4]Loyola University Medical Center, Hinsdale, IL

Disclosures: Recep Nigdelioglu: None; Xianzhong Ding: None; Stefan Pambuccian: None; Xiuzhen Duan: None; Yihong Ma: None

Background: Surgical treatments of hepatocellular carcinoma (HCC) include partial resection and liver transplantation. Transarterial chemoembolization (TACE) and Y90 radioembolization are the most common locoregional therapies for bridging patients to surgery. Pathology evaluation of post-TACE or Y90 treated surgical specimens is mostly focused on the extent of tumor necrosis and cancer staging. The histologic features of the response to the treatments in both HCC and surrounding benign parenchyma have not yet been described in detail. The aim of this study was to characterize the histologic response to TACE and Y90.

Design: We examined 33 HCC hepatectomy specimens from January 2015 to July 2018, including 20 with prior TACE, 4 Y90 and 9 combined treatment. The 9 combined treatment cases were categorized into Y90 group since only the Y90 affected areas were evaluated. H&E slides were examined by two pathologists and histologic changes were recorded. The results were analyzed by chi-square test and $p<0.05$ was considered statistically significant.

Results: There was a significant difference in necrotic patterns between TACE and Y90 treatments. TACE treated HCCs mainly showed coagulative necrosis and sharply demarcated from the background liver (Figure A), while paucicellular fibrosis with edema and gradual transition to adjacent parenchyma was a predominant feature in Y90 treated cases (Figure B). Exuberant dense ductular reaction was frequently seen adjacent to Y90-associated fibrosis. Y90-induced ductular reaction was extensive, multifocal and often associated with reactive atypia of ductular epithelium characterized by maze-like angulated growth pattern, increased nuclear-cytoplasmic ratio and hyperchromasia which could mimic cholangiocarcinoma (Figure C). On the other hand, ductular reaction following TACE was less common (2/20 vs 7/13, $p<0.05$) and was generally inconspicuous. The epithelium in the Y90-induced ductular reaction was immuno-reactive to CD56 (Figure D) in selected cases, which is unusual for cholangiocarcinoma.

Figure 1 - 1549

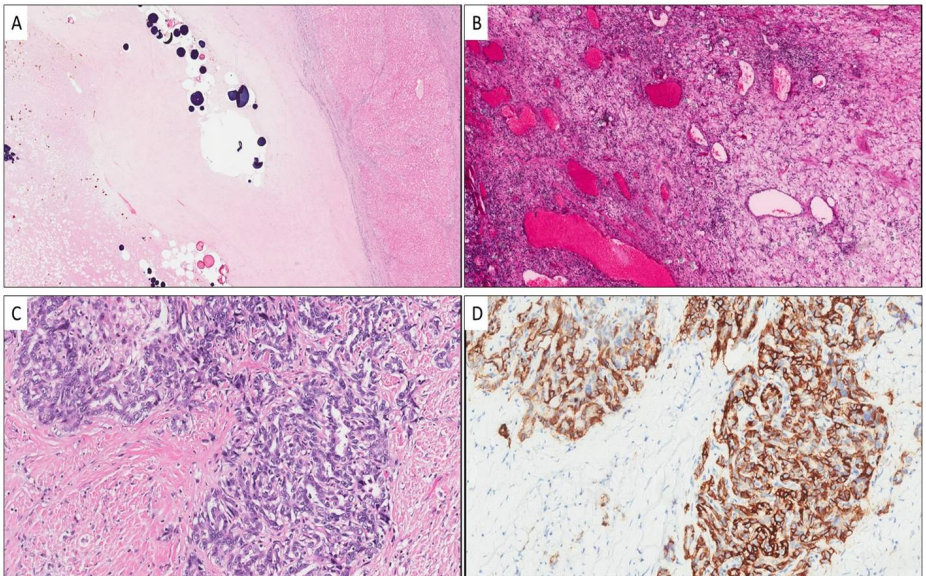

Conclusions: There were distinct histologic differences in response to TACE and Y90 treatments. Y90-induced ductular reaction was exuberant which could be a diagnosis pitfall and should not be over-interpreted as cholangiocarcinoma or combined HCC-cholangiocarcinoma. Immunohistochemical stain for CD56 may be useful to avoid this pitfall.

1550 Histologic Sub-classification of cirrhosis: Comparison of Laennec and Jain-Garcia systems

Maria Olave[1], Ilke Nalbantoglu[2], Guadalupe Garcia-Tsao[3], Dhanpat Jain[4]
[1]Yale University, New Haven, CT, [2]Woodbridge, CT, [3]Yale New Haven Hospital, New Haven, CT, [4]Yale University School of Medicine, New Haven, CT

Disclosures: Maria Olave: None; Ilke Nalbantoglu: None; Dhanpat Jain: None

Background: Cirrhosis is a dynamic process and can regress. Different classification systems exist for assessing regression and architectural remodeling. The two classification systems, namely Laennec and Jain-Garcia, sub-classify it into mild, moderate and severe disease (4a, 4b, 4c). Both of these systems take into consideration the nature of fibrous septa and cirrhotic nodules, show good correlation with clinical severity of cirrhosis, especially hepatic venous pressure gradient (HPVG). Of note, HPVG measurements are operator dependent and not available at all centers, which makes histologic assessment of liver biopsies critical for assessment of severity of cirrhosis. The aim of the study was to compare the inter-observer variability of these two systems among pathologists.

Design: 50 cases of liver needle biopsies with a confirmed pathologic diagnosis of cirrhosis were randomly selected from our pathology database for the study. The inclusion criteria included 1) size of biopsy >2cm 2) availability of reticulin, trichrome and H&E stains for each case. The cases were coded and randomly numbered. The three stains were independently and blindly reviewed by three pathologists with varying degrees of experience; 1 resident, 1 Associate Professor, and 1 Professor, and were scored as 4a, 4b and 4c using both systems. The inter-observer variability was assessed using Fleiss' kappa statistical test.

Results: Among the three pathologists, the kappa agreement of cirrhosis sub-classification using the Jain-Garcia system was 0.64 (substantial agreement), and 0.57 (moderate agreement) using the Laennec system. For each histologic group (4a, 4b, 4c), the kappa agreement was 0.58, 0.48, and 0.79 respectively, using the Jain-Garcia System, and 0.55, 0.45 and 0.66 respectively using the Laennec system.

Conclusions: Cirrhosis progression and regression is now a well-established phenomenon, making histologic sub-classification of cirrhosis clinically relevant. In our study, both systems of cirrhosis sub-classification demonstrate good interobserver correlation, with Jain-Garcia system showing slightly better correlation despite varying levels of pathology experience. Jain-Garcia system also appears to increase the inter-observer agreement between individual histologic categories.

1551 Portal Vein Sclerosis is Associated with Higher Stage of Disease, Portal Inflammation, and Portal and Centrizonal Arterialization in Adults with Classic PI*ZZ Alpha-1 Antitrypsin Deficiency

Andrea Olofson[1], Jinping Lai[2], Xiuli Liu[2]
[1]Gainesville, FL, [2]University of Florida, Gainesville, FL

Disclosures: Andrea Olofson: None; Jinping Lai: None; Xiuli Liu: None

Background: Classic PI*ZZ alpha-1 antitrypsin deficiency (A1ATD) is an inherited metabolic disorder that predisposes the affected individual to chronic liver disease as the retained A1AT glycoprotein in the endoplasmic reticulum contributes directly to liver injury. Our pilot study revealed that liver fibrosis is associated with the presence of portal inflammation and numerous A1AT granules in the liver biopsy. However, vascular changes have not been examined in adults with A1ATD.

Design: Fourteen adults with classic PI*ZZ A1ATD were recruited from North America and prospectively enrolled in teh study. Liver biopsy was performed and analyzed for fibrosis using METAVIR stages F0-F4. PAS-positive, diastase-resistant (PAS/D) staining identified A1AT accumulation. PAS/D+ granules present in a high power field were scored as follows: less than few (none to 5-20 hepatocytes with globules) or numerous (≥ 20 hepatocytes with globules). Portal inflammation (none to minimal vs. at least mild), lobular inflammation (absent or present), hepatocyte ballooning, hepatocyte apoptosis, dysplasia, steatosis (>5%), iron deposition, and lipofuscin were assessed. In addition, portal vein sclerosis, subendotheliitis, arterialization of portal vein, and occurrence of centrizonal arterioles were also recorded using previously published criteria (Gill RM et al., 2011; Lee H et al, 2016).

Results: This cohort included 11 females and 3 males with an average age of 58 years (range 28-74). The biopsies measured 1.6 cm (range 1.0 - 2.7) with an average of 15 portal triads (range: 10-27). Eleven biopsies (78.5%) showed portal vein sclerosis. Portal vein sclerosis is associated with higher fibrosis stage, portal inflammation, as well as portal and centrizonal arterialization [Table 1].

Feature	No portal vein sclerosis (n=3)	Portal vein sclerosis (n=11)	P value
Mean age (SD), years	56.3 (11.1)	58.9 (12.6)	0.75
Gender, male (%)	1 (33.3)	2 (18.2)	0.51
Presence of at least mild portal inflammation, n (%)	0 (33.3)	8 (72.7)	0.024
Presence of lobular inflammation, n (%)	3 (100)	6 (54.5)	0.15
Presence of hepatocyte ballooning, n (%)	1 (33.3)	3 (27.2)	0.84
Presence of hepatocyte apoptosis, n (%)	3 (100)	6 (54.5)	0.15
Presence of large cell dysplasia, n (%)	0 (0)	2 (18.2)	0.42
Presence of numerous PAS/D+ granules, n (%)	0 (0)	6 (54.5)	0.09
Presence of > 5% steatosis, n (%)	1 (33.3)	3 (27.2)	0.83
Presence of iron in hepatocytes, n (%)	0 (0)	0 (0)	1
Significant lipofuscin, n (%)	2 (66.7)	5 (45.4)	0.54
Presence of centrizonal arteriole, n (%)	0 (0)	7 (63.6)	0.05
Portal vein subendotheliitis, n (%)	0 (0)	5 (45.4)	0.15
Presence of portal arterialization, n (%)	1 (33.3)	11 (100)	0.0014
Fibrosis ≥2, n (%)	0 (0)	7 (63.6)	0.02

Conclusions: In adults with classic PI*ZZ A1ATD, portal vein sclerosis occurs in 78.5% liver biopsies and is associated with higher stage of disease, portal inflammation, and portal and centrizonal arterialization.

1552 Evaluation of the American Joint Committee on Cancer (AJCC) 8th Edition Staging System for Hepatocellular Carcinoma in 1,034 Patients with Curative Resection

Sujin Park[1], Sangjoon Choi[1], Cheol-Keun Park[1], Dong Hyun Sinn[1], Jong Man Kim[1], Sang Yun Ha[1]
[1]Samsung Medical Center, Seoul, Korea, Republic of South Korea

Disclosures: Sujin Park: None

Background: Recently, 8th edition staging system of the American Joint Committee on Cancer (AJCC) was released with change in T stage. We validated the prognostic value of the new AJCC staging system in comparison to the previous 7thedition.

Design: Total 1,034 patients who had undergone curative resection as the initial treatment for hepatocellular carcinoma at Samsung Medical Center, Seoul, Korea, between 2008 and 2012, were enrolled in this study. Pathology T stage was determined as AJCC 7th and 8th edition, respectively. Recurrence free survival (RFS) was estimated using the Kaplan-Meier method and compared by log-rank test. The analysis of the time dependent receiver-operating-characteristic (ROC) curves for censored survival data was used to compare the capability of the two models to predict tumor recurrence.

Results: The 1-, 3- and 5-year RFS rates were 77.7%, 61.8% and 56.4%, respectively. Among 478 T1 patients by 7th edition, 157 were re-classified as T1a, and 321 as T1b by 8th edition. Stage migration was observed in 63 patients (6.1%); from T2 to T1a in 45 patients and from T3 to T4 in 18 patients. The 2 year AUC value were comparable in 7th and 8th edition (0.693 vs. 0.690), indicating similar predictive ability. RFS was not different between T1a and T1b by 8th edition (p=0.727). For solitary tumors ≤2cm (T1a by 8th edition), those with microvascular invasion (n=171) had shorter RFS than those without it (n=54) (p=0.016), although there is no such distinction in 8th edition. Tumors involving a major branch of portal vein or hepatic vein (T4 by 8th edition and T3b by 7th edition, n=18) showed shorter RFS than multifocal tumors at least one of which is >5cm (T3 by 8th edition and T3a by 7th edition, n=38) (p=0.006), supporting the change in 8thedition. RFS was comparable between solitary tumors >2cm with vascular invasion (n=375) and multifocal tumors ≤5cm (n=92), which were classified as single category T2 in both 7th and 8th editions. For multifocal tumors≤5cm, survival showed no difference according to presence of vascular invasion.

Conclusions: The AJCC 8th edition staging system for HCC showed comparable predictive performance to the 7th edition. It is desirable in future revision to consider sub-stratification of solitary tumors ≤2cm(T1a) depending on the presence of vascular invasion, which is not included in 8th edition. Further studies are required to validate these findings.

1553 The Prognostic Role of Apelin Receptor Expression in Hepatocellular Carcinoma Treated with Curative Surgical Resection

Sujin Park[1], Taebum Lee[2], Cheol-Keun Park[1], Sang Yun Ha[1]
[1]Samsung Medical Center, Seoul, Korea, Republic of South Korea, [2]Samsung Medical Center, Sungkyunkwan University School of Medicine, Seoul, Korea, Republic of South Korea

Disclosures: Sujin Park: None

Background: Apelin and apelin receptor (APJR) have been known to be involved in the regulation of angiogenesis, and high apelin level is related to poor outcome in several cancer types. Recently, apelin has been highlighted as a promising target in the treatment of metabolic disease, and some significant results on APJR antagonists in cancer treatment has been reported in preclinical level. However, the expression of apelin or APJR and its prognostic effect in hepatocellular carcinoma(HCC) remain unknown.

Design: We evaluated the APJR expression in 288 curatively resected HCCs using immunohistochemistry, and evaluated its correlation with clinicopathologic features and the prognostic effect.

Results: High APJR expression was observed in 72 out of 288 HCCs (25%). High APJR expression was significantly associated with younger age (*P*=0.033), higher Edmondson grade (*P*<.001), advanced AJCC T-stage (*P*<.001), high AFP level (*P*=0.023), presence of microvascular invasion (*P*<.001), intrahepatic metastasis (*P*=0.004), absence of liver cirrhosis (*P*=0.035) and early recurrence (*P*=0.029). During a median 119 months of follow-up period, high expression group showed shorter recurrence free survival (*P*<.001) and overall survival (*P*=0.001) than low expression group. In multivariate analysis, high APJR expression was an independent predictor of shorter recurrence free survival (Hazard Ratio 1.49; 95% confidence interval 1.08-2.05), *P*=0.016), in addition to well-known prognostic factors such as intrahepatic metastasis and hepatitis virus infection.

Conclusions: We described high APJR expression and its prognostic effect in HCC. Emerging target agents against apelin or APJR could be applicable in patients of HCC with high APJR expression.

1554 Co-Expression of Keratin 19 and Mesenchymal Markers for Evaluation of Epithelial-Mesenchymal Transition and Stem Cell Niche Components in Primary Biliary Cholangitis (PBC)

John Paulsen[1], Briana Zeck[2], Luis Chiriboga[3], Katherine Sun[2], Neil Theise[2]
[1]NYU School of Medicine, New York, NY, [2]NYU Langone Health, New York, NY, [3]New York University, New York, NY

Disclosures: John Paulsen: None; Briana Zeck: None; Luis Chiriboga: None; Katherine Sun: None; Neil Theise: None

Background: It is controversial whether epithelial-to-mesenchymal transition (EMT) or mesenchymal-to-epithelial transition (MET) occurs during liver injury and repair. In PBC, small keratin 19 (K19) positive extraportal cholangiocytes (EPCs; comprising canals of Hering, ductules and ductular reactions) can exhibit a spindled morphology suggestive of EMT/MET. EPCs are also thought to harbor the hepatobiliary stem/progenitor cells (HSPCs), the niche for which is thought to comprise an HSPC juxtaposed to a mesenchymal cell. However, positioning of niche components has not yet, to our knowledge, been histologically visualized. The aim of this study was to use

sequential multiplex immunohistochemistry (SM-IHC) to evaluate for epithelial and mesenchymal co-expression by EPCs including S100-A4, a putative marker of EMT/MET. Also, mesenchymal cells associated with K19+ EPCs were assessed as potential HSPC niche components.

Design: 10 archival cases of stage 1-3 PBC were stained by SM-IHC (consisting of repeated cycles of staining, whole-slide digital image acquisition and antibody stripping). This technique allowed the 4 stains to be formed on the identical slide: K19 (epithelial) and vimentin, αSMA, S100-A4 (mesenchymal). Using Leica Slidepath Digital Image Hub software, expression patterns of the 4 antibodies in EPCs and nearby cells were concurrently evaluated for each specimen. Statistical analysis was performed with chi-squared test.

Results: In each specimen, co-expression of K19 and vimentin and/or S100-A4 was observed in some EPCs (Table 1 & Figure 1). Co-expression of K19/αSMA was not observed. There were statistically significant differences in numbers of EPCs that co-expressed K19/S100-A4 and K19/S100-A4/vimentin when comparing early stage (1) and intermediate stage (2-3) PBC (p values ≤ 0.05). In regard to possible mesenchymal components in an HSPC niche, 88.9% (± 9.6) of EPCs were closely associated with a vimentin-positive stromal cell.

Table 1

Case	Patient Age/Sex	Stage of PBC (Scheuer)	% K19+ EPCs with Vimentin Co-Expression Only	% K19+ EPCs with S100-A4 Co-Expression Only	% K19+ EPCs with Vimentin & S100-A4 Co-Expression	% K19+ EPCs Associated with Vimentin+ Stromal Cell
1	58 / F	1	20%	0%	20%	90%
2	55 / M	1	0%	0.4%	0%	100%
3	41 / F	1	27.3%	18.2%	18.2%	90.1%
4	54 / M	1	19.0%	0%	76.6%	85.7%
5	38 / F	1	38.4%	0%	15.4%	92.3%
6	52 / F	1	0%	6.7%	66.7%	66.7%
7	52 / F	2	18.1%	0%	81.9%	100%
8	26 / F	2	5.6%	27.8%	27.8%	83.3%
9	64 / F	3	20%	0%	80%	90%
10	51 / F	3	9.1%	45.5%	0%	90.9%
Mean (x̄)			15.8%	9.9%	38.7%	88.9%

Figure 1 - 1554

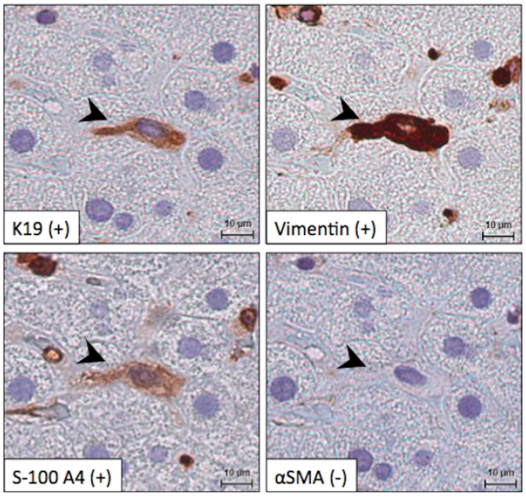

Figure 1: Sequential multiplex immunohistochemical staining shows a spindled extraportal cholangiocyte (*arrowhead*) with co-expression of K19, vimentin and S-100 A4.

Conclusions: Co-expression of epithelial and mesenchymal markers by EPCs is evidence for EMT/MET in PBC. While vimentin positivity may occur in epithelial cells, co-expression with S100-A4 more specifically suggests potential bidirectional transition occurring in EPCs. Lack of αSMA co-expression suggests that this transition does not involve differentiation towards or from hepatic stellate cells/myofibroblasts. Vimentin-positive stromal cells are frequently juxtaposed to EPCs, supporting an epithelial:mesenchymal relationship within the HSPC niche.

1555 Unique Clinicopathologic, Long-term Follow-up and IgG4 Features Distinguishing Plasma cell Rich-rejection and Isolated Central Perivenulitis from Acute Cellular Rejection and De Novo Autoimmune Hepatitis

Maryam Pezhouh[1], David Escobar[2], Audrey Deeken-Draisey[3], M. Sambasiva Rao[4], Guang-Yu Yang[4]
[1]Northwestern University Feinberg School of Medicine, Chicago, IL, [2]McGaw Medical Center of Northwestern University, Chicago, IL, [3]Northwestern Memorial Hospital, Chicago, IL, [4]Northwestern University, Chicago, IL

Disclosures: Maryam Pezhouh: None; David Escobar: None; Audrey Deeken-Draisey: None; M. Sambasiva Rao: None; Guang-Yu Yang: None

Background: Plasma cell rich-rejection (PCR) and isolated central perivenulitis (ICP) are increasingly recognized but poorly understood categories of liver allograft dysfunction. PCR previously known as plasma cell hepatitis can mimic autoimmune hepatitis (AIH) causing diagnostic challenges for pathologists. Although Central perivenulitis (CP) can be seen in conjunction with portal based acute cellular rejection (ACR), pathophysiology and significance of CP in isolation have not been well studied. Here, we seek to investigate the clinicopathologic features, long-term follow-up and IgG4 expression of such patients.

Design: We searched our pathology data base for post-transplant liver biopsies with PCR and ICP and identified 19 and 8 cases, respectively. We included 10 post-transplant age and sex matched liver biopsies with ACR and 16 de novo AIH cases as control groups. Histopathological parameters such as portal and lobular inflammation, presence of necrosis, fibrosis and perivenulitis were documented. Periportal and centrilobular plasma cell infiltration was scored as <30, 31-50 and >50. Immunohistochemichal staining for IgG4 was performed on all samples and counted in one representative high power field (HPF, 40x objective).

Results: PCR and ICP occur significantly late at a mean of 8.5 and 7 years post-transplant respectively compared to ACR occurring at a mean of 3.2 years ($p < 0.05$). Both PCR and AIH showed high plasma cell infiltrate in periportal and centrilobular areas compared to ACR and ICP ($p < 0.05$); however, the number of plasma cell infiltrate in PCR was not significantly different than AIH. PCR group showed higher IgG4+ plasma cells per HPF (mean of 52) compared to AIH group (mean of 10, $p < 0.05$). ICP and ACR group had significantly less IgG4+ plasma cell (2 and 1.5 per HPF, respectively) compared to PCR ($p < 0.05$). More than 25 IgG4+ Plasma cells per HPF was present in 47% (9/19) of PCR compared to 6% (1/16) of AIH ($p<0.05$, table 1). Follow-up data showed that 3/19 (16%) of PCR group died due to complication from liver disease after a mean of 1.6 years and re-transplantation was required in one patient (5%). None of ICP and ACR patients needed re-transplantation.

Table 1. Comparison of cases with absolute number of IgG4+ plasma cells more than 25 per high power field in PCR and AIH group

	Number of cases with IgG4+ Plasma cells >= 25 (%)	Number of cases with IgG4+ Plasma cells <25 (%)
PCR	9/19 (47%)	10/19 (53%)
AIH	1/16 (6%)	15/16 (94%)
The chi-square statistic is 7.1957 (*p*-value=0.007308).		

Conclusions: Our results indicate that marked IgG4 (+) plasmacytic infiltration is a characteristic feature of PCR which had a more aggressive behavior. Although PCR and AIH show overlapping histopathologic features, IgG4 expression seems to be a useful marker to separate liver allografts with PCR from AIH in most cases.

1556 PD-L1/PD-1 In Hepatocellular Carcinoma: An Institutional Review

Julio Poveda[1], Melissa Duarte[2], Patricia Denise Jones[1], Aneesa Chowdhury[1], Kevin Brown[1], Monica Garcia-Buitrago[3]
[1]University of Miami, Miller School of Medicine, Miami, FL, [2]University of Miami/Jackson Health System, Miami, FL, [3]University of Miami Miller School of Medicine/Jackson Health System, Miami, FL

Disclosures: Julio Poveda: None; Melissa Duarte: None; Patricia Denise Jones: None; Aneesa Chowdhury: None; Kevin Brown: None; Monica Garcia-Buitrago: None

Background: Hepatocellular carcinoma (HCC) is the 5th leading cause of cancer. In the modern age of immunotherapy, Keytruda (pembrolizumab) has emerged as a promising chemotherapeutic agent that works against the programmed cell death-1(PD-1)/PD1 ligand (PD-L1) axis. The aim of our study is to determine if age, tumor size or lymphovascular invasion (LVI) influence the pattern of PD-1 and PD-L1 expression and thus, receptiveness to immunotherapy.

Design: A retrospective search of our pathology database at the University of Miami/Jackson Health System over the period of five years was undertaken. A total of 117 explanted and resected liver cases involved by HCC were reviewed. We evaluated the expression of PD-L1 (22C3) in the tumor cell count and PD1 within tumor hot spots using immunohistochemistry (IHC). Tumor proportion scoring (TPS) was performed according to the pembrolizumab guideline for tumor expression. Also, tumor infiltrating lymphocytes (TILs) were quantified within tumor hot spots using CD3 IHC.

Results: PD-L1 show low expression in tumor cells in 12% (15/117) with a TPS up to 20% (range 1-20%), and was negative in 87% (102/117) HCC. Within the positive tumor subset, the average age was 55.7 (range 27-64) and average size of largest tumor was 6.41 cm (range: 1.5-17.0 cm). Within the PD-L1 negative tumor subset, the average age was 61 (range: 50-72), and average size of largest tumor was 4.6 cm (0.6-17.0 cm). Additionally, within the PD-L1 positive tumors, 60% (9/15) showed LVI in contrast to 29% (30/102) in PD-L1 negative tumors.? The mean PD-1 expression in TILs in PD-L1 positive HCC was 750 while the mean in PD-L1 negative HCC was 340. The mean count of CD3 TILs in PDL-positive HCC was 653 while the mean in PD-L1 negative HCC was 239.

Conclusions: Our series demonstrated a PD-L1 expression, shown by TPS, in 12% of HCC cases. PD-L1 positive HCC were associated to more aggressive pathological features such as larger tumor size and presence of LVI compared with PD-L1 negative HCC. Patients with PD-L1 positive tumors tend to be younger than the negative subset. PD-L1 tumor expression positively correlated with higher counts of PD-1 positive and CD3 positive TILS.

Thus, our study identified a subset of PD-L1 positive, high CD3 positive TILs HCC with more aggressive pathologic features which can be treated with pembrolizumab immunotherapy. Further research is necessary to evaluate the clinical response.

1557 Histologic Patterns of Intestinal Failure-Associated Liver Disease: Correlation with Underlying Disease

Madhavi Rayapudi[1], Stephen Ward[2], Swan Thung[3], Thomas Schiano[1], Maria Isabel Fiel[2]
[1]Mount Sinai Medical Center, New York, NY, [2]Icahn School of Medicine at Mount Sinai, New York, NY, [3]Mount Sinai Hospital, New York, NY

Disclosures: Madhavi Rayapudi: None; Stephen Ward: None; Thomas Schiano: None; Maria Isabel Fiel: None

Background: Intestinal failure-associated liver disease (IFALD) is seen in patients treated with parenteral nutrition and can lead to liver failure. Classically, IFALD is associated with cholestatic liver disease in infants and steatohepatitis in older children and adults, though other patterns can be seen. We endeavored to better characterize histologic patterns of IFALD and uncover associations with underlying disease leading to short gut syndrome (SGS).

Design: We collected cases of adult patients with SGS from our institution who underwent either isolated intestinal or combined multi-visceral transplant from 2001-2014 and had available liver tissue for evaluation (biopsy or explant) at the time of intestinal transplant. All liver slides were reviewed by three pathologists. Steatohepatitis, cholestasis, bile duct damage, ductular proliferation, and lobular inflammation were assessed and other features (e.g. ceroid macrophages, nodular regenerative hyperplasia) were noted. Clinical data was obtained retrospectively from the chart review.

Results: We identified 37 adult patients with SGS (mean age 50, range 25-72) that were available for evaluation. Evidence of IFALD was seen in 32 cases (86%). Of the patients who showed IFALD, three histologic patterns were recognized: steatohepatitic (15 cases; 47%), cholestatic (10 cases; 31%), and hepatitic (6 cases; 19%); while 1 case (3%) showed a mixed steatohepatitic/cholestatic pattern. Table 1 shows the average age, length of TPN and underlying disease for the histologic patterns. There was a trend toward older patients in the cholestatic vs steatohepatitic groups ($p=0.07$; Student t test). There was no significant difference in length of TPN. Eight patients underwent intestinal transplantation for Crohn's disease, 6 showed IFALD (3 cholestatic, 2 hepatitic, and 1 mixed cholestatic and steatohepatitic patterns), but none showed isolated steatohepatitic pattern ($p<0.05$ Fisher exact test). Two patients underwent intestinal transplantation for scleroderma and neither showed steatohepatitic pattern (1 cholestatic and 1 hepatitic pattern).

	Steatohepatitic	Cholestatic	Hepatitic	Combined Steatohepatitic and Cholestatic
	(n=15)	(n=10)	(n=6)	(n=1)
Average Age (range)	49(36-60)	56(25-72)	46(36-59)	54
Length of TPN in years	3.3	1.1	1.5	1
Ischemia/trauma	8 (53%)	6 (60%)	2 (33%)	0
Tumor	5 (33%)	0	0	0
Pseudo obstruction	2 (13%)	0	1 (17%)	0
Crohn's disease	0	3 (30%)	2 (33%)	1 (100%)
Scleroderma	0	1 (10%)	1 (17%)	0

Conclusions: Our study shows that the majority (86%) of adult patients with SGS show evidence of IFALD at the time of intestinal transplant. We identified three histologic patterns and correlated them with the underlying disease. Interestingly, we found that Crohn's disease was associated with non-steatohepatitic patterns of liver injury. This may indicate differences in nutritional or inflammatory states of the patients.

1558 Myxoid Hepatic Adenoma: A Subtype with a High Risk for Malignant Transformation

Daniel Rowan[1], Rondell Graham[1], Saba Yasir[1], Michael Torbenson[1]
[1]*Mayo Clinic, Rochester, MN*

Disclosures: Daniel Rowan: None; Rondell Graham: None; Saba Yasir: None; Michael Torbenson: None

Background: Myxoid hepatic adenoma is a rare subtype of hepatic adenoma characterized by abundant extracellular myxoid material dissecting tumor sinusoids. Due to their rarity, the morphology and clinical characteristics of these tumors remain poorly understood. We report additional cases of myxoid hepatic adenoma and their clinicopathologic features.

Design: The surgical pathology database and author's consultation files were searched for hepatic adenomas with myxoid change. Four previously unreported cases were identified. Clinical and gross information were obtained from the original pathology report. Each case was reviewed to assess the histologic features of the tumors and to identify any associated lesions. Immunohistochemical stains for liver fatty acid binding protein-1 (LFABP1), C-reactive protein (CRP), and Beta-catenin were performed on three cases. Alcian blue and mucicarmine stains were also performed.

Results: Four cases of myxoid hepatic adenoma were identified. All patients were female with a mean age of 55 years (range: 27-76). All lesions were unifocal, with a mean tumor size of 12.2 cm (range: 8.8-14.0 cm). All adenomas were located in the right hepatic lobe. Morphologically, the tumors were well circumscribed lesions composed of thin cords of hepatocytes separated by abundant extracellular myxoid material. The hepatocytes contained relatively uniform round nuclei. Mitotic figures were very rare. In all three cases tested, LFABP1 was lost, CRP was negative and there was no nuclear expression of beta-catenin. The extracellular myxoid material was negative for mucicarmine and positive for Alcian blue. Three of the cases had an associated hepatocellular carcinoma (HCC). HCC occurred in the three oldest patients (57, 61, 76 years old) while the youngest patient (27 years old) did not have malignant transformation. Two cases had associated well-differentiated HCCs and one was associated with a moderately differentiated HCC.

Figure 1 - 1558

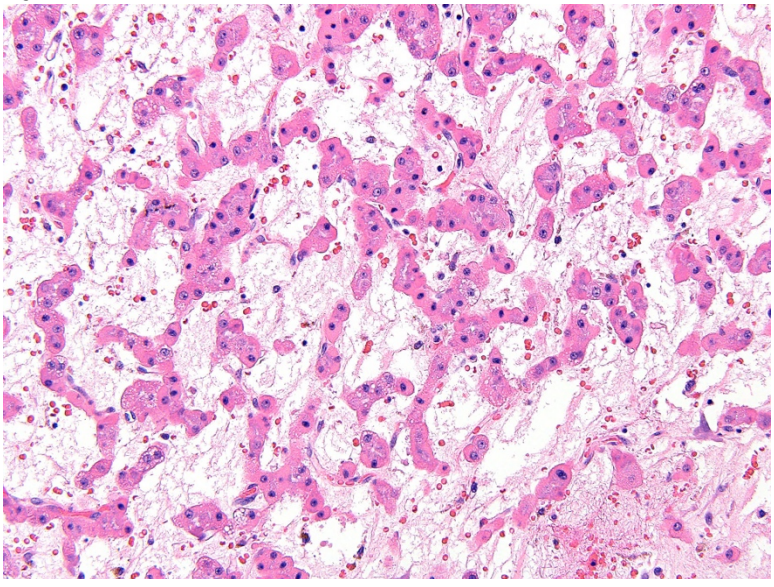

Conclusions: Myxoid hepatic adenomas are rare and have a distinctive morphology. All cases tested showed LFABP1 loss. It is important to recognize this subtype of hepatic adenoma because it appears to be associated with a high risk of malignant transformation.

1559 Histopathological features of Sickle Cell Hepatopathy: a Multi-Institutional Study

Omer Saeed[1], Nicole Panarelli[2], Kavita Umrau[3], Hwajeong Lee[4], Maria Westerhoff[5], Jerome Cheng[5], Jingmei Lin[6]
[1]Indianapolis, IN, [2]Montefiore Medical Center, Scarsdale, NY, [3]Albany Medical College, Albany, NY, [4]Albany Medical Center, Albany, NY, [5]University of Michigan, Ann Arbor, MI, [6]Indiana University, Indianapolis, IN

Disclosures: Omer Saeed: None; Nicole Panarelli: None; Kavita Umrau: None; Hwajeong Lee: None; Maria Westerhoff: None; Jerome Cheng: None; Jingmei Lin: None

Background: Histopathological features of sickle cell hepatopathy (SCH) are not well characterized and the value of liver biopsy remains to be defined. We systematically evaluated features of SCH in liver biopsy samples in order to define the spectrum of histologic abnormalities in this disorder.

Design: A total of 47 liver biopsies from 42 patients who had sickle cell hemoglobinopathy from 4 medical institutes were reviewed. The histopathologic features, including pattern, degree and extent of involvement, were noted in each biopsy. Relevant clinical data were collected retrospectively.

Results: The average age of patients was 27 years (range, 3-64 years). 22 were female (54%). Among 39 patients with known hemoglobin type, 33 had HbSS, 3 had HbSC and 3 had sickle cell trait. The main indications for liver biopsy were hyperbilirubinemia and elevated liver functional tests. Seven out of 21 patients with available clinical data had hepatomegaly confirmed by imaging. The top 3 most common morphological patterns were sinusoidal dilatation (73.9%), intrasinusoidal sickling red cells (73.2%), and sinusoidal congestion (59.5%). Zone 3 hepatocyte atrophy and dropout that were likely associated with severe form of sinusoidal dilatation and congestion presented in 33.4% and 16.7% of cases, respectively. Moderate to severe hepatic hemosiderosis (3+ and above) was a common finding (54.3%). Portal inflammation, lobular inflammation and interface activity were typically mild to minimal and present only in a minority of cases (28.5%, 14.3% and 2.4%, respectively). Mild to moderate bile duct injury occurred in 12.2% of the cases. Advanced fibrosis (bridging or cirrhosis) were present in 26.2% of the cases. Only 2.4% of biopsies showed cholestasis.

Conclusions: SCH is a clinicopathological diagnosis which includes marked hyperbilirubinemia, histopathologic abnormalities and/or hepatomegaly. Common diagnostic histopathological features of SCH include sinusoidal dilatation, intrasinusoidal sickling and sinusoidal congestion in an uninflamed or less inflamed background. Marked hemosiderosis that is related to multiple blood transfusions is a common finding that may result in additional hepatic damage. Liver biopsy is useful to confirm SCH and exclude other, potentially treatable, causes of liver disease. Pathologists should note that significant portal and lobular inflammation, interface activity and bile duct injury are not typical features of SCH and may be suggestive of other pathologies.

1560 Effects of Direct-Acting Antiviral (DAA) Therapy on Hepatic Macrophage and Lymphocyte Populations in Patients with Chronic HCV Infection

Omar A. Saldarriaga[1], Bradley Dye[1], Judy Pham[1], Adam Booth[1], Camila Simoes[1], Netanya Utay[2], Heather Stevenson-Lerner[1]
[1]University of Texas Medical Branch, Galveston, TX, [2]The University of Texas Health Science Center at Houston, Houston, TX

Disclosures: Omar A. Saldarriaga: None; Bradley Dye: None; Judy Pham: None; Adam Booth: None; Camila Simoes: None; Netanya Utay: None; Heather Stevenson-Lerner: None

Background: Hepatitis C virus (HCV) is still the main cause of cirrhosis and hepatocellular carcinoma (HCC) in the US even with DAA treatment. According to the CDC, the incidence of HCV is increasing due to the opioid epidemic. Despite numerous clinical studies, relatively few have evaluated the changes in the hepatic microenvironment after elimination of the virus.

Design: We collected liver biopsies from 10 patients with chronic HCV infection before and after DAA treatment to assess changes in inflammatory activity, intrahepatic macrophage and lymphocyte populations, and fibrosis stage. Initially, conventional scoring systems were used to determine the amount of inflammation and fibrosis, respectively; we then used two multiplex immunofluorescence panels (CD68/CD163/MAC387/CD14/CD16 and CD3/CD4/CD8/FOXP3/CD56) followed by multispectral imaging to phenotype and quantify intrahepatic macrophages and lymphocytes pre- and post-DAA treatment. Multiplex stained slides were acquired using the Vectra 3 Platform (PerkinElmer) and images were analyzed using inForm and Visiopharm software. The amount of fibrosis was quantified by digitally scanning Masson's trichrome stains using an Aperio ImageScope® slide scanner and importing the acquired images into Nikon NIS Elements® software to calculate the collagen proportionate area (CPA= area of fibrosis/total area) x100. Ten control patients without HCV or known liver disease were also analyzed.

Results: All study patients (10/10) achieved sustained virologic response (SVR) with no detection of viral RNA at 24 weeks post-treatment and showed significantly decreased transaminase levels after clearing the virus. Fifty percent (5/10) of the patients showed persistent lymphocytic portal inflammation post-treatment. Multiplex staining and spectral imaging analysis revealed unique macrophage and lymphocyte populations in the portal tracts and lobules in the HCV+ patients when compared to controls and the post-treatment biopsies obtained after SVR. Although the calculated CPA was not significantly different in the liver biopsies before and after treatment,

macrophage and lymphocyte infiltration increased in patients with higher stages of fibrosis when compared to those with low or minimal fibrosis.

Conclusions: In summary, DAA treatment in this patient cohort provided a unique opportunity to compare changes in the hepatic microenvironment in the same patient with and without the presence of the HCV virus.

1561 Autoimmune Hepatitis/Primary Biliary Cholangitis Overlap: Treatment Response and Histologic Correlates

Shula Schechter[1], Maria Westerhoff[1], Jonathan Mowers[2], Alisa Likhitsup[3], Laura Lamps[4]
[1]University of Michigan, Ann Arbor, MI, [2]Ann Arbor, MI, [3]University of Michigan Hospitals, Kansas City, MO, [4]University of Michigan Hospital, Ann Arbor, MI

Disclosures: Shula Schechter: None; Maria Westerhoff: None; Jonathan Mowers: None; Alisa Likhitsup: None; Laura Lamps: None

Background: Autoimmune hepatitis (AIH)-primary biliary cholangitis (PBC) overlap syndrome can be challenging to diagnose. Hepatologists often use the Paris Criteria, which combine clinical, laboratory, and histologic findings. Pathologists, on the other hand, may be unaware of the other variables at the time of biopsy. The goals of this study were to evaluate a cohort of patients with histologically suggested AIH/PBC overlap, determine the proportion who met Paris criteria, and evaluate response to treatment.

Design: Liver biopsies from 23 patients (1 male, 22 females; median age 56, range 13-74) with pathology diagnoses suggestingAIH/PBC overlap were subjected to blinded histologic evaluation (see Table below). Medical records were reviewed for treatment and clinical outcome (follow-up ranging 9 to 174 months; median 76 months). Statistical analysis was performed to see if any histologic parameters correlated with clinical behavior and treatment response.

Results: Paris criteria for AIH/PBC overlap were met in 12/23 cases (52%) at the time of diagnostic liver biopsy. Regardless of histology or Paris criteria, patients were initially treated as AIH with immunosuppression alone, PBC with ursodiol alone, or AIH/PBC overlap with combination therapy (Figure 1). Incomplete response occurred in almost all patients treated with monotherapy, including10 of 11 who met Paris criteria and 3 additional patients who did not meet Paris criteria. Ultimately, the response to therapy for the entire cohort was more similar to PBC in 2 patients, AIH in 7 and overlap in 14.

No histologic features were significantly associated with response to treatment (defined as normalization of laboratory values). However, the presence of ductular reaction was associated with incomplete response to single agent therapy (p=0.02). In addition, biopsies showing at least 3 of the 5 factors with an asterisk (Table 1) had a much greater likelihood of incomplete response to initial monotherapy (p=0.007).

Table 1: Histologic features and association with incomplete response to initial treatment

Feature	Number (%) of biopsies with histologic feature	% with feature who had incomplete initial response to monotherapy
Destructive lymphocytic cholangitis destructive	22 (96%)	61.9%
Ductular reaction*	17 (74%)	75%
Ductopenia*	14 (61%)	71.4%
Cholate stasis*	9 (39%)	77.8%
Florid duct lesion*	8 (35%)	57.1%
Necrosis and collapse*	7 (30%)	57.1%
Granulomas outside of portal tracts	6 (26%)	50%
Cholestasis	4 (17%)	83.3%
Rosettes	2 (9%)	100%
Activity (Value of 3 or More)	12 (53%)	63.6%
Fibrosis (Value of 3 or More)	10 (43%)	77.8%

Figure 1 - 1561

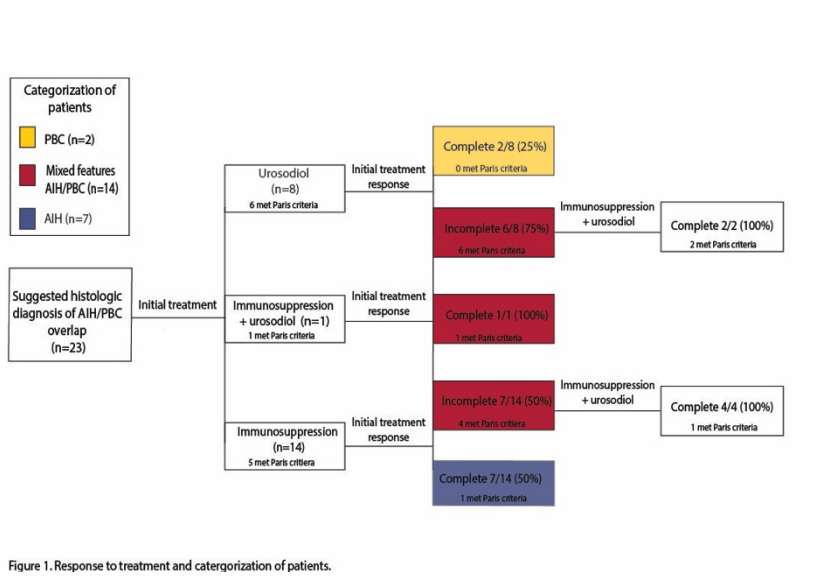

Figure 1. Response to treatment and catergorization of patients.

Conclusions: Therapy for AIH/PBC overlap varies widely and is not necessarily influenced by histology. The majority of patients initially treated with a single therapy do not respond completely. Importantly, laboratory values normalized in the patient who initially received immunosuppression and urosodiol, and in all 6 patients who received combined therapy after incomplete response to monotherapy. Although no histologic features predicted treatment response, several were associated with incomplete response to monotherapy.

1562 Disparities of Cholesteryl Esters Metabolism in Hepatocellular Carcinoma Patients

Akram Shalaby[1], Zhirong Liu[2], Charu Subramony[3], Xinchun Zhou[4]
[1]University of Mississippi Medical Center, Jackson, MS, [2]Shanxi Medical University, Taiyuan, China, [3]University of Mississippi, Jackson, MS, [4]Madison, MS

Disclosures: Akram Shalaby: None

Background: Hepatocellular carcinoma (HCC) is the sixth most prevalent cancer and the third leading cause of cancer-related deaths with prominent disparities in race and gender. Many risk factors for HCC have been identified, however, detailed molecular pathways through which HCC develops, progresses, and disparities remain elusive. Cholesteryl ester (CE) is a group of storage form lipids that is involved in energy and cholesterol metabolism and in the pathogenesis of many cancers. Whether abnormalities of CE metabolism in the liver correlate with pathogenesis and disparities of HCC is currently under-investigated.

Design: A tissue microarray (TMA) was constructed with 192 tissue cores of HCC and tumor-adjacent benign liver tissues (BLT) from African American (AA) and Caucasian American (CA) HCC patients, who were enrolled in the University of Mississippi Medical Center from 2010 to 2017. We performed immunohistochemistry (IHC) for lysosomal lipase (LAL), an enzyme to hydrolyze CEs and Acetyl-CoA acetyltransferase 1 (ACAT1), an enzyme that catalyzes CE synthesis on TMA slides. Each IHC stained core (BLT or HCC) was then evaluated with a scoring system we used previously. Student's T-test and Chi Square test were used in data analysis.

Results: The mean IHC score of LAL for HCC samples was 3.57, which was significantly higher than that in BLT (2.4, p=0.0001), whereas the mean IHC score of ACAT1 was 2.25, which was lower (not significantly) than that in BLT (2.8). Interestingly, there were obvious racial and gender differences in the mean IHC score of LAL (but not ACAT1); it was significantly higher in males and higher in AA HCC patients, as compared to females and CA HCC patients, respectively. In addition, AA HCC patients had earlier clinical onset, higher levels of plasma lipids and worse liver function, but no difference in the rate of viral infections or smoking and alcohol use, as compared to CA HCC patients.

Conclusions: Our study suggests that abnormalities in liver CE metabolism, especially increased expression level of LAL correlate with pathogenesis, progression and disparities in race and gender of HCC.

1563 Clinicopathologic Characteristics of the Hepatitic Variant of Graft Versus Host Disease

Angela Shih[1], Ricard Masia[1], Anthony Mattia[2], Lawrence Zukerberg[3], Vikram Deshpande[1]
[1]Massachusetts General Hospital, Boston, MA, [2]Newton-Wellesley Hospital, Sudbury, MA, [3]Auburndale, MA

Disclosures: Angela Shih: None; Ricard Masia: None; Anthony Mattia: None; Lawrence Zukerberg: None; Vikram Deshpande: None

Background: Graft-versus-host disease (GVHD) of the liver after allogeneic hematopoietic stem cell transplantation is classically a cholestatic pattern of injury, but the more unusual hepatitic variant of GVHD has not been well characterized. Significant elevation of liver enzymes in this clinical context produces a wide etiologic differential, including drug toxicity and infection. This study aims to characterize the clinicopathologic features of the hepatitic variant of GVHD.

Design: Nine cases of the hepatitic variant of GVHD were identified. Clinical information was obtained through the electronic medical record, and non-focal liver core biopsies were reviewed for comparison to a classic GVHD cohort. Chromogenic in situ hybridization (CISH) for XIST was performed using branched DNA technology in five patients who were male recipients of female stem cell donors to determine the distribution of donor-derived lymphocytes.

Results: Patients (n=9) with the hepatitic variant of GVHD had a mean age of 44 years (range: 28 to 71) at a mean of 14 months (SD: 18) from stem cell transplant; none had known subsequent donor lymphocyte infusion. They presented with a mean ALT 594 U/L (SD: 332 U/L), AST 320 U/L (SD: 145 U/L), and alkaline phosphatase 253 U/L (SD: 138 U/L), with near normal resolution of laboratory values with increased immunosuppression. All cases showed histologic findings of bile duct injury of variable severity with expansion of portal tracts by a mixed portal inflammatory infiltrate (n=9/9). All cases also showed varying degrees of lobular injury considerably increased over classic GVHD, with scattered lobular apoptotic hepatocytes, lytic necrosis, and clusters of ceroid-laden macrophages (n=9). Interface activity was present (n=4/9), and centrilobular necrosis and collapse were often observed (n=5/9). XIST CISH shows scattered donor-derived lymphocytes present in both portal and lobular inflammatory infiltrates.

Conclusions: Hepatitic variant of GVHD presents as elevated liver enzymes compared to classic GVHD, and histologically shows varying degrees of biliary and lobular injury. Donor-derived lymphocytes appear to be associated with the hepatitic variant of GVHD and may be informative in select patients. The presence of increased lobular injury, interface activity, and centrilobular injury may help distinguish this variant of GVHD, although there is considerable morphologic overlap with drug reaction and infection.

1564 Diagnostic Utility of 5hmC in Distinguishing Hepatocellular Neoplasia from Non-Neoplastic Liver

Andrew Siref[1], Brent Larson[2], Maha Guindi[3]
[1]Cedars-Sinai, Los Angeles, CA, [2]Cedars-Sinai Medical Center, Los Angeles, CA, [3]Cedars-Sinai Medical Center, Beverly Hills, CA

Disclosures: Andrew Siref: None; Brent Larson: None; Maha Guindi: None

Background: Hepatocellular neoplasia can be a diagnostic challenge. Hepatocellular adenomas (HCA) arise in a background of non-cirrhotic liver and diagnostic histologic features may be lacking in biopsy specimens. Hepatocellular carcinomas (HCC) develop in a background of cirrhosis, where regenerating and dysplastic nodules may mimic carcinoma. Recently, the loss of an epigenetic marker, 5-hydroxymethylcytosine (5hmC), has been reported in a number of other tumors. This pilot study evaluates the utility of 5hmC expression in the liver as a means of differentiating non-neoplastic from neoplastic tissues.

Design: 39 liver sections were collected from the surgical pathology archive and stained with a commercially available 5hmC antibody. Cases included: normal, non-cirrhotic liver (n = 10), cirrhotic liver (n = 10), HCA (n = 9), and HCC (n = 10). All neoplastic cases had no known previous therapy. Evaluation of background, non-neoplastic liver from 7 cases of HCA and 8 HCC (5 of which had a background of cirrhosis) was also available for analysis. 5hmC expression in hepatocyte nuclei was scored for intensity (1 to 3) and quantity (to the nearest 5%) to generate H-scores (intensity multiplied by quantity). A threshold H-score of <200 was employed to designate diminished 5hmC expression. Statistical analysis was performed using a Fisher exact test.

Results: Non-neoplastic hepatocytes consistently demonstrated strong, diffuse nuclear 5hmC immunoreactivity. Hepatocytes in cirrhotic nodules showed no appreciable difference in staining proportion or intensity from non-cirrhotic liver tissue. 5hmC reactivity was significantly reduced in neoplastic hepatocytes (HCC and HCA) compared to non-neoplastic hepatocytes. More specifically, HCC and HCA showed significantly diminished 5hmC reactivity compared to cirrhotic and non-cirrhotic liver, respectively. One well-differentiated HCC and two inflammatory HCAs retained 5hmc staining.

	Diminished 5-hmC	Retained 5-hmC	P value	
Non-neoplastic liver (n = 35)	2	33	<0.0001	Sensitivity: 84.2% Specificity: 94.3%
Neoplastic liver (n = 19)	16	3		
Non-cirrhotic liver (n = 20)	0	20	<0.0001	Sensitivity: 77.7% Specificity: 100%
HCA (n = 9)	7	2		
Cirrhotic liver (n = 15)	2	13	0.0002	Sensitivity: 90% Specificity: 86.7%
HCC (n = 10)	9	1		

Figure 1 - 1564

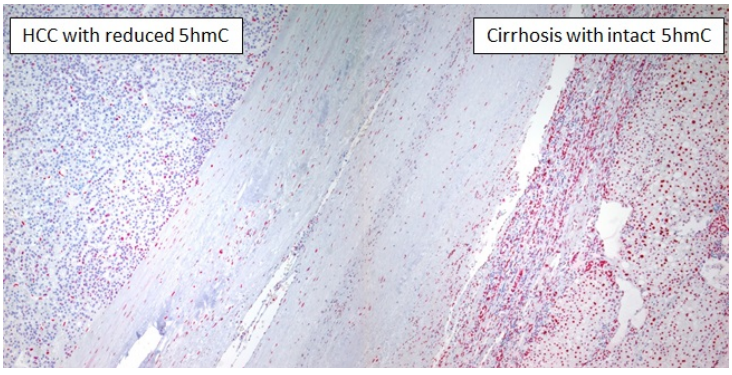

Conclusions: This pilot demonstrates significantly reduced 5hmC reactivity in neoplastic compared to non-neoplastic hepatocytes. 5hmC loss differentiates HCA and HCC from their respective backgrounds with high sensitivity and specificity. The effect of tumor grade, prior therapy, and molecular phenotype remain to be investigated. An expanded study set to evaluate these variables and including small biopsy samples is warranted to further assess the utility of 5hmC staining in clinical immunohistochemical panels for diagnosing hepatocellular neoplasia.

1565 Histologic Patterns of Injury in Acute on Chronic Liver Failure

Jacob Sweeney[1], Meaghan Birch[1], Catherine Lucero[2], Meredith Pittman[3]
[1]Weill Cornell Medicine, New York, NY, [2]Weill Cornell Medicine, New York City, NY, [3]New York-Presbyterian/Weill Cornell Medical Center, New York, NY

Disclosures: Jacob Sweeney: None; Meaghan Birch: None; Catherine Lucero: None; Meredith Pittman: None

Background: Acute on chronic liver failure (ACLF) is a distinct clinical syndrome wherein patients with pre-existing chronic liver disease develop acute hepatic decompensation and extra-hepatic organ failure. Timely recognition of ACLF is critical as short-term mortality is high (33%). Despite its clinical significance, histologic descriptions of this syndrome are limited. The aim of our study was to catalog the histologic features of ACLF and to compare them with those observed in patients with decompensated cirrhosis (DCC) and acute liver failure (ALF).

Design: Over a 2-year period, twenty-five patients who underwent orthotopic liver transplant were categorized as having ALF, DCC, or ACLF using CLIF-EASL criteria. Three pathologists, blinded to clinical information, independently reviewed the liver explant slides (hematoxylin and eosin, trichrome, and reticulin) from each case and recorded histologic features, including the degree and character of necrosis. Pathologic consensus was obtained in each case.

Results: Nine explant livers displayed severe parenchymal necrosis (mean 70%, range 50-90%) in a confluent and geographic pattern in the absence of advanced fibrosis: these patients had been classified as ALF. Histiocytic inflammation and fibrin deposition were common in regions of hepatocellular loss (Figure 1a,b). In contrast, sixteen explants were cirrhotic, and these patients had been classified as ACLF (n=11) or DCC (n=5). Cirrhosis was secondary to alcoholic liver disease (6), viral hepatitis (3), Wilson disease (3), and autoimmune hepatitis (1); etiology was unknown in three cases. In contrast to ALF, the necrosis in ACLF was most prominent at the interface of fibrotic septa and regenerative nodules. Although there was histologic overlap between ACLF and DCC (Table 1), the degree of necrosis,

inflammation, and ductular cholestasis was greater in ACLF, and intralobular necrosis was a feature of ACLF, not DCC. Canalicular cholestasis was significantly associated with ACLF.

Table 1

Histologic feature	ACLF (n=11)	DCC (n=5)	p value
steatosis	6 (55%) 1 (0-2)*	0	0.09
Ductular cholestasis	9 (82%) 1 (0-1)	2 (40%) 0 (0-2)	0.2
Canalicular cholestasis	11 (100%) 2 (1-3)	2 (40%) 1 (0-2)	0.01
Portal inflammation	10 (91%)1 (0-2)	5 (100%) 1 (1-2)	1
Lobular inflammation	11 (100%)2 (1-4)	4 (80%) 1 (0-2)	0.3
Septal inflammation	11 (100%) 3 (1-4)	5 (100%) 2 (1-3)	1
Ductular reaction	100% (11/11)	100% (5/5)	1
Balloon cells	18% (2/11)	20% (1/5)	1
Acidophil bodies	45% (5/11)	20% (1/5)	0.5
Mallory-Denk bodies	36% (4/11)	20% (1/5)	1
Necrosis / collapse	11/11 (100%)	5/5 (100%)	1
Mean percent	23%	3%	
Range percent	5%-50%	5%-10%	
Distribution	64% P, 36% C	100% P	
Necrosis per areas	91% PS, 91% IL, 9% PL	100% PS	
***# cases (%) median value (range)**			
P: patchy, **C**: confluent areas, **PS**: paraseptal, **IL**: intralobular, **PL:** panlobular			

Figure 1 - 1565

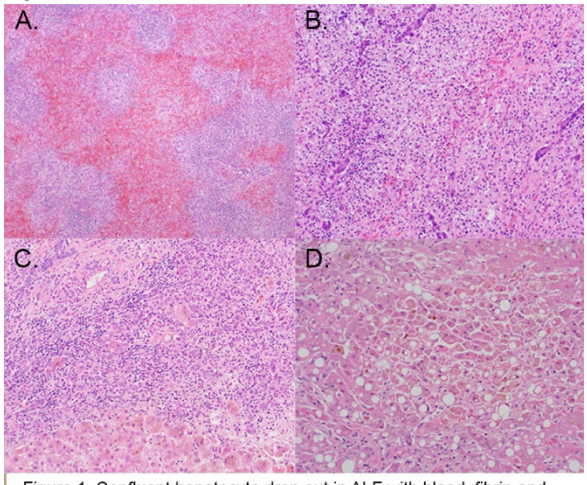

Figure 1. Confluent hepatocyte drop out in ALF with blood, fibrin and histiocytic inflammation (A,B). Paraseptal hepatocyte loss in ACLF with prominent bile ductular proliferation and mononuclear inflammation (C). Intralobular cholestasis and necrosis was also frequently associated with ACLF (D).

Conclusions: The characteristic histologic findings in ACLF include patchy necrosis, cholestasis, marked bile ductular proliferation, and brisk mononuclear inflammation within paraseptal areas. This distinct pattern of injury was consistently observed and independent of cirrhosis etiology, suggesting a discrete causal mechanism unrelated to ischemia or progression of underlying disease in these patients. The recognition and further characterization of ACLF is important given its prognostic significance.

1566 New proposal for macroscopic-based classification in 80 biliary atresia patients post-liver transplant

Roberto Tambucci[1], Catherine De Magnee[1], Xavier Stephenne[1], Françoise Smets[1], Raymond Reding[1], Mina Komuta[1]
[1]Cliniques universitaires Saint-Luc, Brussels, Belgium

Disclosures: Roberto Tambucci: None; Catherine De Magnee: None; Xavier Stephenne: None; Françoise Smets: None; Raymond Reding: None; Mina Komuta: None

Background: Biliary atresia (BA) exhibits various macroscopic features in the explanted liver. An example is the perihilar benign hepatic nodules observed in patients post-Kasai portoenterostomy (KPE), especially in long-surviving Asian cohorts. We hypothesised that a macroscopic-based BA classification may correspond with clinical and histological features. Thus, we aimed to assess correlations between macroscopic and clinicopathological features in 80 BA patients.

Design: We investigated 80 BA patients who underwent a liver transplantation (LT) (median age at LT: 2.5 years, ranging from 4 months to 32 years) at Saint-Luc Hospitals from 2009 to 2017. Clinical information was obtained from patient files. Macro- and microscopic aspects were reviewed by a liver-specialized pathologist.

Results: Macroscopically, 80 BAs were subclassified into 5 groups: group 1-biliary plug (n=22, 27.6%), group 2-biliary plug with biloma (n=15, 18.8%), group 3-small lesion (n=7, 8.6%), group 4-no biliary plug (n=28, 35%), and group 5-large hepatic nodule (n=8, 10%). Histologically, groups 1 and 2 showed marked extravasation of the bile in the perihilar region. Keratin 7 highlighted advanced ductular reaction, ductal plate malformation (DPM)-like structures, without cholate stasis. Groups 3 and 4 showed severe bilirubinostasis and cholate stasis. The small lesions in group 3 corresponded with a regenerative nodule with severe bilirubinostasis and giant cell transformation of the hepatocytes. Group 5 demonstrated a well delineated lesion showing periportal or septal fibrosis with preserved bile ducts, compared to the surrounding cirrhotic parenchyma. Bilirubinostasis ($p=0.0076$), DPM-like structures ($p=0.0323$), and bile extravasation ($p<0.0001$) were statistically less in group 5 compared to the others. Importantly, 2 (20%) of 10 cases had co-incidental, well differentiated HCC. Correlating macroscopic features with clinical aspects showed that group 5 patients were all post-KPE, and had a significantly longer LT-free survival, compared with the other groups ($P=0.0042$). In contrast, groups 1 and 2 comprised far fewer patients who received KPE before LT. Overall, groups 1 and 2 presented so-called typical BA macroscopic and histological features.

Conclusions: BA was macroscopically subclassified into 3 groups that corresponded with relevant clinical features; biliary plug with/without biloma, no bile plug with/without a small lesion, and large hepatic nodular group.

1567 Hepatocellular Adenoma or Benign Liver? -- An Opportunity for Digital Pathology

Harrison Tsai[1], Kun-Hsing Yu[2], John Hart[3], Lei Zhao[4]
[1]Brigham and Women's Hospital, Boston, MA, [2]Harvard Medical School, Boston, MA, [3]University of Chicago, Chicago, IL, [4]Brigham and Women's Hospital, Harvard Medical School, Boston, MA

Disclosures: Harrison Tsai: None; Kun-Hsing Yu: *Primary Investigator*, Harvard Medical School; John Hart: None; Lei Zhao: None

Background: Histologic distinction of hepatocellular adenoma (HCA) from benign liver or other well differentiated hepatocellular proliferations can be challenging in core biopsy samples. Computerized digital imaging studies have recently demonstrated the ability to distinguish neoplastic from non-neoplastic tissue based solely on nuclear architecture, utilizing deep learning analysis. Here, we report on digital imaging extraction of nuclear architecture features from captured liver images and their use in machine learning efforts aimed at the distinction between HCA and benign liver.

Design: H&E slides from 24 HCA cases were retrieved from the archives of 2 institutions, from which 221 H&E images were obtained at 200x (~840 x 660 um). The areas were manually selected (127 HCA & 94 background liver excluding portal triads). Open source software was used for segmentation and feature extraction of nuclei (standard color deconvolution and Otsu thresholding). Cases with poor segmentation performance were re-evaluated utilizing sparse non-negative matrix factorization (SNMF). Since both hepatocytes and non-hepatocytes were captured during the segmentation step, support vector machines (SVM) were then trained to separate hepatocyte nuclei from nuclei of other cell types based on morphometric features. SVMs were also used to explore classification of HCA versus uninvolved liver based on 49 nuclear architectural features derived solely from centroid coordinates of predicted nuclei.

Results: Standard segmentation methods were able to capture 95-100% of hepatocyte nuclei in both the HCA and background liver images of 19/24 cases, and 85-95% in 3/24 cases. In the remaining 2/24 cases, only 40-70% of hepatocyte nuclei from either HCA or background were successfully segmented, due to highly eosinophilic staining. These cases were resolved via SNMF (97-100% of hepatocyte nuclei captured). SVMs trained to predict hepatic nuclei from segmented nuclei yielded an average accuracy of 88% on manually annotated testing data (ranging from 78%-97% by case). Finally, nuclear architecture based SVMs trained to classify adenomas versus background liver yielded a weighted case-based accuracy of **79%** by leave-one-case-out-cross-validation (all HCA and background images from each case removed together).

Conclusions: Computational digital imaging analysis can facilitate accurate diagnosis of HCA. Ongoing trials involving deep learning and convolutional neural networks may result in more accurate discrimination in the future.

1568 Identification of a MicroRNA Signature in Distinguishing Well Differentiated Hepatocellular Carcinoma from Hepatocellular Adenoma

Beena Umar[1], Mehrnoosh Tashakori[1], Marwan Abouljoud[1], Jia LI[1], Lisa Whiteley[1], Dhananjay Chitale[2], Mohammad Raoufi[1]
[1]Henry Ford Health System, Detroit, MI, [2]Henry Ford Hospital, West Bloomfield, MI

Disclosures: Beena Umar: None; Mehrnoosh Tashakori: None; Marwan Abouljoud: None; Jia LI: None; Lisa Whiteley: None; Dhananjay Chitale: None; Mohammad Raoufi: None

Background: MicroRNAs (miRNAs) are globally dysregulated in many tumors and play an integral role in tumorigenesis. In liver, miRNAs are abundant, modulate an array of cellular functions and have shown to play an important role in pathogenesis of liver diseases. Increasing evidence suggests that miRNAs can be used as potential diagnostic marker in various tumors including liver neoplasms. The distinction between well differentiated hepatocellular carcinoma (WDHCC) and hepatic adenoma (HA) can be histologically very challenging, especially when limited tissue is available for evaluation. Ancillary tests are of limited help in distinguishing these lesions. Given the challenges in histopathological diagnosis of WDHCC vs HA and strong evidence of miRNA in hepatic tumorigenesis, we aimed to find a multi-biomarker panel using miRNAs as a diagnostic tool for differentiating WDHCC from HA.

Design: We profiled 17 candidate miRNAs on 31 samples; 9 HA, 4 WDHCC, 6 moderately differentiated HCC (MDHCC), 5 poorly differentiated HCC (PDHCC) and 7 normal liver. Total RNA was isolated from formalin fixed paraffin embedded (FFPE) tissue with Ambion's RecoverAll. cDNA and real-time PCR were performed using ABI TaqMan® microRNA kits and Roche LightCylcer480. miRNAs were normalized using RNU6B as endogenous control. Moderated t-test from the LIMMA package was used to identify differentially expressed miRNAs. To determine a panel of miRNAs discriminating WDHCC from HA, random forest (RF) classification algorithm was performed. Validity was assessed by leave-one-out-cross validation (LOOCV).

Results: Our analysis showed that most miRNAs were underexpressed in HA compared to HCC. Eight miRNAs (miR221, miR222, miR223, miR200, miR375, miR126, miR301, miR422) were significantly underexpressed in HA compared to WD-HCC at a 5% false-discovery rate(fig1). RF identified a panel of six miRNAs (miR222, miR203, miR200, miR126, miR301, miR422) that best distinguish WDHCC from HA. The area under the Receiver Operating Curve (ROC) is 0.83 from LOOCV. This panel was able to distinguish HA from WDHCC with sensitivity of 89% and specificity of 67% from LOOCV(fig2).

Figure 1 - 1568

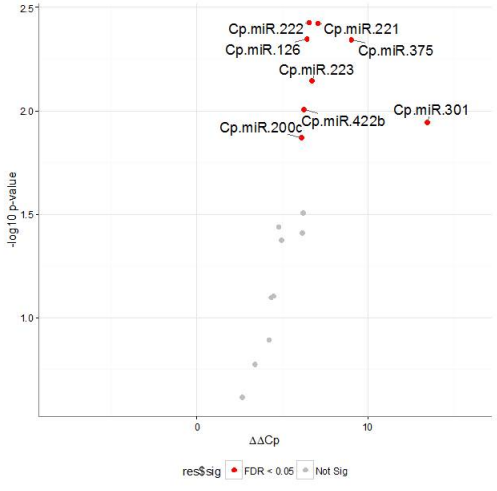

Figure 1. Volcano plot of differentially expressed miRNAs. ΔCp of miRNA of HA samples were compared with WDHCC samples
The x-axis specifies the ΔΔCp (e.g. log2 fold change) and the y-axis specifies the negative logarithm to the base 10 of LIMMA test p-values
Red dots reflect the significantly differentially expressed miRNAs (FDR<=0.05)

Figure 2 - 1568

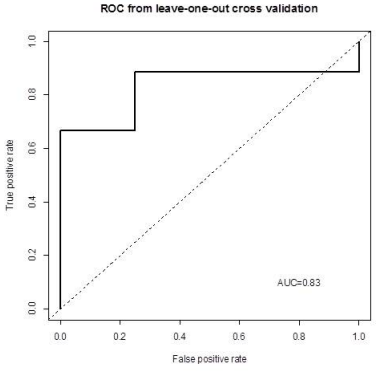

Figure 2. The average ROC curve for 10-repeated 5-fold CV

Conclusions: In summary, our study showed that a six miRNA signature (miR222, miR203, miR200, miR126, miR301, miR422) could serve as novel biomarker panel to differentiate WDHCC from HA. Given our limited sample size, we are currently analyzing this microRNA signature in a larger cohort of patients with hepatocellular neoplasms to validate the clinical utility of our data.

1569 Focal Nodular Hyperplasia-like Nodules Arising in the Setting of Hepatic Chronic Vascular Disorders Show Beta-catenin Activation

Sarah Umetsu[1], Nancy Joseph[1], Soo-Jin Cho[1], Dhanpat Jain[2], Vikram Deshpande[3], Sanjay Kakar[1]
[1]University of California, San Francisco, San Francisco, CA, [2]Yale University School of Medicine, New Haven, CT, [3]Massachusetts General Hospital, Boston, MA

Disclosures: Sarah Umetsu: None; Nancy Joseph: None; Soo-Jin Cho: None; Dhanpat Jain: None; Vikram Deshpande: None; Sanjay Kakar: None

Background: Abernethy malformation is a rare anatomic abnormality in which congenital absence of the portal vein causes venous flow to bypass the liver and drain directly into the systemic venous circulation. As in other hepatic vascular disorders, patients with Abernethy malformations can develop hepatocellular nodules, ranging in appearance from focal nodular hyperplasia (FNH), hepatocellular adenoma (HCA), and hepatocellular carcinoma (HCC). However, it is not known if FNH-like nodules that arise in the setting of a chronic vascular disorders share the same characteristics as conventional FNH.

Design: Three patients with Abernathy malformation and 1 patient with Tetrology of Fallot and a mesocaval shunt with hepatocellular nodules were identified. Reticulin stain and immunohistochemical stains for b-catenin and glutamine synthetase (GS) were performed on 6 nodules (1-2 nodules per patient). GS staining was classified as diffuse (>50% staining), map-like, or pseudomap-like (expanded perivascular zones of staining without broad interconnected zones of positivity that are typical of map-like pattern). DNA was purified from 2 nodules in one patient and next-generation sequencing for 500 cancer genes was performed.

Results: The 6 nodules examined showed well-differentiated hepatocellular lesions with minimal cytological atypia. 5 of 6 nodules showed FNH-like features with fibrous septa and ductular reaction (Figure 1); 4 of these nodules showed vague nodular architecture, and 1 showed prominent nodular architecture. The remaining nodule (1/6) had HCA-like features with no features of HCC. GS showed a pseudomap-like staining pattern in 2 FNH-like nodules (Figure 2); diffuse homogenous staining was seen in the other 4 nodules (3 FNH-like, 1 HCA-like). Nuclear staining for b-catenin was seen in 2 nodules (1 FNH-like, 1 HCA-like). Sequencing revealed activating *CTNNB1* mutations in 2 nodules (both FNH-like) that lacked nuclear b-catenin staining, one with diffuse GS and one with pseudomap-like GS.

	Size (cm)	Histology	B-catenin	Glutamine Synthetase	Reticulin	CTNNB1 alteration
Nodule 1 (patient 1)	5.5	Fibrous septa, ductular reaction	No nuclear staining	Pseudomap-like	Intact	CTNNB1 p. T41A
Nodule 2 (patient 1)	1.2	Fibrous septa, ductular reaction	No nuclear staining	Diffuse	Intact	CTNNB1 p.S45P
Nodule 3 (patient 2)	9.5	Fibrous septa, prominent nodular architecture, ductular reaction	Nuclear staining	Diffuse	Patchy loss	Not done
Nodule 4 (patient 3)	0.4	No fibrous septa or ductular reaction	Nuclear staining	Diffuse	Focal loss	Not done
Nodule 5 (patient 4)	3	Fibrous septa, ductular reaction	No nuclear staining	Pseudomap-like	Intact	Not done
Nodule 6 (patient 4)	2	Fibrous septa, ductular reaction	No nuclear staining	Diffuse	Intact	Not done

Figure 1 - 1569

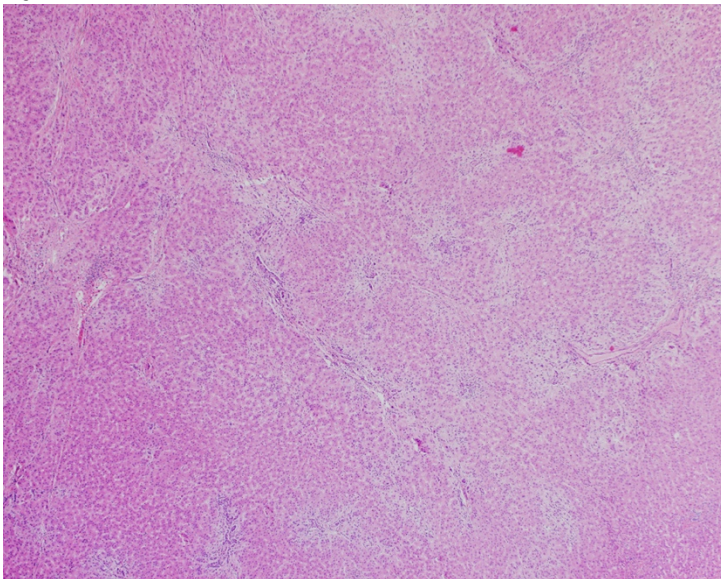

Figure 2 - 1569

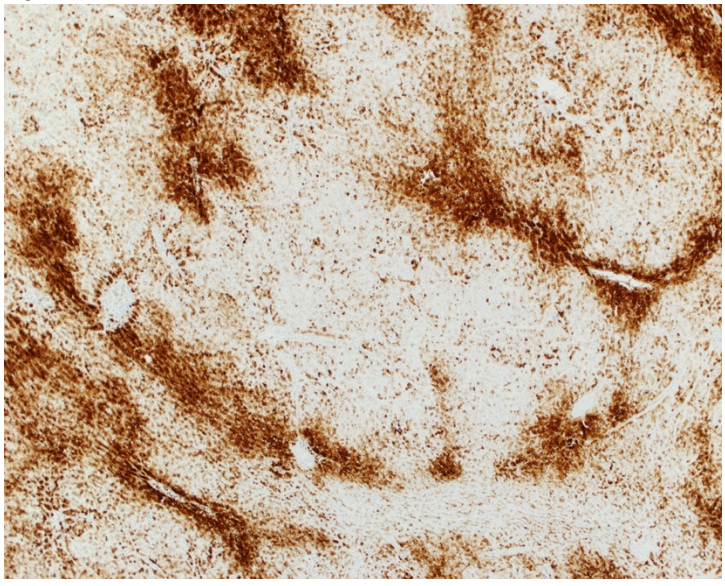

Conclusions: Nodules morphologically resembling FNH arising in the setting of hepatic chronic vascular disorders can show immunohistochemical evidence of b-catenin activation and b-catenin mutations in the absence of significant cytoarchitectural atypia or reticulin loss. These results suggest that unlike sporadic FNH, FNH-like lesions arising in this setting may be neoplastic and potentially at risk for malignant progression. This should be taken into account while making management decisions for these patients.

1570 Transcriptomic and Proteomic Analysis of Steatohepatitic Hepatocellular Carcinoma Reveals Novel Distinct Biologic Features

Benjamin Van Treeck[1], Taofic Mounajjed[1], Roger Moreira[1], Jaime Davila[1], Erik Jessen[1], Rondell Graham[1]
[1]Mayo Clinic, Rochester, MN

Disclosures: Benjamin Van Treeck: None; Taofic Mounajjed: None; Roger Moreira: None; Jaime Davila: None; Erik Jessen: None; Rondell Graham: None

Background: The steatohepatitic variant of hepatocellular carcinoma (SH-HCC) is a recently described variant of hepatocellular carcinoma that is most strongly associated with underlying non-alcoholic steatohepatitis (NASH). The molecular biology of SH-HCC has not been studied.

Design: Ten cases of pure SH-HCC arising in patients with cirrhosis due to non-alcoholic steatohepatitis were retrieved. Transcriptomic analysis was performed on tumor-normal pairs of SH-HCC using formalin fixed paraffin embedded (FFPE) tissue sections. The transcriptomic data were compared with publicly available curated data from The Cancer Genome Atlas (TCGA). Immunohistochemistry (IHC) for liver fatty acid binding protein (LFABP) and glutamate synthetase (GS) was performed on FFPE of the tumor and adjacent non-neoplastic liver to validate RNA level findings.

Results: Morphologically, SH-HCC showed minimal intratumoral inflammation and the characteristic steatosis, ballooned hepatocytes and Mallory bodies (Figure 1). When compared to well curated HCC associated with viral hepatitis C (n= 35 cases) from TCGA, the transcriptome of SH-HCC revealed downregulation of T cell genes *CD3E* (fold change 0.59; p=0.0002; FDR = 0.0048) and *CD8A* (fold change 0.47; $p=9.9x10^{-6}$; FDR 0.0005), activation of the hedgehog pathway (*GLI1* fold change 2.2; p 0.047) and a gene expression pattern indicative of zone 3 type profile with upregulation of *GLUL* (glutamine synthetase; GS) (fold change 1.33), downregulation of *FABP1* (LFABP) (fold change 0.53) and *ASS1* (fold change 0.33) (p = 0.019; 0.00046 and $9.1 x10^{-17}$ respectively). IHC confirmed the zone 3 phenotype at the protein level with diffuse strong GS expression in the neoplastic cells (8 of 10) and loss/diminished LFABP (10 of 10) cases. SH-HCC revealed a distinctive differential gene expression profile when compared to well curated HCC associated with viral hepatitis C (n= 35 cases) and no other documented HCC risk factors from TCGA as shown in Figure 2.

Figure 1 - 1570

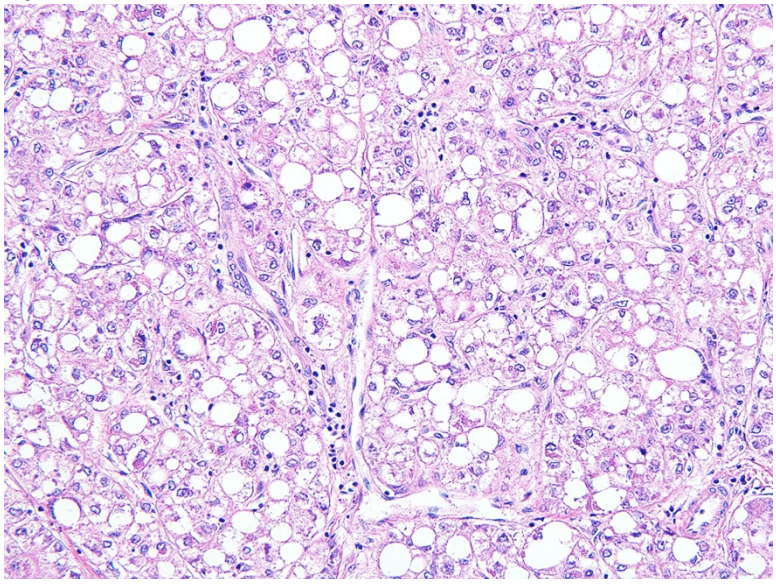

Figure 2 - 1570

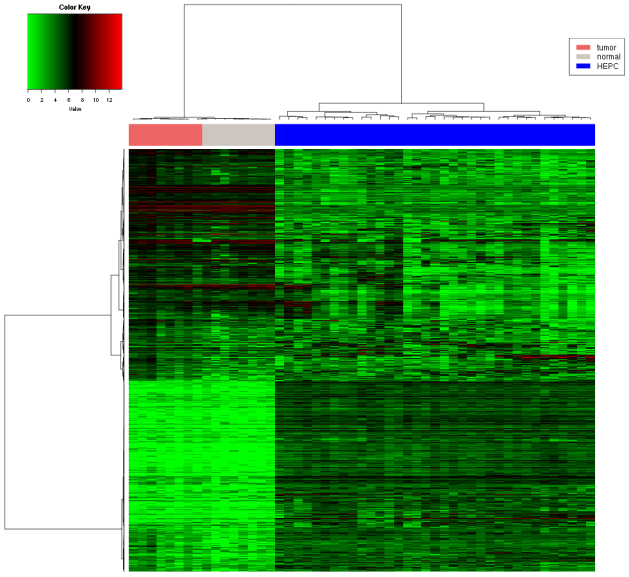

Conclusions: SH-HCC is characterized by a distinctive morphology which corresponds to a distinctive gene expression profile that differs from HCC due to viral hepatitis, reveals downregulation of activated T-cells, a zone 3 like expression profile/ phenotype and activation of the hedgehog pathway. These findings have important biologic implications including that cases of SH-HCC are unlikely to respond to PD-1 axis inhibition.

1571 The Influence of Neoadjuvant Therapy on the Immune Cell Infiltration of Hepatic Colorectal Metastases

Anuj Verma[1], Edwin Parra[1], Riham Katkhuda[1], Mei Jiang[1], Naohiro Uraoka[2], Jose Solorzano[3], Ignacio Wistuba[1], Michael Overman[1], Scott Kopetz[1], Dipen Maru[1]
[1]The University of Texas MD Anderson Cancer Center, Houston, TX, [2]Memorial Sloan Kettering Cancer Center, New York, NY, [3]Madrid, Spain

Disclosures: Anuj Verma: None; Edwin Parra: None; Riham Katkhuda: None; Mei Jiang: None; Naohiro Uraoka: None; Jose Solorzano: None; Ignacio Wistuba: None; Michael Overman: *Consultant*, Roche; Dipen Maru: None

Background: Neoadjuvant chemotherapy plus Bevacizumab is a standard of care therapy in patients with hepatic colorectal metastases (HCRM). However, effects of the neoadjuvant therapies on immune cell make of the HCRM is not known. A better understanding of effects of these therapies on immune microenvironment will provide foundation in understanding synergistic (or antagonistic) mechanism of conventional neoadjuvant therapy with the checkpoint inhibitors.

Design: Multiplex immunofluorescence (mIF) using the Opal 7-color IHC Kit™ (Perkin Elmer, Waltham, MA) was performed in 72 HCRM, 19 treated with surgery only and 53 treated with surgery after 5-Flurouracil, oxaliplatin (FOLFOX) and bevacizumab (n=27) or 5-Fluouracil, irinotecan (FOLFIRI) and bevacizumab (n=26) based neoadjuvant therapy. The mIF markers panel included: AE1/AE3, PD-L1, CD3, CD8, PD-1 and CD68. We performed the quantification in the intra-tumor epithelial and stromal compartment and the different cell phenotypes were expressed as cell by mm^2, using the InForm™ software program.

Results: Table shows the characteristics of tumor infiltrating T cells and macrophages in HCRM with and without neoadjuvant therapy

	HCRM without neoadjuvant therapy (n=19)	HCRM after neoadjuvant therapy (n=53),		Fold change, P-value
		FOLFOX+B (n=27)	FOLFOFIRI+B (n=26)	
CD3+ T cells, mean ±SD (range)	111.7 ±100.6(9.5-429.2)	946.2 ±928.6(29.7-5084.6)		8.5 fold, P <0.001
Cytotoxic T(CD3+CD8+) cells, mean ±SD (range)	8.4±9.7(0-34.6)	262.9±328.8(7.1-1905.5)		32 fold, P <0.001
Tumor Associated macrophages, mean ±SD (range)	335.6±210(78.3-1005)	270.5±189.5(7.3-874.1)		1.2 fold, P= 0.1
PD-L1 positive macrophages, mean ±SD (range)	47.27±16.7(27.7-88.2)	2.2±4.9(0-23.3)		20 fold, P <0.001

Conclusions: Neoadjuvant therapy in HCRM induces immune cell infiltration and activation with higher activation of cytotoxic T cells. PDL-1 downregulation in macrophages after neoadjuvant therapy is a novel finding and should be explored in the context of its efficacy with PD-1 inhibitors.

1572 Systemic Autoimmune Diseases and Liver Histology: Network Analysis Identifies Possible Clinico-biologic Associations

Jeff Wang[1], Xuchen Zhang[2], Romulo Celli[3]
[1]Yale University School of Medicine, New Haven, CT, [2]Yale University School of Medicine, Orange, CT, [3]Branford, CT

Disclosures: Jeff Wang: None; Xuchen Zhang: None; Romulo Celli: None

Background: Systemic autoimmune diseases (SAD), such as lupus (SLE) and rheumatoid arthritis (RA), are a heterogeneous group with myriad clinical and serologic presentations, often associated with elevated liver function tests. The liver histologic manifestations of each disorder are incompletely described. Utilizing network analysis, a hypothesis-generating graphical model, we aim to identify associations among clinical and histologic parameters in these patients.

Design: Liver biopsies from patients with SAD (excluding infectious, drug-induced, fatty liver, PBC, PSC, and autoimmune hepatitis) between 2010 and 2017 were identified at our institution. Cases were assessed blindly for the presence of 26 pathologic characteristics. Clinical data such as age, gender, race, liver function tests, and auto-antibodies were collected. Non-parametric correlation among variables was assessed using the Spearman rho test and all correlations with a p value <0.01 were used. A network graph was created based on the qualifying correlations.

Results: Biopsies from 32 women and 3 men with 11 different SAD were identified. The average patient age was 49 years. RA and SLE were the most common diagnoses (29% and 26% prevalence, respectively). The most common findings among all biopsies were patchy mild portal chronic inflammation (49%), portal Kuppfer cell aggregates (49%), and nodular regenerative changes (40%). The network comprised 25 clinicopathologic characteristics and 42 correlations. Histologic cholestasis was associated with anti-smooth muscle, anti-Ro, and anti-dsDNA antibodies, while an elevated alkaline phosphatase was associated with anti-rheumatoid factor and anti-smooth muscle antibodies (p<0.01) (figure 1). In SLE, histologic findings of mild lobular inflammation (p=0.015) and acidophil bodies (p=0.044) were significantly more prevalent compared to other diagnoses. RA was similar to all other diagnoses for all 26 variables assessed.

Systemic Autoimmune Diseases	Count*
Rheumatoid Arthritis	10
Lupus (SLE)	9
Celiac Disease	5
Graves Disease	3
Hashimoto's Disease	3
Sjogren's Syndrome	2
Type 1 Diabetes Mellitus	2
Polymyositis	2
Scleroderma	1
Shulman Syndrome	1
Juvenile Idiopathic Arthritis	1
Antisynthetase syndrome	1

*A few patients had two systemic autoimmune diseases

Figure 1 - 1572

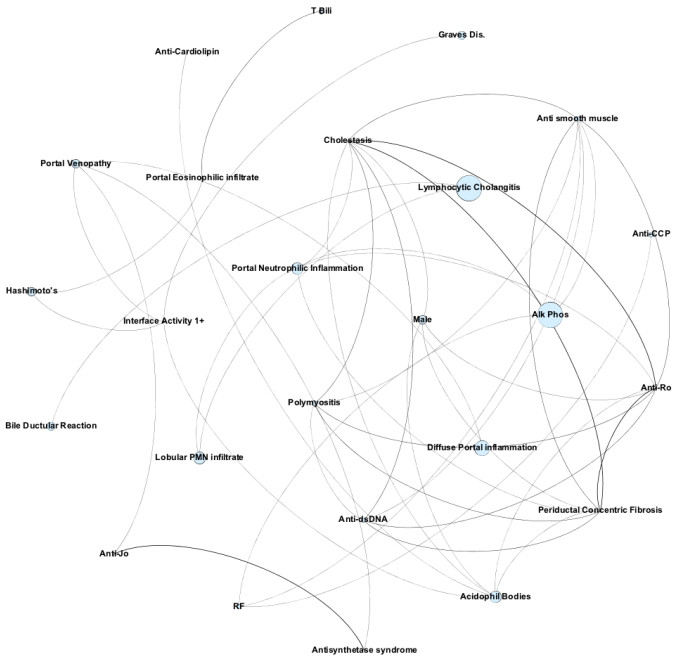

Conclusions: In accordance with prior studies, the most common findings on liver biopsies of patients with SAD are mild and non-specific. Cholestasis and elevated alkaline phosphatase are linked to the presence of multiple autoantibodies, raising the possibility that these demonstrate cross reactivity with biliary epithelium. In patients with an elevated ANA and mild inflammatory changes on biopsy, the diagnosis of SLE can be suggested. Network analysis is a valuable hypothesis-free approach to identifying potential clinico-pathologic associations.

1573 "Sex Cord-Like" Hepatic Carcinoma: a Rare Variant of Intrahepatic Cholangiocarcinoma?

Kwun Wah Wen[1], Amitabh Srivastava[2], Nancy Joseph[1], Tara Saunders[1], Sanjay Kakar[1]
[1]University of California, San Francisco, San Francisco, CA, [2]Brigham and Women's Hospital, Harvard Medical School, Boston, MA

Disclosures: Kwun Wah Wen: None; Amitabh Srivastava: None; Nancy Joseph: None; Tara Saunders: None; Sanjay Kakar: None

Background: Rare primary liver tumors with morphologic resemblance to sex cord tumors and strong inhibin staining have been described. The term "cholangioblastic variant of intrahepatic cholangiocarcinoma (ICC)" has been proposed, but the tumor lacks a definite 'blastic morphology and the reported mutational profile is distinct from ICC (PMID:28232156). The histogenesis and natural history of these tumors is not well understood.

Design: Clinicopathologic data was reviewed for 3 resected cases including immunohistochemistry in all cases, albumin in situ hybridization (ISH) in 2 cases and 300-gene panel sequencing in 1 case. Treatment and follow-up data were obtained.

Results: All 3 tumors occurred as solitary tumors in young women (Table) with no extrahepatic masses. One patient was treated with chemotherapy and died of metastatic disease after 2 years. Recurrence or metastasis did not occur in the other 2 cases (follow-up 5 months and 2 years). All 3 cases had characteristic morphologic features with tumor cells arranged in sheets interrupted by small lumina alternating with areas showing small cystic/microcystic structures. Ribbon-like/retiform areas and gland-like spaces with eosinophilic material (reminiscent of Call-Exner bodies or thyroid follicles) were present. Cytologic atypia was mild, mitotic activity was low and there was no necrosis. All cases had strong diffuse staining with inhibin and CK7, focal positivity with synaptophysin (SYN) and chromogranin (CG), and negative hepatocellular markers. Albumin ISH (n=2) was strongly positive. NGS (n=1) did not show mutations typical of ICC (*IDH, BAP1, PBRM1, KRAS, BRAF, TP53, FGFR2* fusion). Copy number analysis (n=1) did not reveal any significant alterations.

	Age (yr)/ gender	Size (cm)	Recurrence/ metastasis	CK7, Inhibin	Albumin ISH	CG, SYN	Arginase, Glypican, Hep Par	FOXL2, SF-1
Case 1	37/F	6.9	No (2 yrs)	P	P	F	N	Not done
Case 2	28/F	10	No (5 mths)	P	P	F	N	N
Case 3	19/F	14	Yes (2 yrs)	P	Not done	F	N	N
P-positive, N-negative, F-focal, CG-chromogranin, SYN-synaptophysin								

Conclusions: "Sex cord-like" primary hepatic carcinoma is a rare tumor with predilection for young women and potential for aggressive behavior. Focal SYN and CG staining can be mistaken for neuroendocrine neoplasm. Albumin ISH positivity supports cholangiocytic lineage and suggests that it may be a unique variant of ICC. The distinct morphology, strong inhibin staining and lack of typical ICC mutations (based on limited data) suggests a distinct molecular pathway. Recognition of this variant and additional study is necessary to determine the reason for strong inhibin staining, driving molecular alterations and detailed natural history.

1574 Clinical and pathologic significance of antinuclear antibodies in pediatric nonalcoholic fatty liver diseases

Hao Wu[1], Liang Zhu[2], Norma Quintanilla[3], Darryl Kinnear[3], Ryan Himes[3], Kalyani Patel[1], Daniel Leung[3]
[1]Texas Children's Hospital, Houston, TX, [2]The University of Texas Health Science Center at Houston, Houston, TX, [3]Texas Children's Hospital and Baylor College of Medicine, Houston, TX

Disclosures: Hao Wu: None; Darryl Kinnear: None; Ryan Himes: None; Kalyani Patel: None; Daniel Leung: None

Background: The clinical and histologic relevance of ANA-positivity in NAFLD remains controversial among adult-only or adult-predominant studies. Pediatric NAFLD differs from that of adult diseases at least histologically. The significance of ANA positivity in pediatric NAFLD is unknown.

Design: Patients with a pathologic diagnosis of NAFLD and ANA testing within 3 months were identified through a pathology database query and chart review. The correlation between ANA status and clinical/ histologic parameters was tested with appropriate statistical methods.

Results: Of the forty patients (29 M and 11 F) identified between 2011 and 2015, 95% were Hispanic. The age at liver biopsy ranged from 6 to 18.7 years (median 12.1), with elevated liver biochemistries as the indication for biopsy. Twenty-two patients (55%) had positive ANA. There were no significant differences in gender, age, BMI, hypergammaglobulinemia, hypercholesterolemia, hypertriglyceridemia, AST/ALT/GGT fold elevation, diabetes, obstructive sleep apnea, or positivity for F-actin antibody when comparing ANA+ patients to ANA- (Table). Patients tended to have higher risk for insulin resistance with ANA+, and the difference reached statistical significance when only those with high ANA titers (1:160) were compared to ANA- ($p=0.04$). Histologically, all biopsies had lobular inflammation. There was no significant difference with regard to moderate-to-severe steatosis (>33%), more than minimal portal inflammation, presence/degree of interface inflammation, presence of plasma cells, ballooning degeneration/bridging fibrosis, grade 2 lobular inflammation, or NAS score between those with ANA positivity and those without. ANA positive biopsies tended to have portal eosinophils, but the difference was not statistically significant ($p=0.07$). AIH scores were ≥10 in 5 patients; four (18.2%) were ANA positive.

All patients were treated with lifestyle and dietary modifications only. At a median follow up of 2.6 years, BMI was significantly increased from baseline ($p<0.001$), while both AST and ALT levels were significantly lower than baseline ($p=0.01$ and $p< 0.001$, respectively). Two patients with repeat liver biopsy demonstrated no interval histologic changes. In one patient with ANA re-testing the titer normalized from a baseline of 1:1280 3.8 years prior.

	ANA-positive (n=22)	ANA-negative (n=18)	p-value (test)
Female (%)	36.4% (8/22)	16.7% (3/18)	0.16 (chi-square)
Age (median, range)	11.8 (6-18.7)	12.4 (9.1-17.8)	0.33 (t test)
BMI (median, range)	29.73 (20.8-49.5)	31.6 (23.9-42.2)	0.62 (Wilcoxon rank-sum)
Diabetes	6.3% (1/16)	26.7% (4/15)	0.17 (Fisher Exact)
Hypertension	4.5% (1/22)	16.7% (3/18)	0.31 (Fisher Exact)
Insulin resistance	50% (6/12)	10% (1/10)	**0.074 (Fisher Exact)**
Obstructive sleep apnea	22.7% (5/22)	11.1% (2/18)	1 (Fisher Exact)
Acanthosis nigrans	36.4% (8/22)	33.3% (6/18)	0.84 (chi-square)
Positive F-actin	14.3% (3/21)	0% (0/17)	0.23 (Fisher Exact)
hypergammaglobulinemia	10.5% (2/19)	17.6% (3/17)	0.65 (Fisher Exact)
hypercholesterolemia	11.8% (2/17)	45.5% (5/11)	0.22 (Fisher Exact)
hypertriglyceridemia	35.3% (6/17)	50% (6/12)	0.43 (chi square)
AST xULN (mean, median)	1.9, 1	2.3, 1.5	0.44 (Wilcoxon rank-sum)
ALT xULN (mean, median)	4.8, 4	5.1, 3	0.86 (Wilcoxon rank-sum)
GGT xULN (mean, median)	1.2, 1	1.4, 1	0.72 (Wilcoxon rank-sum)
Grade 2 steatosis	31.8% (7/22)	16.7% (3/18)	0.46 (Fisher Exact)
Grade 3 steatosis	22.7% (5/22)	38.9% (7/18)	0.31 (Fisher Exact)
More than minimal portal inflammation	27.3% (6/22)	33.3% (6/18)	0.67 (chi-square)
Interface inflammation	77.3% (17/22)	61.1% (11/18)	0.32 (Fisher Exact)
More than minimal interface inflammation	13.6% (3/22)	38.9% (7/18)	0.14 (Fisher Exact)
Presence of plasma cells	68.2% (15/22)	66.7% (12/18)	0.91 (chi-square)
More than minimal plasma cells	27.3% (6/22)	4 (22.2%)	1.00 (Fisher Exact)
Presence of portal eosinophil	72.7% (16/22)	44.4% (8/18)	**0.07 (chi-square)**
Portal eosinophil cluster	27.3% (6/22)	5.6% (1/18)	**0.10 (Fisher Exact)**
Grade 2 lobular inflammation	50% (11/22)	33.3% (6/18)	0.36 (chi-square)
Presence of ballooning (NASH)	27.2% (6/22)	33.3% (6/18)	0.68 (chi-square)
NAS score (mean, median)	3.6, 3.5	3.7, 3.5	0.91 (Wilcoxon rank-sum)
Fibrosis stage 3	27.3% (6/22)	16.7% (3/18)	0.47 (Fisher Exact)

Conclusions: In children, positive ANA alone does not appear to correlate with clinical or pathologic severity of NAFLD. ANA at high tiers is associated with higher risk for insulin resistance.

1575 Significant Necrosis in Liver Allograft Is a Survival Predicator

Xin Zhang[1], Jingmei Lin[2]
[1]Indiana University School of Medicine, Indianapolis, IN, [2]Indiana University, Indianapolis, IN

Disclosures: Xin Zhang: None; Jingmei Lin: None

Background: Allograft biopsy plays an important role in monitoring the status of transplanted livers. Necrosis can be a worse complication; however, the association between the extent of necrosis and organ survival has not been well studied.

Design: Sixty-eight patients who had 69 liver transplantations with allograft necrosis (1 patient received 2 transplantations) between 2004 and 2018 were included in the study. Histological features including necrosis and parenchyma collapse were graded. Allograft outcome and patient survival were reviewed retrospectively. MELD scores were calculated using the laboratory data obtained on the same day of biopsy. The correlation of necrosis, MELD score, allograft and patient survival were analyzed using Chi-Square test.

Results: The core biopsy length ranged from 3 to 37 mm with an average of 16 mm (94% > 10 mm). The cause of allograft necrosis was mainly ischemia due to reperfusion failure, bleeding and compromised blood supply. Allograft failure rate within 1 month after index biopsy was worse in patients with a higher extent of necrosis (2.5%, 6.7%, 25% and 40% in groups with necrosis of 1-25%, 26-50%, 51-75%, and >75%, respectively) (Table1). More than 50% necrosis was significantly associated with allograft failure ($p < 0.001$). Among patients with >75% massive necrosis, one who received an immediate second transplant survived; 3 out of 9 patients (33.3%) who had not received an additional transplant deceased within 1 month. MELD score is widely accepted for mortality assessment to rank transplant waiting list, however it didn't predict fatality accordingly in liver allografts that failed shortly due to massive necrosis. MELD scores didn't correlate well with the extent of necrosis ($p>0.05$), indicating that necrosis is an independent tool in assessing allograft outcome.

Figure 1 - 1575

Table 1. One-month prognosis of allograft liver with significant necrosis

Extent of necrosis (n=69)	Failed allograft (n=7)	Received further transplant within 1-month (n=1)		No further transplant within 1-month (n=68)	
		Failed allograft	Survived allograft	Failed allograft	Survived allograft
1-25% (n=40)	1 (2.5%)	NA	NA	1 (2.5%)	39 (97.5 %)
26-50% (n=15)	1 (6.7%)	NA	NA	1 (6.7%)	14 (93.4%)
51-75% (n=4)	1 (25%)	NA	NA	1 (25%)	3 (75%)
76-100% (n=10)	4 (40%)	NA	1 (100%)	3 (33.3%)	6 (66.7%)

Conclusions: Extent of necrosis in liver allograft correlates with organ survival. Adequate biopsy with more than 50% necrosis is associated with significant transplant-free mortality. Besides MELD score, necrosis is an independent valuable risk assessment for patient management. Immediate retransplantation is crucial for patients with substantial allograft necrosis.

1576 Distinction of Autoimmune Hepatitis from Drug Induced Autoimmune Hepatitis: The Answer Lies at the Interface

Xin Zhang[1], Craig Lammert[1], Raj Vuppalanchi[1], Romil Saxena[1]
[1]Indiana University School of Medicine, Indianapolis, IN

Disclosures: Xin Zhang: None; Romil Saxena: None

Background: Clinical and pathological differentiation of conventional AIH (cAIH) from drug induced AIH (dAIH) represents an unmet need in hepatology.

Design: A list of patients with cAIH or dAIH was provided by clinical hepatologists. Blinded to the diagnosis, a trainee and a practicing pathologist scored the corresponding liver biopsies for portal tract inflammation, interface hepatitis, lobular inflammation, central perivenular inflammation, central vein endothelitis and perivenular necrosis as none, mild, moderate or severe (scores 0,1,2,3). Presence of plasma cells, eosinophils, portal and perivenular macrophages, duct proliferation, and duct damage were scored as rare, few and many (Scores 0,1,2). A pathologic diagnosis was provided with the knowledge that the cases represented either cAIH or drug induced liver injury (DILI). The clinical diagnoses were then made available, and correlated with pathologic features and pathologic diagnoses. $P<0.05$ was considered statistically significant at cut-off values 0/1.

Results: Slides were available in 23 cases, 4 (3, NAFLD; 1, advanced cirrhosis) were excluded. Nine of 13 cases of cAIH showed moderate to severe, whereas 4 showed mild interface hepatitis; the latter were all under immunosuppressive therapy (Table, cases 10-13).

Of 6 dAIH cases, 1 showed severe interface hepatitis (Table, case 18). cAIH showed more portal, interface and perivenular inflammation, and numbers of plasma cells and eosinophils than dAIH (all, $p<0.05$). Five cAIH cases showed no fibrosis, 4 showed fibrosis of portal tracts, 2 showed central perivenular fibrosis and 1 showed thin fibrous septa (trichrome not available, 1 case).

Eleven of 13 cAIH cases, and 5 of 6 DILI cases were diagnosed as such (Table). Case 7 diagnosed as DILI showed moderate interface and severe perivenular inflammation. Case 15 diagnosed as "treated AIH" showed mild interface hepatitis and no perivenular inflammation; trichrome and reticulin stains showed architectural distortion suspicious for advanced fibrosis.

Figure 1 - 1576

Table 1: Correlation of Pathologic Parameters and Pathologic Diagnoses with Clinical Diagnoses

Case	Portal inflammation	Plasma cells	Eosinophils	Interface hepatitis	Perivenular inflammation	Clinical Diagnosis	Blinded pathologic diagnosis
1	2	2	2	3	3	AIH	Favor AIH
2	2	2	0	2	1	AIH	AIH long standing
3	3	2	3	3	3	AIH	AIH
4	2	2	3	2	3	AIH	AIH
5	3	2	1	3	3	AIH	AIH
6	3	1	1	3	3	AIH	Favor AIH
7	1	1	1	2	3	AIH	DILI
8	3	2	1	3	2	AIH	AIH
9	3	2	1	3	1	AIH	AIH
10	2	1	1	1	0	AIH (on treatment)	Favor treated AIH
11	1	0	0	1	0	AIH (treated)	Not AIH
12	1	1	0	1	3	AIH (treated)	Not AIH
13	2	3	3	1	0	AIH (treated)	Favor DILI
14	1	1	0	1	0	DILI	Favor DILI
15	1	1	0	0	0	DILI	c/w treated AIH
16	2	1	0	1	1	DILI	Favor DILI
17	1	1	0	1	1	DILI	Favor DILI
18	3	1	1	3	2	DILI	Favor DILI
19	1	1	1	1	0	DILI	DILI

1. Moderate to severe interface hepatitis is the most important criterion for diagnosis of cAIH over dAIH; there may or may not be accompanying central perivenular inflammation.
2. Presence of numerous plasma cells and, counterintuitively, eosinophils favors a diagnosis of cAIH over dAIH.
3. Presence or absence of fibrosis is not a valid criterion for differential diagnosis: fibrosis is not present in many cases of acute AIH and there may be underlying fibrosis in cases of DILI.

1577 Hepatocellular Carcinoma in Nonalcoholic Fatty Liver Disease

Lei Zhao[1], Fei Dong[2], Harrison Tsai[2], Jason Hornick[1], Lipika Goyal[3], Nikroo Hashemi[2], Kathleen Corey[4], Joseph Misdraji[5]
[1]Brigham and Women's Hospital, Harvard Medical School, Boston, MA, [2]Brigham and Women's Hospital, Boston, MA, [3]Boston, MA, [4]Massachusetts General Hospital, Boston, MA, [5]Massachusetts General Hospital, Harvard Medical School, Boston, MA

Disclosures: Lei Zhao: None; Fei Dong: None; Harrison Tsai: None; Jason Hornick: None; Lipika Goyal: None; Nikroo Hashemi: None; Kathleen Corey: *Consultant*, Novo Nordisk; Joseph Misdraji: None

Background: Although the association between hepatocellular carcinoma (HCC) and nonalcoholic fatty liver disease (NAFLD) was made two decades ago by epidemiological studies, the mechanisms that link these conditions are still poorly understood. This study aims to summarize the demographical, morphological and molecular features that are associated with HCC arising in the setting of nonalcoholic fatty liver disease.

Design: Cases were identified by searching for all liver partial resection/liver transplantation performed at Massachusetts General Hospital and Brigham and Women's Hospital from 2004 to 2015; cases were included if the patient had known NAFLD, and as comparison cases of known chronic viral hepatitis C or B. Clinical information was confirmed by reviewing electronic medical records. Pathologic features were evaluated by reviewing pathology report and examination of selected cases. Genetic alterations were analyzed in 62 cases (9 NAFLD without cirrhosis, 53 viral hepatitis) by targeted massive parallel sequencing.

Results: A total of 274 cases of resection or liver transplantation for HCC were identified. Among these patients, 65 patients had clinical diagnosis of NAFLD with no other well-known risk factors (HCV, HBV, hemochromatosis, alcohol) for HCC. Patient age was higher in the NAFLD group compared to the viral hepatitis group ($p=0.0007$). Tumors were larger in the NAFLD group ($p=0.003$).

By massive parallel sequencing, most tumors demonstrate low mutational burden. Alterations in TSC1/TSC2 gene were present in 44.4% (4/9) of tumors associated with NAFLD and were only observed in 1.9% (1/53) tumors associated with viral hepatitis.

	HCC associated with NAFLD	HCC associated with virial hepatitis
Clinical and Pathologic Features	n=65	n=165
Age at diagnosis (years)**	31 to 79, mean=69	29 to 80, mean=62
Tumor size (cm)**	7.4	5.7
Tumor stage n for T1/T2/T3/T4	29/19/9/0	67/53/26/1
Tumor differentiation n for G1/G2/G3	9/42/11	27/98/31
Vascular invasion % of cases	39.6	44.4
Gene Alterations (including mutations and copy number variations)	n=9	n=53
CTNNB1	22.2	29.6
TP53	22.2	31.5
ARID1A	11.1	13.0
ARID2	11.1	3.7
ATM	0	3.7
TSC1/TSC2*	44.4	1.9
TERT promotor	33.3	33.3

Conclusions: HCC arising in the setting of NAFLD appears to separate from HCC arising from other well-known risk factors by clinical, pathologic parameters and genetic alterations.

1578 Assessment of the Diagnostic Value of C4d Immunostaining in Antibody-Mediated Rejection in Liver Allograft Biopsy: A Single Institution Experience

Wei Zheng[1], Hanlin Wang[2]
[1]University of California, Los Angeles, Los Angeles, CA, [2]David Geffen School of Medicine at UCLA, Los Angeles, CA

Disclosures: Wei Zheng: None; Hanlin Wang: None

Background: The recently published Banff criteria require positive C4d and positive donor-specific antibodies (DSA) for the diagnosis of antibody-mediated rejection (AMR) in posttransplant liver allograft biopsy. This retrospective single center study was conducted to further assess the diagnostic value of C4d immunostaining in AMR diagnosis.

Design: A total of 149 posttransplant liver biopsies (from 149 patients) were included in this study. C4d immunohistochemistry was performed on every biopsy, which was evaluated following the recommendation by the Banff Working Group (Am J Transplant 2016; 16:603-14). HLA class I and II DSA status was retrieved from the HLA lab database, which was examined on every case. Chart review was also conducted for each case.

Results: Cases were classified into four groups according to their C4d and DSA results: C4d+/DSA+ (n=37), C4d-/DSA- (n=19), C4d+/DSA- (n=6), C4d-/DSA+ (n=87). Fifty-six cases (38%) exhibited a concordant C4d/DSA status. Among the C4d+/DSA+ group, 18 (49%) cases matched the clinical impression of AMR; 10 (27%) showed histologic features of T cell-mediated rejection; and 9 (24%) exhibited features of non-rejection-type injury on biopsies such as ischemia or biliary obstruction. Among the C4d-/DSA- group, 9 (37%) showed no features of rejection; 10 (53%) showed features of acute T cell-mediated rejection or chronic rejection. Ninety-three cases (62%) exhibited a non-concordant C4d/DSA status. Among the C4d+/DSA- group, 3 (50%) exhibited no evidence of rejection and the remaining 3 biopsies showed features of acute T cell-mediated rejection. Among the C4d-/DSA+ group, 4 (5%) were thought to be AMR clinically, 37 (42%) showed acute T cell-mediated rejection or chronic rejection; 46 (53%) showed no evidence of rejection.

Conclusions: The data presented in this study demonstrate a concordant C4d/DSA status in <40% of cases included in our study. No direct correlation between C4d and DSA was observed in >60% of our cases. Though remaining useful, the diagnostic value of C4d immunostaining needs to be further defined.

1579 OATP1B3 Is A Novel Immunohistochemical Marker to Discriminate Well Differentiated Hepatocellular Carcinoma from Its Benign Hepatocellular Mimickers

Wei Zheng[1], Alyssa Krasinskas[2], Wei Yue[3], Hanlin Wang[4]
[1]University of California, Los Angeles, Los Angeles, CA, [2]Emory University, Atlanta, GA, [3]University of Oklahoma Health Sciences Center, Oklahoma City, OK, [4]David Geffen School of Medicine at UCLA, Los Angeles, CA

Disclosures: Wei Zheng: None; Alyssa Krasinskas: None; Wei Yue: None; Hanlin Wang: None

Background: Histopathologic distinction between well differentiated hepatocellular carcinoma (WDHCC) and benign hepatic mimickers, such as hepatocellular adenoma (HCA), focal nodular hyperplasia (FNH) and dysplastic/regenerative nodule, is a known diagnostic challenge. Immunohistochemistry and reticulin stain have been widely used for the distinction, but none of the current available immunomarkers is highly sensitive nor highly specific. Organic anion transporting polypeptide 1B3 (OATP1B3) is a hepatocyte-specific plasma membrane protein that is exclusively distributed in zone 3 in normal human liver. In this study, we examined the diagnostic value of OATP1B3 as a novel immunohistochemical marker in the distinction between WDHCC and its benign hepatic mimickers, particularly on biopsy specimens.

Design: A total of 185 formalin-fixed, paraffin-embedded tissue blocks from 95 liver core biopsies and 90 resection specimens were selected (including 10 normal liver tissues, 65 WDHCCs, 22 cirrhotic nodules (CN), 15 high-grade dysplastic nodules (HGDN), 45 HCAs, and 28 FNHs). Immunohistochemical staining using a rabbit polyclonal antibody directed against OATP1B3 was performed with appropriate positive and negative controls.

Results: We found that, in normal liver tissue, OATP1B3 was exclusively expressed in zone 3 hepatocytes with a strong membranous staining pattern (Fig.1A-1B). This unique expression pattern was somewhat similar to that detected by glutamine synthetase immunostaining. Unlike GS, however, OATP1B3 expression was completely negative in all 65 WDHCC cases (Fig. 2A-2C). HCA, FNH, CN and HGDN cases were either diffusely or focally positive for OATP1B3 expression. Diffuse and strong membranous expression was observed in all 8 beta-catenin mutated HCAs (Fig.2D-2F). A patchy cytoplasmic granular staining pattern was noted in all steatotic HCAs (Fig. 2J-2L). Interestingly, a 'map-like' staining pattern was observed in all 28 (100%) FNH cases (Fig. 2G-2I), also similar to the staining pattern by glutamine synthetase for this lesion.

Figure 1 - 1579

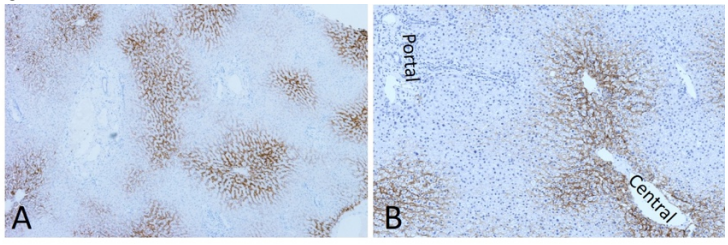

Figure 2 - 1579

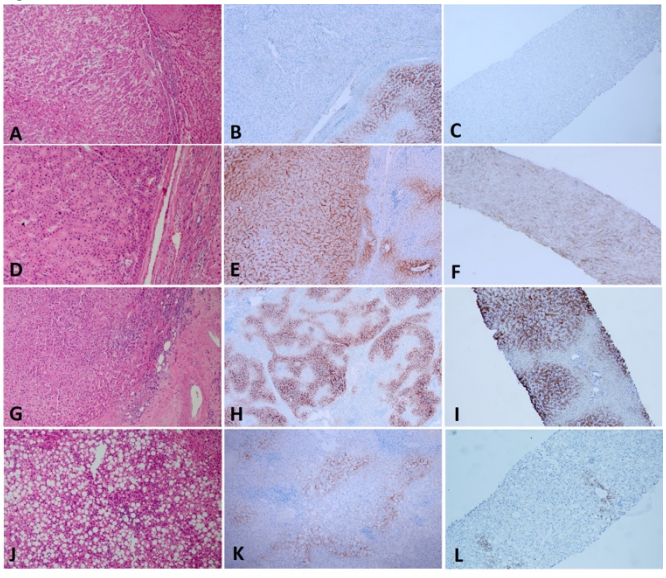

Conclusions: The unique immunostaining patterns in hepatocellular nodular lesions observed in our study demonstrate that OATP1B3 is a promising immunomarker that can be used to distinguish WDHCC from its benign hepatic mimickers and precancerous lesions. OATP1B3 may also have a diagnostic value in the subclassification of HCA and in the distinction between HCA and FNH.

1580 Histologic Overlap in Liver Biopsies from Patients With and Without Non-Cirrhotic Portal Hypertension (NCPH): Interobserver Agreement Study

Chunlai Zuo[1], Jingmei Lin[2], Kajsa Affolter[3], Won-Tak Choi[4], Stephen Lagana[5], Xiuli Liu[6], Eun-Young Choi[7], Zhaohai Yang[8], Maria Isabel Fiel[9], Maria Westerhoff[7], Hwajeong Lee[10]
[1]Albany Medical Center, Guilderland, NY, [2]Indiana University, Indianapolis, IN, [3]Salt Lake City, UT, [4]University of California, San Francisco, San Francisco, CA, [5]New York, NY, [6]University of Florida, Gainesville, FL, [7]University of Michigan, Ann Arbor, MI, [8]Penn State Hershey Medical Center, Hershey, PA, [9]Icahn School of Medicine at Mount Sinai, New York, NY, [10]Albany Medical Center, Albany, NY

Disclosures: Chunlai Zuo: None; Jingmei Lin: None; Kajsa Affolter: None; Won-Tak Choi: None; Stephen Lagana: None; Xiuli Liu: None; Eun-Young Choi: None; Zhaohai Yang: None; Maria Isabel Fiel: None; Maria Westerhoff: None; Hwajeong Lee: None

Background: Histologic features of NCPH in a liver biopsy may be subtle and overlap with those without NCPH. We assessed interobserver agreement on individual histologic features that are associated with NCPH and studied whether a provision of relevant clinical history improves interobserver agreement.

Design: Archived liver samples (38 biopsies, 1 resection) from patients with NCPH/nodular regenerative hyperplasia (NRH) (n=17, group A (A)) and without NCPH and advanced fibrosis (n=21, group B (B)) were retrieved. Static H&E images of lobules (L, x100, A=27, B=23) and portal tracts (P, x200, A=23, B=27) were captured. A total of 100 images of L and P were distributed among 9 gastrointestinal/liver pathologists blinded to clinical history. Each pathologist answered multiple choice questions based on two scenarios – Q1: no clinical history of portal hypertension or advanced fibrosis in the sample, Q2: history of portal hypertension without advanced fibrosis in the sample (Figure 1, Table 1). The lobular change was categorized as normal or abnormal (anisocytosis, nodular regeneration, sinusoidal dilatation, increased draining vessels, incomplete septa). The portal change was categorized as normal or abnormal (paraportal shunting, portal tract remnants, increased number of portal vessels, phlebosclerosis). Fleiss' kappa coefficient analysis was performed to assess interobserver agreement on normal vs. abnormal diagnosis, in L and P, based on Q1 and Q2. The choice selected by >=6 pathologists was considered consensus answer for the image.

Results: The k value regarding normal vs. abnormal diagnosis among the 9 pathologists was 0.26, 0.25, 0.19, and 0.18, and consensus was reached in 37, 34, 28, and 34 images, for LQ1, LQ2, PQ1, and PQ2, respectively. With clinical history, the k value was (A)LQ2: 0.33, (A)PQ2: 0.17, (B)LQ1: 0.17, and (B)PQ1: 0.15. Clinical scenarios affected the consensus status in 13 (26%) and 20 (40%) images of L and P, respectively. Consensus changed from normal to abnormal from Q1 to Q2 in 4 (8%) and 7 (14%) images of L and P, respectively.

	Lobule	Portal tract
a	Within normal limits (single choice)	Within normal limits (single choice)
	Or (b-f: multiple choices)	Or (b-e: multiple choices)
b	Anisocytosis	Paraportal shunting vessel(s)
c	Nodular regeneration	Portal tract remnants
d	Sinusoidal dilatation	Increased number of portal vessels
e	Increased parenchymal draining vessels	Phlebosclerosis
f	Thin, incomplete fibrous septa	

Figure 1 - 1580

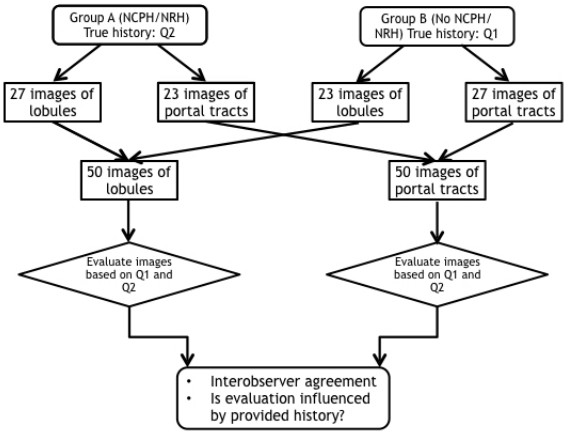

Conclusions: Interobserver agreement on the interpretation of L and P as normal vs. abnormal from both NCPH and non-NCPH biopsy is fair at most, regardless of provision of clinical history. Interpreting individual histologic features of NCPH is likely to remain a challenge due to the histologic overlap in liver biopsies with or without NCPH. Consensus discussion and constellation of clinical and other histologic findings may improve diagnostic yield.